Probing the Mechanism of Viral Inhibition by the Radical S-adenosyl-L-methionine (SAM) Dependent Enzyme- Viperin

by

Soumi Ghosh

A dissertation submitted in partial fulfillment of
the requirements for the degree of
Doctor of Philosophy
(Chemistry)
in The University of Michigan
2020

Doctoral Committee:

Professor E. Neil G. Marsh, Chair
Professor Ryan Bailey
Assistant Professor Jennifer Bridwell-Rabb
Professor Stephen Ragsdale

Soumi Ghosh

soumigho@umich.edu

ORCID iD: 0000-0001-6101-0147

Dedication

To my parents, who always inspire me to reach the zenith of hope

Acknowledgements

I would like to express my deepest appreciation to all the people who continuously encouraged me to pursue scientific research in higher studies. First and foremost, I thank my advisor and Committee chair, Professor E. Neil G. Marsh, who constantly mentored me in my research in graduate school. He inspired me to develop as an independent researcher, providing intellectual freedom. The knowledge I gained in designing and conducting experiments and writing scientific publications under his supervision is invaluable. He was extremely supportive in my attendance at various conferences, applications for fellowships and applications for postdoctoral fellowship. It is an honor for me to share the authorship of three publications with him. Thank you, Professor Marsh, for your constant motivation during the ups and downs in my graduate school, and appreciating my effort as I paved my way through this challenging project.

I am extremely thankful to the present committee members, Professor Stephen Ragsdale, Professor Ryan Bailey, Dr. Jennifer Bridwell-Rabb, and the former committee members Professor Carol Fierke, Professor Bruce Palfey and Dr. Brent Martin. Their valuable advices and suggestions enriched my research and opened new scientific insights.

My journey in graduate school at the department of Chemistry, University of Michigan, became a memorable part of life. This came true because of my departmental colleague, especially the fellow members in Prof. Marsh's laboratory. Their

contribution to this project is invaluable and their support made my life less stressful in the graduate school.

This challenging project would have been impossible without the help from my collaborators. I am thankful to Dr. Paige Malec, Kelcie Zegalia and Professor Robert Kennedy at the department of Chemistry, University of Michigan for assisting me in conducting the mass spectrometric analysis of 5'-deoxyadenosine. I also thank Damon Hoff at the SMART Center, University of Michigan for assisting me in imaging the mammalian cells in the immunofluorescence study. I thank Professor Alexey Nesvizhskii's laboratory, department of Pathology, University of Michigan and Dr. Venkatesha Basrur, bioinformatics and proteomics core, University of Michigan for providing us the wonderful collaboration in conducting the protemics study of viperin.

Lastly, but not the least, I express my deep gratitude to my parents, without whom my dream in pursuing research would not have been possible. I thank all my relatives and teachers who constantly supported and inspired me from India. And needless to say, I am greatful to all my friends here and my beloved friend Saswata at the Ohio state University, for making this new country a *home*, away from home.

Table of Contents

List of Figures

List of Tables

List of Appendices

Abstract

Viperin (Virus Inhibitory Protein; Endoplasmic Reticulum associated, INterferon inducible) is an endoplasmic reticulum (ER)-associated antiviral responsive protein that is highly up regulated in eukaryotic cells upon viral infection. Viperin is a radical S-adenosyl-L-methionine (SAM) enzyme, that catalyses the synthesis of antiviral nucleotide 3'-deoxy-3', 4'-didehydro-CTP (ddhCTP) exploiting radical SAM chemistry. However, the modulation of its catalytic activity by other intracellular proteins is not well understood and needs further investigation. In this dissertation, I use enzymology-based approaches to investigate how viperin's enzymatic activity is regulated through its interaction with various cellular and viral proteins that are involved in cellular metabolic and signalling pathways and viral replication. I showed that viperin can reduce the intracellular expression level of the cholesterol biosynthetic enzyme, farnesyl pyrophosphate synthase (FPPS). This, in turn perturbing the intracellular cholesterol synthesis, thereby retarding budding of enveloped viruses from cholesterol-rich lipid rafts of host cell membranes. I also undertook a proteomics study that revealed that viperin interacts with several other endogenous cholesterol biosynthetic enzymes. I also demonstrated that viperin promotes the degradation of viral non-structural protein A (NS5A) from hepatitis C virus through proteasome-mediated degradation in the presence of sterol-regulatory protein VAP-33. In turn, co-expression of viperin with VAP-33 and NS5A reduced the specific activity of viperin by ~ 3-fold. Lastly, this study showed that viperin is activated by innate immune signalling proteins kinase IRAK1 and ubiquitin ligase TRAF6, as it facilitates the ubiquitination of

IRAK1 by TRAF6. The results provide valuable insights into the mechanism of action of viperin in regulating these target proteins and its significance as a SAM-dependent enzyme.

Chapter 1

Introduction: The Radical *S*-adenosylmethionine Enzyme Viperin is an Anti-viral Responsive Protein

1.1 Overview of radical enzymes: Many enzymatic reactions proceed through mechanisms involving free radical intermediates. Enzymes use the reactivity of the unpaired electron to overcome the energy barrier in chemically challenging reactions. Radical-based reactions in enzymology are often associated with redox-active (flavin, quinone, pterin) (1-9) or metal-based (cobalamin, heme, non-heme, mononuclear copper) (1,9-18) cofactors. The importance of 5-'deoxyadenosyl radical in biological transformations has gained attention due to its ability to catalyze a diverse range of reactions. The two classes of enzymes generate 5'-deoxyadenosyl radical as a part of their mechanism. Adenosylcobalamin (AdoCbl) and radical *S*-adenosylmethionine (AdoMet) dependent enzymes initiate the free radical chemistry by generating 5'-deoxyadenosyl radical either by homolytic cleavage of adenosylcobalamin or single-electron reduction of S-adenosylmethionine (AdoMet), respectively ***[Figure 1.1]***. Although both of these classes of enzymes perform similar chemistry, the Radical SAM enzymes use a cofactor that is much simpler to synthesize, with less complicated biosynthetic and transport machinery. With the addition of new enzymes to this superfamily, Radical SAM enzymes are the subject of extensive research to understand their structural and functional diversity (12,19).

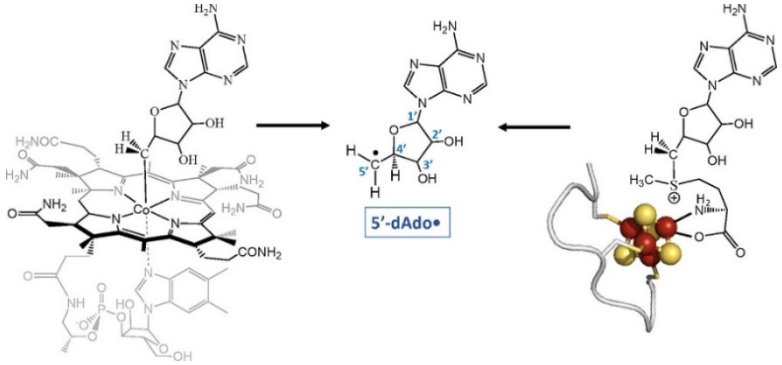

Figure 1.1: Generation of 5'-deoxyadenosyl radical by Adenosylcobalamine (AdoCbl) and *S*-adenosylmethionine (AdoMet) superfamily of enzymes. Figure reproduced from *J. Am. Chem. Soc.* 2019, 141, 30, 12139-12146 (20)

1.2 Introduction to radical SAM enzymes: The Radical S-adenosyl-L-methionine enzymes superfamily (12,21,22) is one of the more recently recognized classes of radical enzymes, but also extremely widespread comprising more than 300,000 members. The enzymes in the superfamily catalyze a diverse range of chemical reactions, participating in numerous biosynthetic pathways, such as cofactor, antibiotics and small molecule biosynthesis, DNA repair and metabolism (12,21,22,31,32). Well-studied examples include ribosomal RNA methyltransferases RlmN and Cfr (23,24) (adenine methylation), lysine-2,3-amiomutase (25) (isomerization), biotin synthase (26) (sulfur insertion), methythiotransferases MiaB, RimO, and MtaB (27) (thiomethyl insertion), molybdopterin cofactor biosynthetic enzyme MoaA (28) (cyclization of GTP to molybdopterin precursor), protein activating enzymes PFL-AE (29) and aRNR-AE (30) (protein radical generation) ***[Figure 1.2]***.

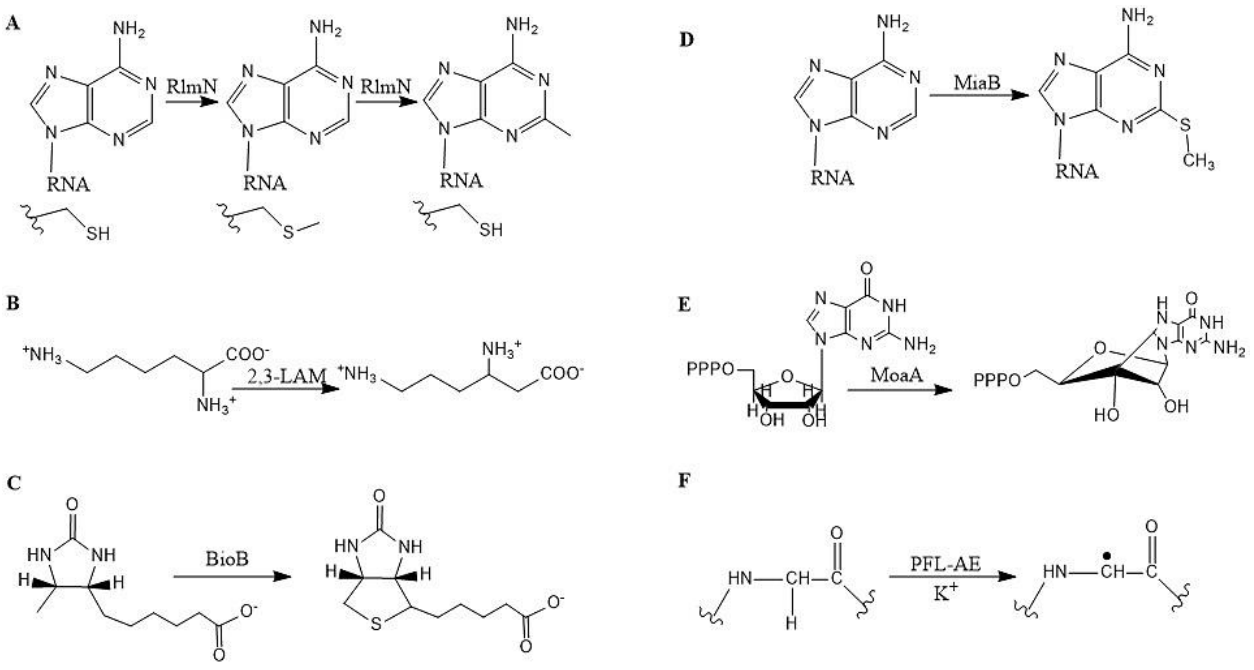

Figure 1.2: Reactions catalyzed by different radical *S*-adenosylmethionine superfamily of enzymes. (A) Methylation by ribosomal RNA methyltransferase RlmN; (B) Isomerisation by lysine-2,3-aminomutase (LAM); (C) Sulfur insertion by biotin synthase (BioB); (D) Thiomethylation by methylthiotransferase MiaB; (E) Cyclisation of GTP by molybdenum cofactor biosynthesis protein MoaA; (F) Glycyl radical generation by pyruvate-formate lysae activating-enzyme (PFL-AE).

Despite their functional diversity, these enzymes share some common features (33-35). They are characterized by the presence of a conserved CxxxCxxC motif, the cysteines chelating three iron atoms of a $[4Fe\text{-}4S]^{2+/+}$ cluster. The cofactor/co-substrate S-adenosyl-L-methionine (SAM/AdoMet) is directly coordinated to the fourth, unique iron atom of the cluster to allow electron transfer during the course of the reaction ***[Figure 3]***. Most of the enzymes adopt a partial TIM-barrel structure, comprised of six (β/α) motif ***[Figure 1.3 (A)].*** The iron-sulfur cluster is bound at the top of the partial β-barrel core domain. The AdoMet moiety coordinates the iron-sulfur cluster in a hydrophilic binding site, adopting anti-conformation at the glycosidic bond ***[Figure 1.3 (B)].***

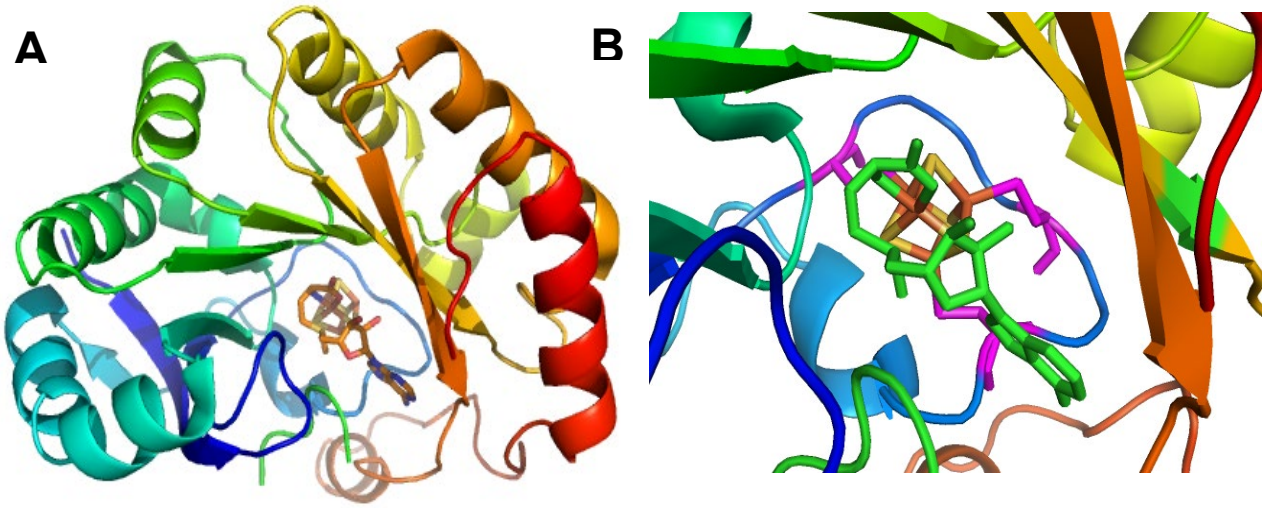

Figure 1.3: Structure of radical SAM enzyme pyruvate-formate lysae activating enzyme (PFL-AE) (PDB ID 3CB8). (A) Enzyme adopting a partial TIM-barrel structure, comprising of six (β/α) motif; (B) Zoomed in view of the ligand binding site with the iron-sulfur cluster (yellow-orange) and S-adesnosyl-Lmethionine cofactor (green), chelated to CxxxCxxC signature motif (magenta).

The structural similarity among the radical SAM enzymes allows them to share a common reaction mechanism, involving a single-electron reductive cleavage of SAM by the iron-sulfur cluster and generation of a highly reactive radical intermediate, 5'-deoxyadenosyl radical (dAdo·). In the presence of substrate, the radical abstracts a hydrogen atom from the substrate and forms 5'-deoxyadenosine (dAdoH) as a by-product ***[Figure 1.4]*** (21). The substrate radical thus generated undergoes a wide variety of reactions in the subsequent steps, dependent on the enzymes. In the absence of the substrate, uncoupled turnover can occur, leading to the radical being quenched by the solvent or protein moiety (21).

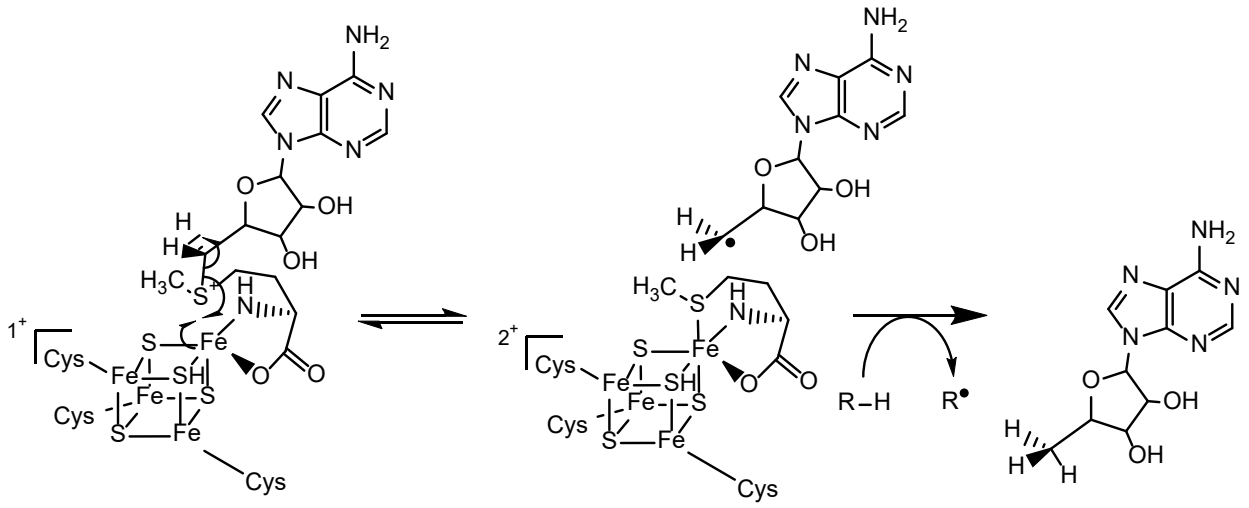

Figure 1.4: General reaction mechanism of radical SAM enzymes: one-electron reductive cleavage of SAM by the iron-sulfur cluster to generate 5'-deoxyadenosyl radical. The radical abstracts hydrogen atom from the substrate of the protein, generating a substrate radical and 5'-deoxyadenosine as the by-product.

1.3 Viperin (Radical SAM domain-containing protein 2) is a member of the radical SAM enzyme superfamily that shows antiviral activity: Investigating the reaction mechanisms of radical SAM enzymes is quite challenging due to the oxygen sensitivity of the iron-sulfur cluster and the instability of radical intermediates. Although the presence of radical SAM enzymes was thought to be confined to anaerobic microorganisms, the recent emergence of their importance in human metabolism and signaling pathways provides new insights into the function of these enzymes (32). To date, eight radical SAM enzymes have been found in humans: they are involved in molybdenum cofactor biosynthesis, fatty acid synthesis, tRNA modifications, and the antiviral response(32). The Radical *S*-adenosylmethionine domain-containing protein 2 (RSAD2) or viperin (virus inhibitory protein, endoplasmic reticulum-associated, interferon-inducible) is one enzyme (36-42), that is increasingly receiving attention due to its ability to restrict a broad range of viruses, including human cytomegalovirus (HCMV)(44-46), influenza A virus(47),

HIV(48), hepatitis C virus(49-51), zika virus(52-54), Encephalitis virus (52,55), and Dengue virus (56,57) ***[Figure 1.5].*** The mechanisms by which viperin mitigates viral infection appear to be dependent on the identity of the virus and are quite variable in nature. It has been shown to interact with numerous cellular and viral proteins. However, the involvement of catalytic mechanism of viperin as a radical SAM enzyme while exerting antiviral activity by regulating the protein targets lacks proper explanation and needs further investigation. Taking biochemical and cellular biology approaches, my major goal in this study is to establish molecular-level insights into the interactions between viperin and its cellular targets, while behaving as a radical SAM enzyme.

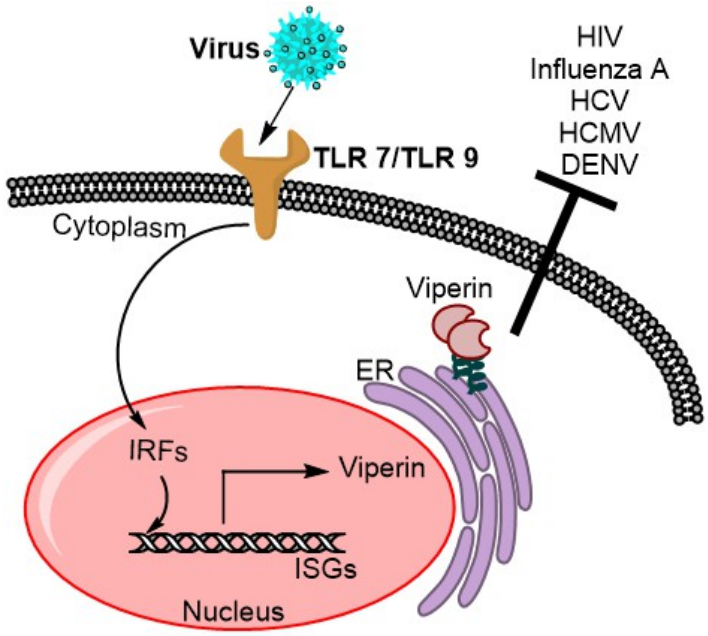

Figure 1.5: Overview of anti-viral response of viperin: Viperin is up-regulated in the cells by innate immune Toll-like receptors (TLR7/9) and it inhibits a broad range of viruses.

In 1997, the mRNA of RSAD2/viperin was first identified as cytomegalovirus-inducible gene 5 (cig5) through differential display PCR from a cell culture infected with human

cytomegalovirus (HCMV) (58) and later its sequence identity with radical SAM enzyme MoaA was confirmed (59). In 2001, the gene was isolated from human cytomegalovirus (HCMV) infected fibroblasts (44). When stably expressed, viperin was shown to restrict HCMV replication and abolish the expression of structural glycoproteins of the virus, while localized to the endoplasmic reticulum. Furthermore, this highly species-conserved protein was recognized in various mammals, fish, and reptiles (60).

Viperin is expressed at a low basal level in most cells and induced by type I, II, III interferon, double-stranded DNA and RNA, lipopolysaccharides, Poly I:C and multiple viruses(40,59,61,62). Especially, the expression of mammalian viperin is found to be induced by interferon-dependent and independent pathways or through direct activation of Toll-like-receptor (TLR) or RIG-I-receptors (RLR) by viruses. The interferon-stimulating gene factor 3 (ISGF3) shows strong regulation of viperin expression in the interferon-dependent pathway, whereas its interferon-independent expression is controlled by interferon regulatory factors (IRF1 and IRF3)(62).

1.4: Structure of viperin: Sequence analysis and a recent crystal structure of mouse viperin predict that this 361 amino acid protein, with 42 kDa molecular mass, contains three distinct domains (36,39-41,63). The N-terminal domain, which shows variability between species in length and sequence, has an amphipathic α helix that binds at the cytosolic face of the endoplasmic reticulum (ER) and lipid droplets (64-66). In contrast, the central SAM-binding domain and C-terminal domain are highly conserved. The central domain (71-182) contains a tri-cysteine motif (CxxxCxxC), responsible for binding the iron-sulfur cluster. The AdoMet cofactor interacts with a conserved GGE motif and arginine 194 and serine 180, observed in this central domain region (63). Although the

Fe-S binding motif seems to be essential for viperin's anti-viral activity against HCV and HCMV, the role of this domain has yet to be determined. The C-terminal domain is mostly disordered and shown to be crucial in substrate recognition. Studies show that the C-terminal tryptophan in this domain interacts with CIAO1, a [Fe-S] cluster installing protein. Thereby, truncation of C-terminal results in an enzymatically inactive viperin, compromising its antiviral activity against HCV, HIV-1 and Dengue virus type-2. The crystal structure of mouse viperin showed that amino acid residues 75-284 adopt a partial $(\beta\alpha)_6$ fold ***[Figure 1.6 (A)],*** similar to other radical SAM enzymes; whereas the N-terminal (45-73) and last 26 amino acids in the C-terminal (337-362) are disordered. The C-terminal extension is flexible and folds over the barrel, mimicking a closed $(\beta\alpha)_8$ - barrel fold (63).

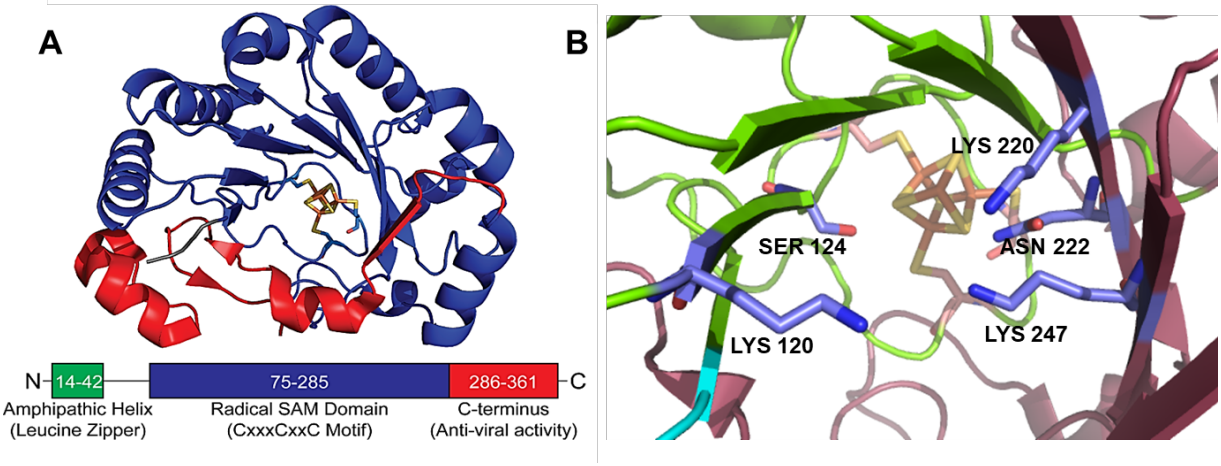

Figure 1.6: Structure of mouse viperin (PDB ID 5VSL): (A) Overall partial TIM barrel folds of viperin. The radical SAM domain and the C-terminal domain are shown in blue and red, respectively. (B) Zoomed in view of active site, containing the positively charged amino acids (Blue), and facing the iron-sulfur cluster (Yellow-orange) binding site, comprised of β-sheet and loops from radical SAM domain (green) and C-terminal domain (maroon).

A close structural similarity has been observed between and viperin and radical SAM enzyme MoaA, that catalyze the cyclization of GTP to 3′, 8-cyclic-GTP in the first step of molybdenum cofactor biosynthesis. It shows a similar β-barrel fold with a flexible C-

terminal extension as does viperin ***[Figure 1.7].*** A remarkable structural alignment is observed at the second β-strand between these two proteins, bearing the SAM binding motif and positively charged and hydrophilic amino acid residues at the active site (Lys69, Lys163, Arg192, Thr73, Asn165 in MoaA and Lys120, Lys220, Lys247, Ser124, Asn222 in viperin) ***[Figure 1.6 (B)].*** From this structural basis, it was predicted that viperin might contain a nucleoside-triphosphate binding site and use an NTP as potential substrate (36,63).

Figure 1.7: Overlay of crystal structures of viperin (5VSL) in cyan and molybdenum cofactor biosynthesis protein MoaA (2FB3) in magenta.

1.5: Prediction of the substrate of viperin: Initially, there was no direct evidence of the identity of the substrate of viperin. Numerous biochemical and virological phenomena provided indirect evidence regarding the structure or characteristics of the substrate of viperin. Overexpression of wild-type human viperin in *E.coli* showed an elongated morphology in *E.coli*, whereas cells overexpressing a mutant enzyme unable to bind the iron-sulfur cluster did not show any morphological change (67). This suggests that viperin

utilizes cellular metabolites, common to both bacteria and humans, in a SAM-dependent manner; and alter the lipid metabolism and perturb cell-division. Supporting this observation, geranyl pyrophosphate (GPP) and farnesyl pyrophosphate (FPP), two terpene intermediates in the mevalonate and cholesterol biosynthesis pathway were tentatively identified as potential substrates of viperin (68). During SAM- cleavage activity, recombinant human viperin showed enhanced production of 5'-deoxyadenosine in the presence of these two small molecules, coupled with the incorporation of a nonexchangeable hydrogen atom from GPP and FPP in a deuterium oxide exchanged buffer solution ***[Figure 1.8].*** However, the biochemical significance of viperin's activity on the cholesterol level in the presence of these small molecules remains unexplained.

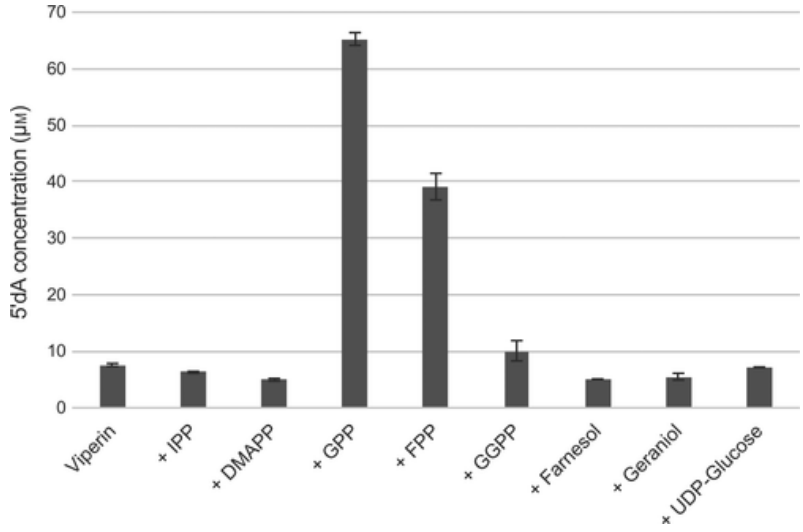

Figure 1.8: The production of 5'-deoxyadenosine (5'dA) by viperin in the presence of different small molecules: Geranyl pyrophosphate (GPP) and Farnesyl pyrophosphate (FPP) showed increase in the production of 5'-dA, when assayed with viperin in the presence of SAM and dithionite. Figure reproduced from *FEBS Lett.,* 592, 2, 199-208

Similarly, a nucleoside-sugar was characterized to be a possible small molecule substrate of viperin, as viperin interacts with several viral glycoproteins to limit the viral assembly and maturation process. *In-vitro* radical SAM activity of fungal viperin in the presence of

uridine diphosphate glucose (UDP-glucose) produced a modified nucleoside-sugar via a coupling reaction between UDP-glucose, 5'-deoxyadenosine radical and a hydrogen atom from the solvent ***[Figure 1.9]***. These observations support the hypothesis that viperin can prevent the formation of oligosaccharide precursors, required for the expression of viral glycoproteins; however, direct evidence for viperin's inhibitory activity against glycosylation was not studied in this case(69).

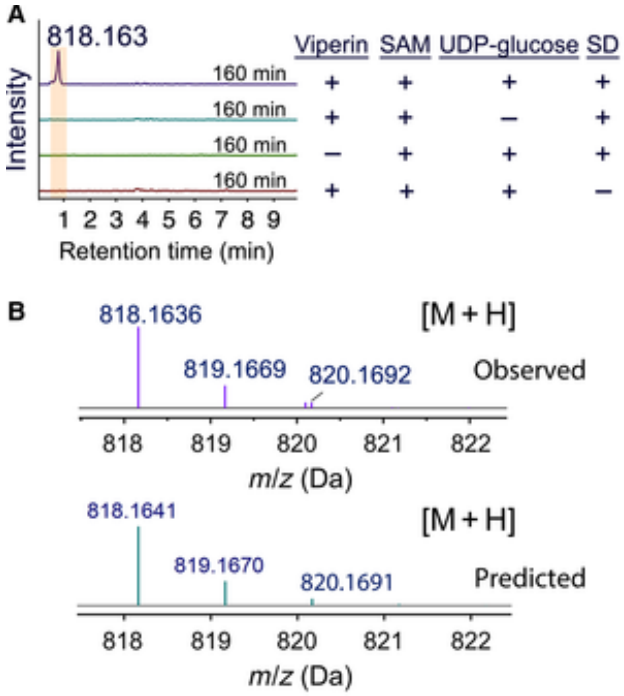

Figure 1.9: The addition reaction of a 5′-dAdo radical and a hydrogen atom to UDP-glucose, catalyzed by viperin: (A) A product [M + H] with m/z of 818.1, denoting the presence of the addition product, was detected only in the presence of Viperin, SAM, UDP-glucose, and sodium dithionite (SD). (B) The observed mass matches accurately with the predicted mass of the addition product. Figure reproduced from *FEBS Lett.,* 591, 16, 2394-2405.

Based on the fact that the gene encoding viperin is found adjacent to nucleotide monophosphate phosphorylating enzyme cytidylate monophosphate kinase 2 (CMPK2), it was predicted that viperin might have similar nucleotide modifying activity. Indeed,

recently, rat viperin was shown to catalyze the conversion of cytidine triphosphate to 3′-deoxy-3′,4′-didehydro-cytidine triphosphate (ddhCTP) in a radical dependent manner, both in mammalian cells and in vitro (70). The 5'-deoxyadenosyl radical generated by viperin from reductive cleavage of SAM, abstracts a hydrogen atom from the 4'-carbon of CTP forming a substrate radical, which rearranges to ddhCTP ***[Figure 1.10].*** Lacking the 3'-hydroxyl, this ribonucleotide acts as a viral RNA polymerase chain terminator, for RNA-depepndent RNA polymerases from flaviviruses such as the Hepatitis C virus, Dengue virus, West Nile virus and Zika virus. However, this antiviral nucleotide is not sensitive in inhibiting all RNA viruses, suggesting that this is not the general mechanism of viperin to exert its antiviral activity (70).

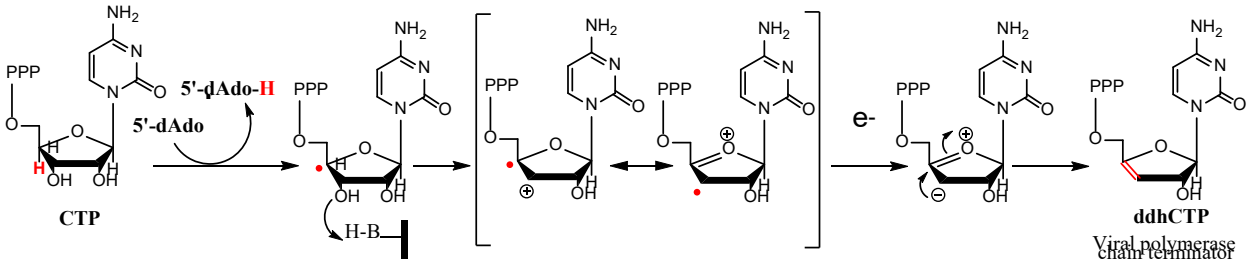

Figure 1.10: The conversation of CTP to 3′-deoxy-3′,4′-didehydro-cytidine triphosphate (ddhCTP) by viperin.

1.6: Regulation of cellular and viral proteins by viperin: Although a direct biochemical function of the enzyme activity of viperin was established in this study, its virus-specific inhibitory mechanism is not well understood to date. Viperin has been reported to target several cellular and viral proteins while modulating metabolic and signaling pathways that restrict replication of a broad spectrum of DNA and RNA viruses, including herpesviruses (HCMV) (44,45), flaviviruses (HCV, West Nile virus/WNV, Zika virus and Dengue virus)(49-54,56,57,61,71-73), retrovirus (HIV-1) (44,48), alphavirus (Sindbis virus) (42),

orthomyxovirus (Influenza A virus) (44,47), paramyxovirus (Sendai virus) (42), and rhabdovirus (VSV) (42). Viperin was shown to reduce the human cytomegalovirus (HCMV) infection by perturbing the expression of viral structural proteins (gB, pp28, and pp65), required for virus maturation and assembly (44,46). Viperin was also shown to interact with both structural and non-structural proteins for several Flaviviridae viruses and prevent viral replication in host cells(71). In fact, the flaviviruses responded differently upon viperin induction; for example; the non-structural protein NS3 from the tick-borne encephalitis virus (TBEV) and Zika virus (ZIKV) (52), but not from JEV and YFV, was shown to interact and be degraded by viperin through the proteasomal-degradation pathway(74). In another case, the Dengue virus C protein was shown to interact with viperin, but not the TBEV C protein (56,72). To explain a broader mechanism of inhibition, viperin was also shown to inhibit the activity of bacteriophage T7 DNA-dependent RNA polymerase, as T7 polymerase is widely used as a model to study transcription (75). Overall, the antiviral activity of viperin relies on how it regulates its target proteins ***[Figure 1.11].***

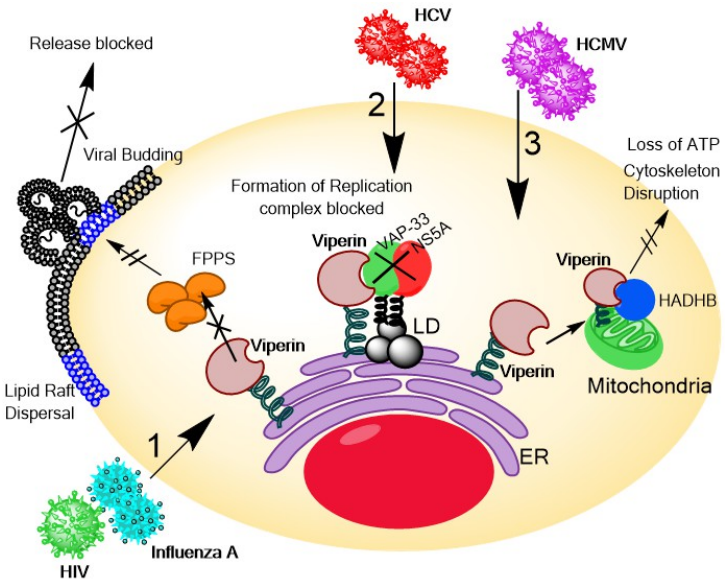

Figure 1.11: Regulation of different metabolic pathways by viperin through its interaction with multiple cellular and viral proteins *in vivo*, upon viral infection.

Apart from viral proteins, viperin is also demonstrated to regulate cellular metabolic and signaling pathways, responsible for the progress of virus infection. Viral budding of enveloped viruses, e.g, influenza virus, and HIV, from the host cell membrane-associated lipid-rafts, was shown to be stalled due to overexpression of viperin, potentially due to its regulatory effect on the lipid metabolism during infection. This might be achieved through the interaction of viperin and farnesyl pyrophosphate synthase (FPPS), a key enzyme for isoprenoid and cholesterol biosynthesis. The inhibition of viral release of the influenza virus by viperin was significantly reversed by overexpression of FPPS in HeLa cells(47). A similar effect was observed during inhibition of HIV by viperin in macrophages, where the addition of exogenous farnesol restored viral egress, consistent with the interaction between viperin and FPPS was responsible for this viral-repression ***[Figure 1.11]*** (48).

The importance of viperin as a key regulator in lipid metabolism was also established during human cytomegalovirus infection, as viperin was observed to relocalize to mitochondria and interact with the mitochondrial trifunctional protein (TFP) beta subunit (HADHB) that mediates fatty acid β-oxidation. This protein-protein interaction resulted in a decrease in cellular ATP level, in turn, weakening the actin cyto-skeleton to facilitate egress of the virus from the cells ***[Figure 1.11]*** (45,76).

In several cases, viperin was described to exert its antiviral activity by regulating protein and lipid secretion pathways. The N-terminal amphipathic helix of viperin was observed to be responsible for restraining the secretion of soluble proteins, required for ER-to-Golgi trafficking (65). Consistent with this observation, an interactome analysis of viperin

identified the Golgi brefeldin A-resistant guanine nucleotide exchange factor 1 (GBF1), a cellular protein involved in ER to Golgi vesicle-mediated transport, as one of its targets (72).

While there is definite proof that viperin can exert antiviral activity over a broad range of pathogens, its role in directly modulating innate immune signaling is also recognized. Viperin enhanced signal transduction through Toll-like receptors 7 and 9 (TLR7/9) which recognize viral nucleic acids and stimulate antiviral effector genes. Viperin was shown to interact with interleukin-1 receptor-associated kinase (IRAK1) and tumor necrosis factor receptor-associated factor 6 (TRAF6) in the signaling complex on lipid bodies; thereby facilitating the ubiquitination of IRAK1 by Ubiquitin ligase protein TRAF6. This, in turn, aided the translocation of IRF7 to the nucleus, where the antiviral interferon-stimulated genes were activated ***[Figure 1.12]*** (77).

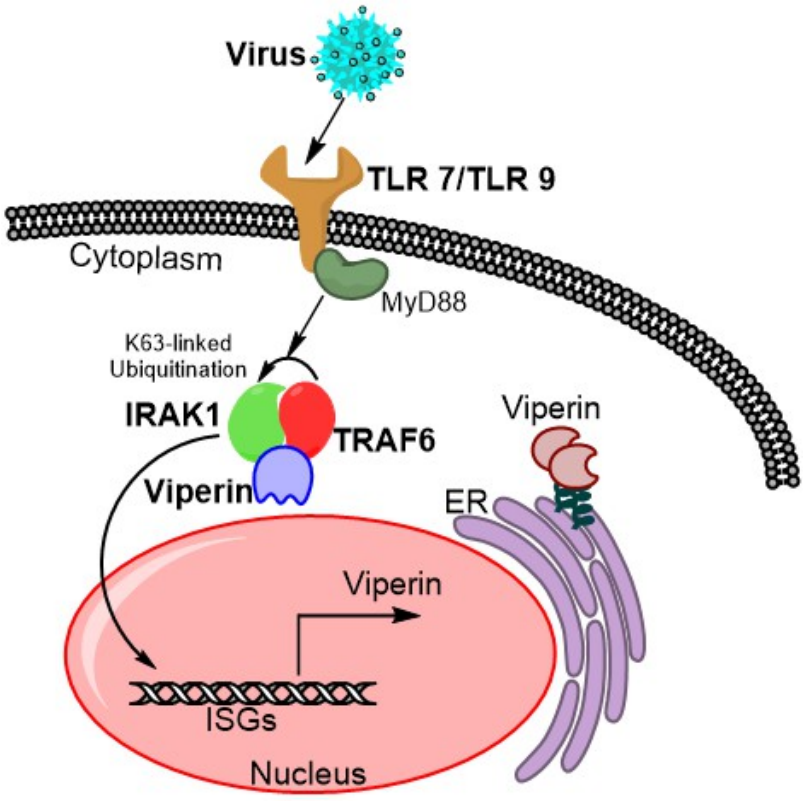

Figure 1.12: Viperin directly participate in innate immune signaling pathways by interacting with Toll-like receptor proteins IRAK1 and TRAF6 and mediating the ubiquitination of IRAK1 by TRAF6.

1.7: Goal of the dissertation research: While structurally and functionally viperin behaves as a radical SAM enzyme, it is still unclear how radical SAM chemistry is imparting immune system regulation by viperin, as it interacts with cellular and viral proteins. To this end, the goal of my dissertation project is to find out how viperin regulates its target proteins and thereby plays a role in suppressing metabolic pathways important in viral replication. I further aim to determine whether viperin exploits its radical SAM activity in regulating its target proteins.

In this dissertation project, I studied the regulation of two potential protein targets by viperin; a cellular protein, farnesyl pyrophosphate synthase (FPPS) and a viral protein, non-structural protein (NS5A). Cell-based *in vivo* and purified protein-based *in vitro* studies were being employed to validate the protein-protein interactions and enzymatic activities of viperin and these two targets. Taking a similar experimental approach, the modulation of viperin's enzymatic activity through its interaction with two innate immune proteins, was also investigated. Lastly, mass spectrometry-based proteomics analysis on immunoprecipitated viperin was also performed to identify other potential binding partners that may facilitate complex formation between viperin and its target proteins. Moreover, a detailed pathway analysis of the proteomics data revealed which cellular pathways viperin is involved. Overall, in this dissertation project, I have focused on enzymatic and biochemical approaches to address the mechanism of viperin at the molecular level, aiming to resolve a unifying course of action of its seemingly diverse anti-

viral activity. The involvement of radical SAM chemistry in the mammalian antiviral responsive system is unexpected and sets viperin apart from other radical SAM enzymes. This study at the interface of immunology and enzymology represents a unique approach to understand this enzyme and aims to break new ground in our understanding of the innate immune system.

References

1. Frey, P. A., Hegeman, A. D., and Reed, G. H. (2006) Free Radical Mechanisms in Enzymology. *Chem. Rev.* **106**, 3302-3316
2. Kay, C. W. M., Feicht, R., Schulz, K., Sadewater, P., Sancar, A., Bacher, A., Möbius, K., Richter, G., and Weber, S. (1999) EPR, ENDOR, and TRIPLE Resonance Spectroscopy on the Neutral Flavin Radical in Escherichia coli DNA Photolyase. *Biochemistry* **38**, 16740-16748
3. Guan, Z.-W., Kamatani, D., Kimura, S., and Iyanagi, T. (2003) Mechanistic Studies on the Intramolecular One-electron Transfer between the Two Flavins in the Human Neuronal Nitric-oxide Synthase and Inducible Nitric-oxide Synthase Flavin Domains. *J. Biol. Chem.* **278**, 30859-30868
4. Tittmann, K., Wille, G., Golbik, R., Weidner, A., Ghisla, S., and Hübner, G. (2005) Radical Phosphate Transfer Mechanism for the Thiamin Diphosphate- and FAD-Dependent Pyruvate Oxidase from Lactobacillus plantarum. Kinetic Coupling of Intercofactor Electron Transfer with Phosphate Transfer to Acetyl-thiamin Diphosphate via a Transient FAD Semiquinone/Hydroxyethyl-ThDP Radical Pair. *Biochemistry* **44**, 13291-13303
5. Fitzpatrick, P. F. (1999) Tetrahydropterin-Dependent Amino Acid Hydroxylases. *Annu. Rev. Biochem.* **68**, 355-381
6. Kappock, T. J., and Caradonna, J. P. (1996) Pterin-Dependent Amino Acid Hydroxylases. *Chem. Rev.* **96**, 2659-2756
7. Anthony, C. (2004) The quinoprotein dehydrogenases for methanol and glucose. *Arch. Biochem. Biophys.* **428**, 2-9
8. Davidson, V. L. (2004) Electron transfer in quinoproteins. *Arch. Biochem. Biophys.* **428**, 32-40
9. Shibata, N., and Toraya, T. (2015) Molecular architectures and functions of radical enzymes and their (re)activating proteins. *The Journal of Biochemistry* **158**, 271-292
10. Meunier, B., de Visser, S. P., and Shaik, S. (2004) Mechanism of Oxidation Reactions Catalyzed by Cytochrome P450 Enzymes. *Chem. Rev.* **104**, 3947-3980

11. Hiner, A. N. P., Raven, E. L., Thorneley, R. N. F., García-Cánovas, F., and Rodríguez-López, J. N. (2002) Mechanisms of compound I formation in heme peroxidases. *J. Inorg. Biochem.* **91**, 27-34
12. Marsh, E. N. G., Patterson, D. P., and Li, L. (2010) Adenosyl Radical: Reagent and Catalyst in Enzyme Reactions. *Chembiochem* **11**, 604-621
13. Banerjee, R. (2003) Radical Carbon Skeleton Rearrangements: Catalysis by Coenzyme B12-Dependent Mutases. *Chem. Rev.* **103**, 2083-2094
14. Cheng, M.-C., and Marsh, E. N. G. (2005) Isotope Effects for Deuterium Transfer between Substrate and Coenzyme in Adenosylcobalamin-Dependent Glutamate Mutase. *Biochemistry* **44**, 2686-2691
15. Gruber, K., and Kratky, C. (2002) Coenzyme B12 dependent glutamate mutase. *Curr. Opin. Chem. Biol.* **6**, 598-603
16. Baik, M.-H., Newcomb, M., Friesner, R. A., and Lippard, S. J. (2003) Mechanistic Studies on the Hydroxylation of Methane by Methane Monooxygenase. *Chem. Rev.* **103**, 2385-2420
17. Lendzian, F. (2005) Structure and interactions of amino acid radicals in class I ribonucleotide reductase studied by ENDOR and high-field EPR spectroscopy. *Biochimica et Biophysica Acta (BBA) - Bioenergetics* **1707**, 67-90
18. Nelson, M. J., and Seitz, S. P. (1994) The structure and function of lipoxygenase. *Curr. Opin. Struct. Biol.* **4**, 878-884
19. Bridwell-Rabb, J., Grell, T. A. J., and Drennan, C. L. (2018) A rich man, poor man story of S-adebosylmethionine and cobalamin revisited. *Annu. Rev. Biochem.* **87**, 555-584
20. Yang, H., McDaniel, E. C., Impano, S., Byer, A. S., Jodts, R. J., Yokoyama, K., Broderick, W. E., Broderick, J. B., and Hoffman, B. M. (2019) The Elusive 5′-Deoxyadenosyl Radical: Captured and Characterized by Electron Paramagnetic Resonance and Electron Nuclear Double Resonance Spectroscopies. *J. Am. Chem. Soc.* **141**, 12139-12146
21. Broderick, J. B., Duffus, B. R., Duschene, K. S., and Shepard, E. M. (2014) Radical S-Adenosylmethionine Enzymes. *Chem. Rev.* **114**, 4229-4317
22. Sofia, H. J., Chen, G., Hetzler, B. G., Reyes-Spindola, J. F., and Miller, N. E. (2001) Radical SAM, a novel protein superfamily linking unresolved steps in familiar biosynthetic pathways with radical mechanisms: functional characterization using new analysis and information visualization methods. *Nucleic Acids Res.* **29**, 1097-1106
23. Grove, T. L., Radle, M. I., Krebs, C., and Booker, S. J. (2011) Cfr and RlmN Contain a Single [4Fe-4S] Cluster, which Directs Two Distinct Reactivities for S-Adenosylmethionine: Methyl Transfer by SN2 Displacement and Radical Generation. *J. Am. Chem. Soc.* **133**, 19586-19589
24. Yan, F., LaMarre, J. M., Röhrich, R., Wiesner, J., Jomaa, H., Mankin, A. S., and Fujimori, D. G. (2010) RlmN and Cfr are Radical SAM Enzymes Involved in Methylation of Ribosomal RNA. *J. Am. Chem. Soc.* **132**, 3953-3964
25. Moss, M., and Frey, P. A. (1987) The role of S-adenosylmethionine in the lysine 2,3-aminomutase reaction. *J. Biol. Chem.* **262**, 14859-14862
26. Lotierzo, M., Tse Sum Bui, B., Florentin, D., Escalettes, F., and Marquet, A. (2005) Biotin synthase mechanism: an overview. *Biochem. Soc. Trans.* **33**, 820-823

27. Atta, M., Arragain, S., Fontecave, M., Mulliez, E., Hunt, J. F., Luff, J. D., and Forouhar, F. (2012) The methylthiolation reaction mediated by the Radical-SAM enzymes. *Biochim. Biophys. Acta* **1824**, 1223-1230
28. Hänzelmann, P., and Schindelin, H. (2004) Crystal structure of the S-adenosylmethionine-dependent enzyme MoaA and its implications for molybdenum cofactor deficiency in humans. *Proc. Natl. Acad. Sci. U. S. A.* **101**, 12870-12875
29. Yang, J., Naik, S. G., Ortillo, D. O., García-Serres, R., Li, M., Broderick, W. E., Huynh, B. H., and Broderick, J. B. (2009) The iron-sulfur cluster of pyruvate formate-lyase activating enzyme in whole cells: cluster interconversion and a valence-localized [4Fe-4S]2+ state. *Biochemistry* **48**, 9234-9241
30. Reichard, P. (1993) The anaerobic ribonucleotide reductase from Escherichia coli. *J. Biol. Chem.* **268**, 8383-8386
31. Zhang, Q., and Liu, W. (2011) Complex biotransformations catalyzed by radical S-adenosylmethionine enzymes. *The Journal of biological chemistry* **286**, 30245-30252
32. Landgraf, B. J., McCarthy, E. L., and Booker, S. J. (2016) Radical S-Adenosylmethionine Enzymes in Human Health and Disease. *Annu. Rev. Biochem.* **85**, 485-514
33. Layer, G., Heinz, D. W., Jahn, D., and Schubert, W.-D. (2004) Structure and function of radical SAM enzymes. *Curr. Opin. Chem. Biol.* **8**, 468-476
34. Vey, J. L., and Drennan, C. L. (2011) Structural Insights into Radical Generation by the Radical SAM Superfamily. *Chem. Rev.* **111**, 2487-2506
35. Boal, A. K., Grove, T. L., McLaughlin, M. I., Yennawar, N. H., Booker, S. J., and Rosenzweig, A. C. (2011) Structural Basis for Methyl Transfer by a Radical SAM Enzyme. *Science* **332**, 1089-1092
36. Shaveta, G., Shi, J., Chow, V. T. K., and Song, J. (2010) Structural characterization reveals that viperin is a radical S-adenosyl-l-methionine (SAM) enzyme. *Biochemical and Biophysical Research Communications* **391**, 1390-1395
37. Duschene, K. S., and Broderick, J. B. (2010) The antiviral protein viperin is a radical SAM enzyme. *FEBS Letters* **584**, 1263-1267
38. Honarmand Ebrahimi, K. (2018) A unifying view of the broad-spectrum antiviral activity of RSAD2 (viperin) based on its radical-SAM chemistry. *Metallomics* **10**, 539-552
39. Mattijssen, S., and Pruijn, G. J. M. (2012) Viperin, a key player in the antiviral response. *Microbes Infect* **14**, 419-426
40. Fitzgerald, K. A. (2011) The interferon inducible gene: Viperin. *Journal of interferon & cytokine research : the official journal of the International Society for Interferon and Cytokine Research* **31**, 131-135
41. Duschene, K. S., and Broderick, J. B. (2012) Viperin: a radical response to viral infection. *Biomol. Concepts* **3**, 255-266
42. Seo, J.-Y., Yaneva, R., and Cresswell, P. (2011) Viperin: a multifunctional, interferon-inducible protein that regulates virus replication. *Cell Host Microbe* **10**, 534-539

43. Crosse, K. M., Monson, E. A., Beard, M. R., and Helbig, K. J. (2018) Interferon-Stimulated Genes as Enhancers of Antiviral Innate Immune Signaling. *J. Innate Immun.* **10**, 85-93
44. Chin, K. C., and Cresswell, P. (2001) Viperin (cig5), an IFN-inducible antiviral protein directly induced by human cytomegalovirus. *Proc. Natl. Acad. Sci. U. S. A.* **98**, 15125-15130
45. Seo, J.-Y., and Cresswell, P. (2013) Viperin Regulates Cellular Lipid Metabolism during Human Cytomegalovirus Infection. *PLoS Pathog.* **9**, e1003497
46. Seo, J.-Y., Yaneva, R., Hinson, E. R., and Cresswell, P. (2011) Human Cytomegalovirus Directly Induces the Antiviral Protein Viperin to Enhance Infectivity. *Science* **332**, 1093
47. Wang, X., Hinson, E. R., and Cresswell, P. (2007) The Interferon-Inducible Protein Viperin Inhibits Influenza Virus Release by Perturbing Lipid Rafts. *Cell Host Microbe* **2**, 96-105
48. Nasr, N., Maddocks, S., Turville, S. G., Harman, A. N., Woolger, N., Helbig, K. J., Wilkinson, J., Bye, C. R., Wright, T. K., Rambukwelle, D., Donaghy, H., Beard, M. R., and Cunningham, A. L. (2012) HIV-1 infection of human macrophages directly induces viperin which inhibits viral production. *Blood* **120**, 778-788
49. Helbig, K. J., Eyre, N. S., Yip, E., Narayana, S., Li, K., Fiches, G., McCartney, E. M., Jangra, R. K., Lemon, S. M., and Beard, M. R. (2011) The antiviral protein viperin inhibits hepatitis C virus replication via interaction with nonstructural protein 5A. *Hepatology* **54**, 1506-1517
50. Jiang, D., Guo, H., Xu, C., Chang, J., Gu, B., Wang, L., Block, T. M., and Guo, J.-T. (2008) Identification of Three Interferon-Inducible Cellular Enzymes That Inhibit the Replication of Hepatitis C Virus. *J. Virol* **82**, 1665-1678
51. Wang, S., Wu, X., Pan, T., Song, W., Wang, Y., Zhang, F., and Yuan, Z. (2012) Viperin inhibits hepatitis C virus replication by interfering with binding of NS5A to host protein hVAP-33. *J Gen Virol* **93**, 83-92
52. Panayiotou, C., Lindqvist, R., Kurhade, C., Vonderstein, K., Pasto, J., Edlund, K., Upadhyay, A. S., and Överby, A. K. (2018) Viperin Restricts Zika Virus and Tick-Borne Encephalitis Virus Replication by Targeting NS3 for Proteasomal Degradation. *J Virol* **92**, e02054-02017
53. Van der Hoek, K. H., Eyre, N. S., Shue, B., Khantisitthiporn, O., Glab-Ampi, K., Carr, J. M., Gartner, M. J., Jolly, L. A., Thomas, P. Q., Adikusuma, F., Jankovic-Karasoulos, T., Roberts, C. T., Helbig, K. J., and Beard, M. R. (2017) Viperin is an important host restriction factor in control of Zika virus infection. *Sci Rep* **7**, 4475
54. Vanwalscappel, B., Tada, T., and Landau, N. R. (2018) Toll-like receptor agonist R848 blocks Zika virus replication by inducing the antiviral protein viperin. *Virology* **522**, 199-208
55. Upadhyay, A. S., Vonderstein, K., Pichlmair, A., Stehling, O., Bennett, K. L., Dobler, G., Guo, J.-T., Superti-Furga, G., Lill, R., Överby, A. K., and Weber, F. (2014) Viperin is an iron-sulfur protein that inhibits genome synthesis of tick-borne encephalitis virus via radical SAM domain activity. *Cell Microbiol* **16**, 834-848
56. Helbig, K. J., Carr, J. M., Calvert, J. K., Wati, S., Clarke, J. N., Eyre, N. S., Narayana, S. K., Fiches, G. N., McCartney, E. M., and Beard, M. R. (2013) Viperin Is Induced following Dengue Virus Type-2 (DENV-2) Infection and Has Anti-viral

Actions Requiring the C-terminal End of Viperin. *PLOS Neglected Tropical Diseases* **7**, e2178
57. Jiang, D., Weidner, J. M., Qing, M., Pan, X.-B., Guo, H., Xu, C., Zhang, X., Birk, A., Chang, J., Shi, P.-Y., Block, T. M., and Guo, J.-T. (2010) Identification of Five Interferon-Induced Cellular Proteins That Inhibit West Nile Virus and Dengue Virus Infections. *J Virol* **84**, 8332-8341
58. Zhu, H., Cong, J.-P., and Shenk, T. (1997) Use of differential display analysis to assess the effect of human cytomegalovirus infection on the accumulation of cellular RNAs: Induction of interferon-responsive RNAs. *Proc. Natl. Acad. Sci.* **94**, 13985
59. Boudinot, P., Massin, P., Blanco, M., Riffault, S., and Benmansour, A. (1999) vig-1, a new fish gene induced by the rhabdovirus glycoprotein, has a virus-induced homologue in humans and shares conserved motifs with the MoaA family. *J. Virol.* **73**, 1846-1852
60. Padhi, A. (2013) Positive selection drives rapid evolution of certain amino acid residues in an evolutionarily highly conserved interferon-inducible antiviral protein of fishes. *Immunogenetics* **65**, 75-81
61. Helbig, K. J., Lau, D. T. Y., Semendric, L., Harley, H. A. J., and Beard, M. R. (2005) Analysis of ISG expression in chronic hepatitis C identifies viperin as a potential antiviral effector. *Hepatology* **42**, 702-710
62. Severa, M., Coccia, E. M., and Fitzgerald, K. A. (2006) Toll-like Receptor-dependent and -independent Viperin Gene Expression and Counter-regulation by PRDI-binding Factor-1/BLIMP1. *J. Biol. Chem.* **281**, 26188-26195
63. Fenwick, M. K., Li, Y., Cresswell, P., Modis, Y., and Ealick, S. E. (2017) Structural studies of viperin, an antiviral radical SAM enzyme. *Proceedings of the National Academy of Sciences* **114**, 6806-6811
64. Gale, M., Jr., Blakely, C. M., Kwieciszewski, B., Tan, S. L., Dossett, M., Tang, N. M., Korth, M. J., Polyak, S. J., Gretch, D. R., and Katze, M. G. (1998) Control of PKR protein kinase by hepatitis C virus nonstructural 5A protein: molecular mechanisms of kinase regulation. *Mol Cell Biol* **18**, 5208-5218
65. Hinson, E. R., and Cresswell, P. (2009) The N-terminal amphipathic alpha-helix of viperin mediates localization to the cytosolic face of the endoplasmic reticulum and inhibits protein secretion. *J Biol Chem* **284**, 4705-4712
66. Hinson, E. R., and Cresswell, P. (2009) The antiviral protein, viperin, localizes to lipid droplets via its N-terminal amphipathic alpha-helix. *Proc. Natl. Acad. Sci. U. S. A.* **106**, 20452-20457
67. Nelp, M. T., Young, A. P., Stepanski, B. M., and Bandarian, V. (2017) Human Viperin Causes Radical SAM-Dependent Elongation of Escherichia coli, Hinting at Its Physiological Role. *Biochemistry* **56**, 3874-3876
68. Mikulecky, P., Andreeva, E., Amara, P., Weissenhorn, W., Nicolet, Y., and Macheboeuf, P. (2018) Human viperin catalyzes the modification of GPP and FPP potentially affecting cholesterol synthesis. *FEBS Lett.* **592**, 199-208
69. Honarmand Ebrahimi, K., Carr, S. B., McCullagh, J., Wickens, J., Rees, N. H., Cantley, J., and Armstrong, F. A. (2017) The radical-SAM enzyme Viperin catalyzes reductive addition of a 5′-deoxyadenosyl radical to UDP-glucose in vitro. *FEBS Lett.* **591**, 2394-2405

70. Gizzi, A. S., Grove, T. L., Arnold, J. J., Jose, J., Jangra, R. K., Garforth, S. J., Du, Q., Cahill, S. M., Dulyaninova, N. G., Love, J. D., Chandran, K., Bresnick, A. R., Cameron, C. E., and Almo, S. C. (2018) A naturally occurring antiviral ribonucleotide encoded by the human genome. *Nature* **558**, 610-614
71. Richard, L., and K., Ö. A. (2018) The Role of Viperin in Antiflavivirus Responses. *DNA and Cell Biology* **37**, 725-730
72. Vonderstein, K., Nilsson, E., Hubel, P., Nygård Skalman, L., Upadhyay, A., Pasto, J., Pichlmair, A., Lundmark, R., and Överby, A. K. (2018) Viperin Targets Flavivirus Virulence by Inducing Assembly of Noninfectious Capsid Particles. *J Virol* **92**, e01751-01717
73. Xu, C., Feng, L., Chen, P., Li, A., Guo, S., Jiao, X., Zhang, C., Zhao, Y., Jin, X., Zhong, K., Guo, Y., Zhu, H., Han, L., Yang, G., Li, H., and Wang, Y. Viperin inhibits classical swine fever virus replication by interacting with viral nonstructural 5A protein. *J Med Virol* **0**
74. Chan, Y.-L., Chang, T.-H., Liao, C.-L., and Lin, Y.-L. (2008) The cellular antiviral protein viperin is attenuated by proteasome-mediated protein degradation in Japanese encephalitis virus-infected cells. *J. Virol.* **82**, 10455-10464
75. Dukhovny, A., Shlomai, A., and Sklan, E. H. (2018) The antiviral protein Viperin suppresses T7 promoter dependent RNA synthesis-possible implications for its antiviral activity. *Sci. Rep.* **8**, 8100-8100
76. Eom, J., Kim, J. J., Yoon, S. G., Jeong, H., Son, S., Lee, J. B., Yoo, J., Seo, H. J., Cho, Y., Kim, K. S., Choi, K. M., Kim, I. Y., Lee, H.-Y., Nam, K. T., Cresswell, P., Seong, J. K., and Seo, J.-Y. (2019) Intrinsic expression of viperin regulates thermogenesis in adipose tissues. *Proc Natl Acad Sci USA* **116**, 17419
77. Saitoh, T., Satoh, T., Yamamoto, N., Uematsu, S., Takeuchi, O., Kawai, T., and Akira, S. (2011) Antiviral Protein Viperin Promotes Toll-like Receptor 7- and Toll-like Receptor 9-Mediated Type I Interferon Production in Plasmacytoid Dendritic Cells. *Immunity* **34**, 352-363

Chapter 2

Probing the Radical SAM Activity of Viperin in Regulating Cellular Protein Farnesyl Pyrophosphate Synthase

(Works in this chapter are mostly published in *J.Biol. Chem*. (2016) **291**, 26806-26815.)

2.1 Introduction Numerous enveloped viruses exploit lipid rafts in host cell plasma membranes for viral assembly and budding from the cell (1-3). Lipid rafts are cholesterol and sphingolipid rich micro-domains in the plasma membrane that maintain the fluidity of the membranes (3). These rafts provide a platform for viral inner structural proteins to bind to the host cell membrane (1). This facilitates various steps in the viral assembly process, including the interaction between viral capsid glycoproteins and structural proteins, multimerization of internal structural and transmembrane proteins and budding and release of viral particles (1,2). Most enveloped viruses and a few non-enveloped viruses (e.g Simian virus 40 or SV40)(1) employ lipid rafts in the host cell membrane for virus entry, replication, and egress. Depletion of cellular cholesterol levels, using cholesterol reducing drugs, such as, lovastatin and gemfibrozil, significantly reduces the expression of viral glycoproteins and reduces viral stability and infectivity (4,5). Therefore, targeting cholesterol and lipid biosynthesis pathways may be a promising broad-spectrum antiviral strategy against enveloped viruses.

The expression of viperin is an anti-viral strategy taken by the host cell to regulate the cellular level of cholesterol ***[Figure 2.1]*** (6,7). Viperin was shown to prevent the release

of Influenza A virus by down-regulating cholesterol synthesis and perturbing lipid-raft formation (6). Viperin mediated inhibition of Human Immuno-deficiency Virus replication was reversed in the presence of exogenous farnesol, a precursor of cholesterol synthesis (8). Regulation of cellular lipid levels by viperin was also observed during the repression of respiratory syncytial virus (RSV) infection, as it disrupted the formation of viral filament structure (9). In another study, overexpressed viperin in hamster derived kidney cells decreased the level of cholesterol and sphingomyelin in the cell membrane (10).

The underlying mechanism involved in the regulation of cellular lipid levels by viperin was studied by Wang *et al (6)*. Their study showed that viperin binds and inhibits farnesyl pyrophosphate synthase (FPPS), a key enzyme in the mevalonate pathway, that leads to synthesis of isoprenoids and sterols. FPPS is a cytoplasmic enzyme that catalyses the condensation of geranyl pyrophosphate (GPP) with isopentenyl pyrophosphate (IPP) to form farnesyl pyrophosphate, a key intermediate in the biosynthesis of isoprenoids and cholesterol (11). Overexpression of viperin in the HeLa cells for 48 hours resulted in a reduction of endogenous FPPS activity by 50% (6).

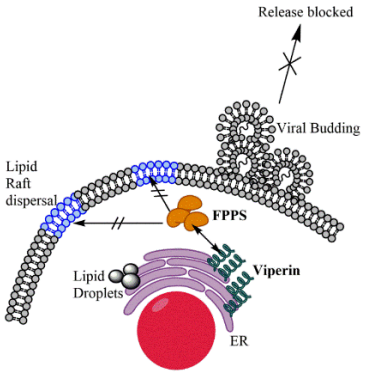

Figure 2.1: Regulation of FPPS by viperin: Reduction of cellular FPPS level can retard cholesterol biosynthesis, thereby disrupting formation of lipid rafts and stalling viral budding process.

Given that many enveloped viruses exploit cholesterol-rich lipid rafts in the cell membrane during the process of viral budding, it was proposed that inhibiting FPPS (and thereby

inhibiting cholesterol production), viperin can prevent viral release from the infected cell. Alternatively, through inhibition of FPPS activity and therefore the production of isoprenoid moieties, viperin may be affecting the prenylation state of various cellular proteins that are necessary for viral release. In either case, the exact mechanism by which viperin inhibits FPPS is still unknown. Also, it was not clear from previous study whether viperin acts as a radical SAM enzyme while inhibiting FPPS.

The goal of this work was to investigate the nature of the inhibitory interaction between viperin and FPPS. This work established that viperin reduces FPPS activity by lowering the steady-state level of the enzyme within the cell, rather than directly inhibiting its catalytic turnover rate. Even though full-length viperin can reductively cleave SAM in a slow, uncoupled fashion and produce 5'-deoxyadenosine, this cleavage reaction is independent of FPPS. However, at the time of this study, it was not known that CTP is a co-substrate of viperin, therefore, the activity of viperin measured here in the absence of CTP only reflects the uncoupled reaction. Furthermore, mutation of key cysteinyl residues (conserved CxxxCxxC motif) ligating the catalytic [4Fe-4S] cluster in the radical SAM domain, surprisingly, does not abolish the inhibitory activity of viperin against FPPS; indeed some mutations potentiate viperin activity. Further characterization of viperin activity through deletion and substitution experiments showed that the observed decrease in the intracellular amount of FPPS is dependent on localization of viperin to the endoplasmic reticulum by its native N-terminal amphipathic α-helix. These results were done collaboratively with Caitlyn Makins and Gabriel David Román-Meléndez and published in *J.Biol. Chem*. (2016) **291**, 26806-26815.

2.2 Results Our initial experiments took a reductive approach and focused on studying the interaction of viperin with FPPS using recombinant proteins over-expressed and purified from *E. coli*. FPPS could be over-expressed and purified from *E. coli* without difficulty and possessed a specific activity similar to that reported in the literature (12). Viperin lacking the first 50 residues that comprise the N-terminal the amphipathic helical domain (designated viperinΔN50 here) was over-expressed as an N-terminal 6xHis-tagged construct and purified using standard approaches; similar to those described previously (13), inside Coy chamber to minimize exposure to oxygen. The [4Fe-4S] cluster could be reconstituted by incubating viperinΔN50 with Na_2S, $Na_2S_2O_4$ and $Fe(NH_3)_6SO_4$ under anaerobic conditions, followed by desalting to remove excess reagents. In the presence of dithionite and SAM, the reconstituted enzyme catalyzed the slow, uncoupled reductive cleavage of SAM to form 5'-deoxyadenosine as previously reported by Duschene and Broderick (13). Attempts to express the full-length enzyme in *E. coli* proved unsuccessful; for reasons that are unclear no protein expression could be detected from cells transformed with the appropriate pET28 expression construct and induced with IPTG (25).

[4Fe-4S]-reconstituted viperinΔN50 and FPPS were incubated together in at equimolar concentrations, ~ 10 μM each, (10 mM Tris-Cl buffer, pH 8.0, containing 300 mM NaCl and 10% glycerol) in the presence of 5 mM dithionite, 5 mM DTT and 200 μM SAM under anaerobic conditions at room temperature for 60 min. After the incubation period, the activity of FPPS was determined under anaerobic conditions using ^{14}C-isopentenyl pyrophosphate (IPP) and geranyl-pyrophosphate (GPP) as substrates and following the incorporation of radioactivity into farnesyl-pyrophosphate (FPP). However, despite

multiple trials in which the incubation times and temperature were varied around these initial conditions, in no change in the activity of FPPS was detected in these experiments. Similarly, the presence of FPPS did not stimulate the reductive cleavage of SAM by viperinΔN50, as might be expected if FPPS was a substrate for viperin. This work was done collaboratively with Gabriel David Román-Meléndez.

Faced with these negative results we concluded that either viperin requires the N-terminal domain for activity against FPPS and/or those additional cellular components are necessary for viperin to interact with FPPS. We therefore pursued our investigation of the effect of viperin on FPPS in a human cell line, HEK293T. We reasoned that this environment should provide: a) the cellular machinery to correctly install the viperin [4Fe-4S] cluster; b) any additional proteins that might be necessary for its activity, and c) the membrane structures to which viperin is localized and which might be important for its activity.

2.2.1. Viperin reduces cellular levels of FPPS. Genes encoding full-length viperin and FPPS were introduced into pcDNA3.1 vectors to facilitate constitutive expression from the CMV promoter and equipped with N-terminal FLAG- and His-tags respectively to allow expression levels to be determined by immuno-staining. Equal amounts of DNA were used to co-transfect HEK293T cells and the expression of both proteins followed for 48 h. Expression levels were compared with cells that were singly transfected. Co-expression of viperin and FPPS resulted in a significant reduction (>2-fold) of the intracellular level of FPPS relative to the FPPS only control, FPPS levels were significantly reduced after 48 h compared to when FPPS was expressed on its own ***[Figure 2.2(A)]***. An examination of the time-course of FPPS expression revealed that under single and co-expression conditions, FPPS levels increased linearly from 24 to 42 h post-transfection ***[Figure 2.2(B)]***. However, the rate of accumulation of FPPS in the presence of viperin

was ~3-fold slower. In contrast, expression of viperin was independent of FPPS and reached a maximum at about 36 h ***[Figure 2.2(C)]***.

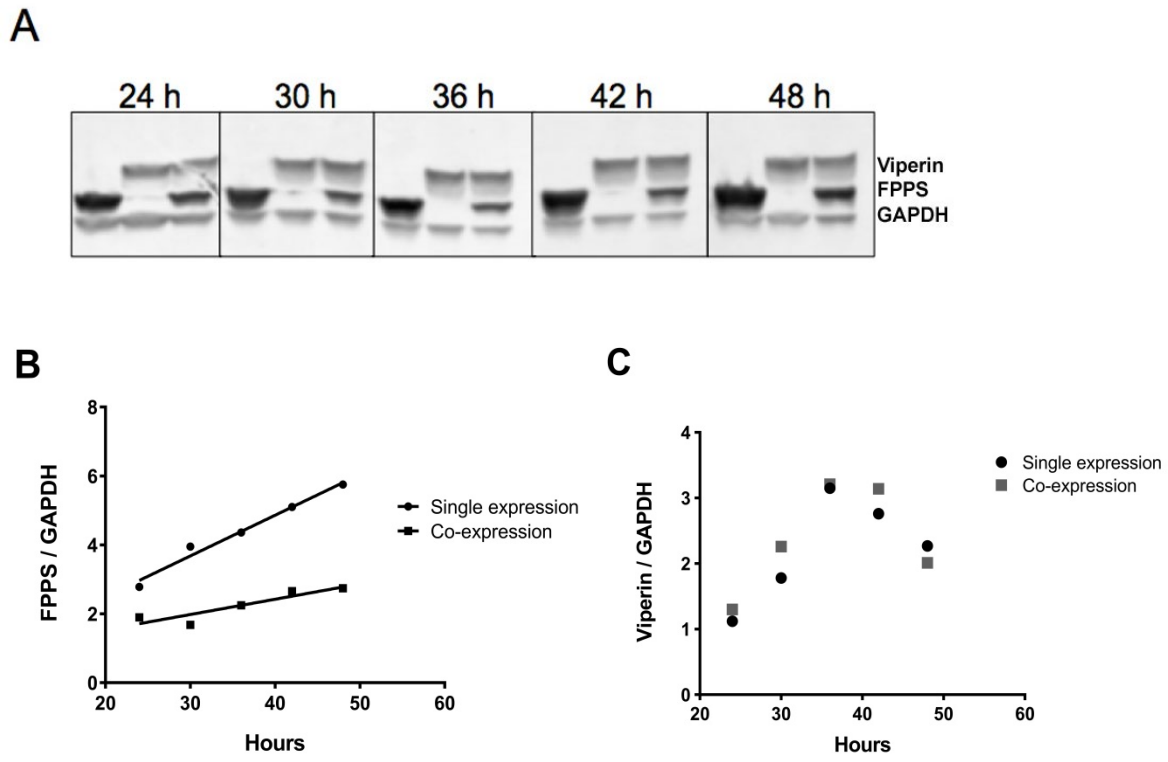

Figure 2.2. Reduction of cellular FPPS levels by viperin in co-transfected HEK293T cells **A**: Western blot analysis of viperin and FPPS expression levels as a function of time after transfection. GAPDH was used as the loading control. **B:** Quantification of intracellular levels of FPPS relative to GAPDH as a function of time in the absence and presence of co-expressed viperin. **C:** Quantification of intracellular levels of viperin relative to GAPDH as a function time in the absence and presence of co-expressed FPPS.

2.2.2 Full-length viperin cleaves SAM. We examined the ability of full-length human viperin, expressed in HEK293T cells, to catalyze the reductive cleavage of SAM to produce AdoH. Tris-buffered saline (50 mM Tris-Cl, pH 7.6, 150 mM NaCl), sonicated within an anaerobic glovebox (Coy Chamber), and centrifuged at 14,000 × g for 10 minutes. Extracts from cells transfected with either viperin and/or FPPS were prepared in Tris-buffered saline containing 1% Triton X-100 and incubated anaerobically at room temperature with 5 mM DTT and 5 mM dithionite for 30 min prior

to the addition of 200 μM SAM. After 1 h the nucleotide pool was extracted and analyzed by LC-MS using established protocols (14). No AdoH was detected in cell extracts lacking viperin, whereas AdoH was readily detected extracts prepared from viperin-expressing HEK293T cells ***[Figure 2.3]***. However, the amounts of AdoH were low, 0.50 ± 0.05 nM, which is less than one turnover based on the concentration of viperin estimated by immuno-staining. Interestingly, co-expression of FPPS with viperin had no effect on SAM cleavage (5'-deoxyadenosine = 0.49 ± 0.05 nM). These results mirrored those obtained in our *in vitro* studies described above, and suggested that either viperin may utilize SAM as a true cofactor (rather than a co-substrate) or that radical SAM chemistry is not involved in viperin's regulation of FPPS.

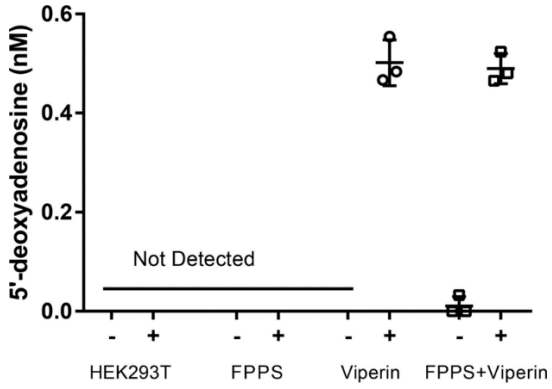

Figure 2.3. Viperin reductively cleaves S-adenosyl-L-methionine in an uncoupled reaction. *Left to right* un-transfected HEK293T cells; HEK293T cells transfected with FPPS; HEK293T cells transfected with viperin; HEK293T cells transfected with FPPS and viperin. The data represent the means and standard deviation of three independent biological replicates.

2.2.3 Mutation of active site residues in viperin. In a complementary approach to depleting the substrate for viperin, we sought to generate inactive viperin variants by mutating each of the conserved cysteine residues within the CxxxCxxC motif to alanine. The C-terminal tryptophan residue (W361), which is thought to be an important recognition element for the cellular iron-sulfur cluster assembly proteins, was also mutated to alanine. Each of these mutations abolished the radical SAM activity of viperin and resulted in slightly lower expression levels of viperin in the cells, suggesting that the mutations destabilize the enzyme slightly. (The C87A, C90A and

C83/87/90A mutations had lower expression compared to WT viperin by ~1.3 fold, ~2.6 fold and ~4.5 fold, respectively; data not shown). Most surprisingly, however, none of the mutations abolished the activity of viperin against FPPS ***[Figure 2.4]***. Indeed, the C87A, C90A, and triple mutant variants proved to be significantly more effective at reducing the intracellular level of FPPS (~6-fold) compared to wild-type viperin (~2-fold). These results demonstrate that the iron-sulfur cluster is *not* required for viperin to reduce FPPS levels and imply that radical SAM chemistry is *not* involved in the regulation of FPPS by viperin.

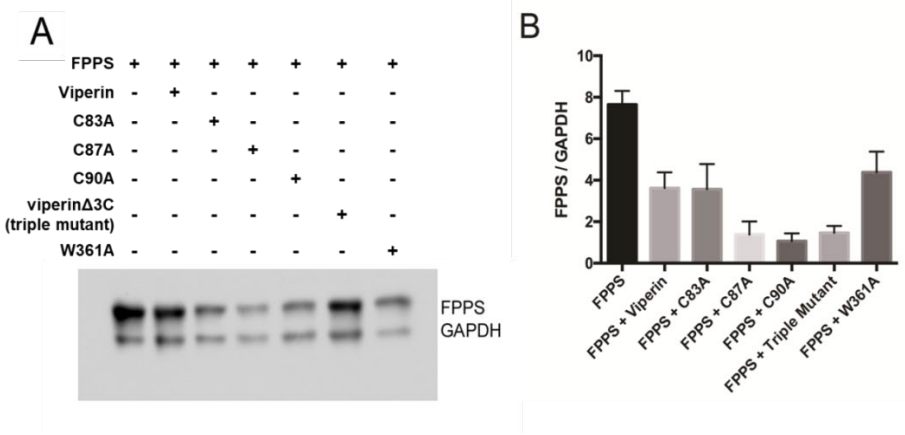

Figure 2.4. Deletion of cysteinyl ligands to the catalytic [4Fe-4S] cluster in viperin does not abolish viperin's activity against FPPS. A. Immunoblot of FPPS, co-expressed with viperin or radical SAM domain mutant constructs of viperin. B**.** Cellular level of FPPS are normalized to GAPDH, and in all cases were significantly reduced when co-expressed with wildtype or mutant viperin enzymes; P = 0.001 - 0.0002.

2.2.4 Effect of cycloleucine on viperin activity. To examine further the mechanism by which viperin reduces FPPS expression we investigated the effect of suppressing intracellular levels of SAM by growing the cells in the presence of cycloleucine. Cycloleucine inhibits SAM synthase and at high concentrations can reduce cellular SAM concentration by up to 80 % (15), thereby depleting the co-substrate for viperin. Consistent with a requirement for SAM, cells transfected with FPPS and viperin and grown in the presence of either 20 mM or 50 mM cycloleucine did not exhibit the reduction in cellular FPPS levels as controls grown in the absence of cycloleucine

[Figure 2.5(A and B)]. However, it should be noted that expression levels of both FPPS and viperin relative to the GAPDH loading control were much lower, likely due to the general cytotoxicity of cycloleucine. Therefore, this result should be interpreted with caution.

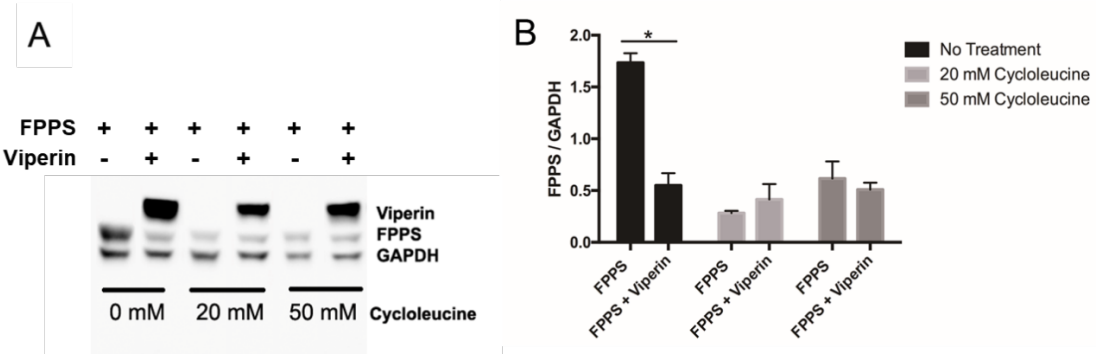

Figure 2.5. Sensitivity of viperin activity to cycloleucine-induced reduction of *intra*-cellular SAM concentration. **A:** Western blot analysis of viperin-induced reduction of FPPS levels in the presence of increasing cycloleucine concentrations. GAPDH is used as loading control. **B:** Quantification of FPPS levels relative to GAPDH in the presence and absence of co-transfected viperin as a function of cycloleucine concentration. (* Significantly significant reduction of FPPS: P = 0.0002; cycloleucine-treated cells did not show a statistically significant reduction in FPPS levels when viperin was co-expressed.)

2.2.5 The native N-terminal amphipathic α-helix of viperin is necessary for reducing cellular FPPS levels. To examine whether association of viperin with the ER or lipid droplets is required for activity against FPPS, we employed the truncated version of viperin lacking the first 50 amino acids comprising of the membrane-targeting N-terminal amphipathic α-helix, but retaining the N-terminal FLAG tag (designated as viperin-ΔN50). Immunofluorescence imaging of HEK293T cells expressing viperin-ΔN50 indicated that, as expected, the truncated protein no longer localized to the ER (Fig. 6A). Viperin-ΔN50 expressed at similar levels to wild-type enzyme but did not significantly reduce the cellular levels of co-transfected FPPS (Fig 6B).

To determine whether the activity of viperin is simply dependent on its localization to the ER, or whether the N-terminal plays a role in the recognition of FPPS, we replaced the N-terminal

amphipathic helix of viperin with the 30-residue N-terminal membrane-localizing sequence of hepatitis C non-structural protein 5A (NS5A) which has been demonstrated to localize NS5A to the ER and lipid droplets as part of the viral replication cycle (16). The chimeric viperin was expressed at similar levels to wild type enzyme and the NS5A sequence effectively re-localized viperin to the ER ***[Figure. 2.6(A)]***. However, the NS5A-TN50 chimeric enzyme displayed no activity against co-transfected FPPS ***[Figure. 2.6(B)].*** These results suggest that the N-terminal amphipathic helix of viperin is important in facilitating the enzyme's ability to decrease cellular FPPS levels and that localization to the ER is not of itself sufficient for this activity.

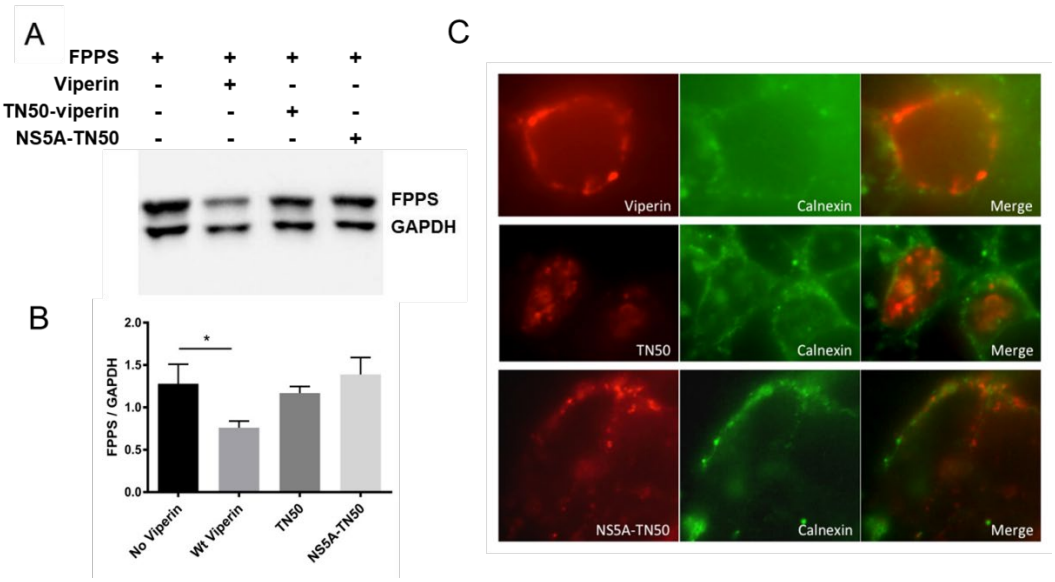

Figure 2.6. ER-localization of viperin is necessary but not sufficient for its activity against FPPS**. A:** Western blot analysis of viperin-induced reduction of FPPS levels in the presence of N-terminal mutated viperin. GAPDH is used as loading control. **B:** The NS5A ER-targeting sequence fails to restore the activity of viperin to reduce the cellular levels of co-expressed FPPS (* $P < 0.05$). **C:** *Top panel* Viperin (red channel) co-localizes with the ER-marker protein calnexin (green channel). *Middle panel* Deletion of the N-terminal amphipathic helix releases viperin to the cytosol. *Bottom panel* Replacing the N-terminal amphipathic helix with the ER-targeting sequence of the viral protein NS5A restores viperin localization to the ER.

2.2.6 Purified FPPS is unmodified by viperin. We examined whether viperin catalyzed any covalent modification of FPPS that might alter its activity or lead to its degradation in the cell. His-

tagged FPPS was co-transfected with viperin into HEK293T, and the cells were cultured for 48 h. The cells were lysed and FPPS-purified from the lysate using nickel-nitrilotriacetic acid affinity resin. Control experiments were set up where FPPS was purified from HEK293T cells that lacked viperin. Native PAGE analysis ***[Figure 2.7(A)]*** revealed no significant difference in the electrophoretic mobility of FPPS isolated from the two preparations that would have been indicative of a post-translational modification. The specific activities of the two enzyme preparations were also compared and found not to differ significantly ***[Figure 2.7(B)]***. k_{cat} for FPPS expressed on its own was 20 ± 2.3 min^{-1}, whereas k_{cat} for FPPS co-expressed with viperin was 15 ± 4.0 min^{-1}; these values are similar to those reported previously(12). LC-ESI-MS analysis of FPPS from each preparation showed no difference in the mass indicative of a covalent modification ***[Figure 2.7(C and D)]*** The observed weight of 42,838 Da differs from the predicted mass of 42,926 Da by 88 Da, which corresponds to the loss of the N-terminal methionine followed by N-terminal acetylation (17). Lastly, no proteolytic fragments of FPPS were evident when FPPS was co-expressed with viperin as judged by immunoblots probed with a polyclonal antibody to FPPS. These observations all indicate that the FPPS remaining in the cell after 48 h is unmodified by viperin.

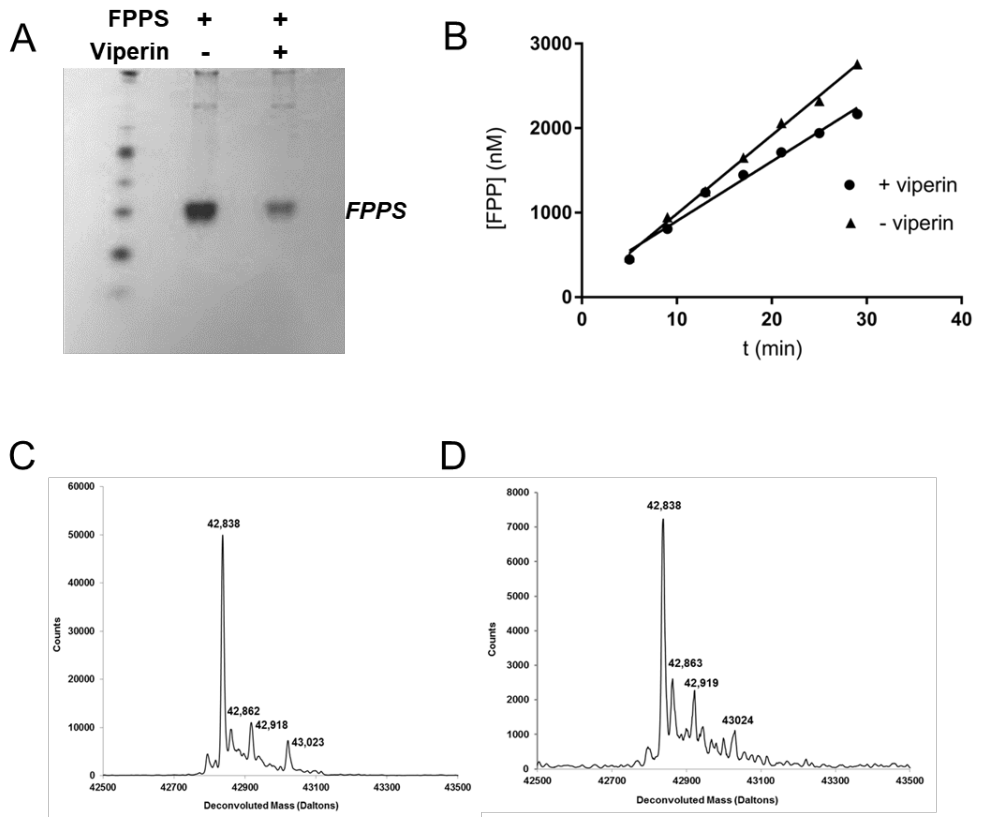

Figure 2.7. FPPS recovered from viperin-expressing cells is un-modified. *A*, native-PAGE analysis of FPPS purified from HEK293T cells. *Lane 1* standard proteins (native molecular masses in kDa indicated on the *left*); *lane 2*, FPPS expressed in the absence of viperin; *lane 3*, FPPS co-expressed with viperin. *B*, activity of FPPS purified from HEK293T cells in absence and in presence of co-expressed viperin; the small difference in rates is not considered significant. *C* and *D*, LC-MS of FPPS purified from HEK293T cells in the absence (*C*) and presence of co-expressed viperin (*D*). No significant differences in the spectra are apparent.

2.3 Discussion Most studies have focused on investigating the antiviral activity of viperin in cell-culture based experiments in which the antiviral activity of the enzyme was assayed either by measuring decreases in viral titer or viral RNA levels. The consensus from these studies is that viperin likely exerts its activity through different pathways that depend on the particular virus and that it interacts with multiple cellular and viral proteins in the process (8,16,18-20). Viperin was only predicted to be a member of radical SAM superfamily during this preliminary stage of study, and it was unclear what reaction, if any, the enzyme catalyzes to effect it's antiviral activity. To partly address this question, recombinantly produced viperin has been characterized *in vitro* and

its ability to reductively cleave SAM to form 5'-deoxyadenosine, a hallmark of radical SAM enzymes, has been demonstrated, both in this work and previously (13). However, the activity was measured only based on the uncoupled reductive SAM cleavage of viperin, as the role of CTP as co-substrate of viperin was not discovered at that time. Therefore, in the light of the new information, there can be a new explanation to the relevance of radical SAM chemistry to viperin's physiological function in targeting FPPS.

Our studies aimed to investigate, at the biochemical level, the interaction of viperin with its best-documented target, FPPS (6). Our initial, unsuccessful, attempts to demonstrate any effect of viperin on FPPS using purified proteins *in vitro*, necessitated a change of approach to studying their interaction *in cellulo*. The over-expression of both proteins in HEK293T cells, which may not be considered truly physiological conditions, nevertheless allows the proteins' interaction to be examined under conditions in which any necessary accessory proteins and cofactors are likely to be present. Moreover, it proved possible to recover FPPS from the cells and biochemically characterize the effect of viperin on the enzyme.

Our experiments demonstrate that viperin depresses the cellular levels of co-expressed FPPS. This is consistent with earlier observations that viperin reduced the activity of endogenously expressed FPPS (6). Our results suggest the reduction in activity is due to increased degradation of FPPS, rather than a covalent modification of the enzyme. This supported by the fact that FPPS purified from HEK293T cells co-transfected with viperin exhibited the same specific activity as FPPS expressed in the absence of viperin and furthermore contained no covalent modifications as assessed by ESI-MS. We consider it very unlikely that viperin in some way regulates transcription, due to the fact that FPPS is expressed from an artificial plasmid; it is similarly unlikely that viperin regulates the translation of FPPS mRNA, as FPPS is a cytoplasmic enzyme whereas viperin is localized to the ER.

A surprising result is that viperin does not appear to depress FPPS levels by a radical SAM mechanism. Our observation that mutating the conserved cysteinyl ligands to the catalytic FeS cluster actually potentiates, rather than abolishes, viperin's ability to decrease FPPS levels is intriguing and leaves open the molecular basis for viperin's activity. These observations are in accord with previous studies in which mutating the conserved cysteinyl residues failed to abolish the ability of viperin to inhibit the replication of HCV (16) and DENV-2 (19) viruses. The sensitivity of viperin activity to cycloleucine suggests that SAM may still be required for activity. However, this result should be interpreted with caution as given the general toxicity of cycloleucine it may be that it decouples FPPS regulation by viperin through another, indirect mechanism.

The N-terminal of viperin appears to be essential for viperin's activity against of FPPS, as replacing this region by a different ER-localizing sequence failed to restore activity. This suggests that the N-terminus plays an important role in recognizing FPPS. We hypothesize that viperin might operate by recruiting additional, as yet unidentified, proteins that would be necessary for FPPS degradation, for example by targeting it for degradation by the proteasome. In fact, viperin is shown to promote the degradation of its cellular and viral target proteins through proteasome-mediated degradation (e.g. mitochondrial protein HADHB, viral protein NS5A and NS3) (21). Interestingly, viperin also has been shown to facilitate K63-linked ubiquitination of the kinase, IRAK1, by the E3 ubiquitin ligase, TRAF6, which are proteins that play a central role in innate immune signaling (22). Viperin appears to do this by co-localizing these proteins to lipid bodies and thus it appears reasonable that a similar mechanism may be operating in the case of FPPS (although we detected no evidence for ubiquitination in our studies).

The question now arises as to whether viperin really is a radical SAM enzyme. We have demonstrated for, the first time, that the full-length enzyme expressed in human cells possesses the ability to reductively cleave SAM to form 5'-deoxyadenosine. However less than one turnover was observed and this presumably represented uncoupled activity. Further investigation on

viperin's radical SAM activity to produce 5'-deoxyadenosine with FPPS in the presence of CTP may results in a higher turnover number. Our results discount a radical mechanism for its interaction with FPPS, but it is still possible that radical SAM chemistry plays a role in regulating other cellular or viral proteins. For example, in contrast to viruses such as Influenza A virus that bud from cholesterol rich lipid rafts and are thus sensitive to FPPS inhibition, flaviviruses such as tick-born encephalitis virus (TBEV) are restricted by viperin but do not require lipid rafts for budding. Indeed it has been shown that inhibition of FPPS by ibandronate has no effect TBEV replication (23).

For TBEV, it was shown that whereas localization to the ER was essential to reduce viral titer, that this was not dependent on identity of the ER-localizing sequence (23). Inhibition of intracellular SAM levels by cycloleucine attenuated viperin's activity against TBEV although this result may be subject to the caveats noted above for our experiments. Significantly, mutation of the conserved cysteine residues or the C-terminal tryptophan of viperin, which is important for installation of the FeS cluster by CIAO1, abolished viperin's inhibition of TBEV replication indicating that an intact FeS cluster was essential for activity. These observations all point to a different mode of action pertaining to viperin's activity against TBEV and other flaviviruses such as DENV-2 and WNV. The results obtained with TBEV are consistent with the involvement of radical SAM chemistry, although they do not demonstrate that such chemistry occurs *in vivo*.

In summary, our studies demonstrate that viperin reduces FPPS activity by reducing cellular levels of the enzyme. This activity is dependent on the N-terminal sequence of viperin but *not* dependent on radical SAM chemistry. It appears most likely that viperin targets proteins using different recognition elements, however the molecular basis of viperin's antiviral action remains unclear, as does the involvement of radical SAM chemistry in it cellular functions.

2.4 Experimental Procedures

Materials. S-adenosyl-L-methionine, 5'-deoxyadenosine, cycloleucine, and mouse monoclonal FLAG antibody (M2) were obtained from Sigma. Mouse monoclonal glyceraldehyde-3-phosphate dehydrogenase (GAPDH) antibody (6C5) was from EMD Millipore. Mouse monoclonal 6x-His tag antibody (HIS.H8) was purchased from Thermo Scientific. Isopentenyl pyrophosphate (IPP) and geranyl pyrophosphate (GPP) were purchased from Isoprenoids, LC. [4-^{14}C]-IPP was purchased from Perkin Elmer. HEK293T cell line was obtained from ATCC. The pcDNA3.1(+) expression vector was purchased from Invitrogen. FuGENE HD transfection reagent was purchased from Promega. All other reagents and materials were purchased from commercial suppliers and were of the highest grade available.

Cloning of viperin for bacterial expression in E. coli. The gene encoding viperin (GenBank: AAL50053.1) was engineered to contain two unique Spe1 sites, allowing the removal of the N-terminal amphipathic alpha helix if necessary. This new construct was named M1Q/W2L-viperin. A naturally occurring Spe1 site (5'-A▼CTAGT-3') occurs between residues Q50 and L51. The first 6 residues of the wild-type viperin sequence (MWVLTP) lend itself to addition of a Spe1 site by simple point mutation of M1 to Q and W2 to L. Addition of a new start methionine yields the final M1Q/W2L-viperin sequence of MQLVLTP. Since the radical SAM domain begins at residue Y77, this design provides a simple strategy at generating truncated viperin. The gene for M1Q/W2L-viperin was codon-optimized for expression in E. coli with an N-terminal 6x histidine tag and purchased from GenScript sub-cloned into pET28 expression vector. A TEV protease cleavage site was included for optional removal of the histidine tag post purification. This yields a 383 amino acid protein with a predicted molecular weight of 44,630.31 Da.

Cloning of truncated M1Q/W2L-viperin for bacterial expression in E. coli. Truncated M1Q/W2L-viperin, in which residues L24-Q72 were removed, was created by standard molecular biology techniques through Spe1 restriction digestion of the M1Q/W2L-viperin pET28 plasmid and confirmed by sequencing. This yields a 334 amino acid protein with an expected molecular weight

of 38,932.4 Da. Without considering the His tag and TEV site, residues L24-Q72 correspond to the removal of residues 3-50 of M1Q/W2L-viperin leaving 27 residues before the radical SAM domain.

Cloning of FPPS for bacterial expression in E. coli. The FPPS gene (GenBank: AAA52423.1) was codon-optimized for expression in E. coli with an N-terminal 6x HIS tag and purchased from GenScript sub-cloned into pET28 expression vector. A TEV protease cleavage site was included for optional removal of the histidine tag post purification. This yields a protein of 374 residues with a calculated molecular weight of 42,925.8 Da.

Bacterial expression of M1Q/W2L-viperin and FPPS from E. coli. To prepare 1 L main culture, a 5 mL seed culture of sterile LB containing 50 µg/mL kanamycin was inoculated with BL21(DE3) E. coli cells containing the pET28 vector containing the appropriate gene. The cells were incubated at 37 °C with shaking at 240 rpm overnight. The next morning, the saturated 5 mL overnight was transferred to 1 L of sterile 2xYT media containing 50 µg/mL kanamycin. The 1 L culture was incubated at 37 °C with shaking at 150 rpm until the OD600 reached approximately 1.0 (5-6 h). The culture was chilled at 4 °C for 30 min and protein expression was induced by adding IPTG to a final concentration of 0.1 mM. The culture was further incubated at 18 °C with shaking at 150 rpm overnight (approx. 18 h). Cells were harvested by centrifugation at 5,000 rpm for 30 min at 4 °C. Cell pellet was stored at -80 °C until ready for use. Protein expression was confirmed by SDS-PAGE.

Purification of truncated M1Q/W2L-viperin from BL21(DE3) E. coli cells. All steps were performed in a Coy chamber (O2 <25 ppm) or under a nitrogen atmosphere using anoxic buffers unless otherwise noted. The cell pellet from a 6 L culture was resuspended in 100 mL lysis buffer (10 mM tris-HCl, 300 mM NaCl, 5 mM imidazole, 1 mM β-mercaptoethanol, 5mM dithionite to act as oxygen scavenger, 1 tablet/10 mL complete mini protease inhibitor tablet - Roche, 1 mg/mL lysozyme, benzonase nuclease, 10% glycerol, pH 8.0) and the suspension shaken for 30 min.

Cell lysis completed by minimal sonication outside the Coy chamber. The lysate was taken back into the Coy chamber and allowed to briefly equilibrate with the anoxic environment prior to removal of the cell debris by centrifugation (17,000 rpm, 30 min,

4 °C). The supernatant loaded onto a super-loop connected to a 5 mL HIS-Trap (GE)

equilibrated in Buffer A (10 mM tris-HCl, 300 mM NaCl, 10 mM imidazole, 10% glycerol, pH 8.0) and the purification carried out by FPLC outside the Coy chamber with a flow rate of 1 mL/min (the column was kept at 10-15 °C by surrounding it with cold packs). The column was washed with Buffer A until the absorbance at 280 nm stabilized and the protein eluted with a linear gradient of 0-100% Buffer B (10 mM tris-HCl, 300 mM NaCl, 500 mM imidazole, 10% glycerol, pH 8.0) over 60 min at 1 mL/min. Elution fractions (15 total) were collected in 2.5 mL aliquots into vials followed by the addition of 500 uL of a 30 mM dithionite solution (Cf = 5 mM dithionite in 3 mL). Fractions containing truncated M1Q/W2L-viperin were pooled, centrifuged to remove precipitated protein, divided into 2mL aliquots, and stored at -80 °C until ready for reconstitution.

Bradford analysis (which was used instead of the calculated extinction coefficient because the purified protein contained high levels of imidazole which would interfere with the A280 reading) established the enzyme stock to be 1 mg/mL (prior attempts to dialyze the pooled enzyme stock resulted in significant protein precipitation). Protein yield was ~ 4 mg/L culture.

Reconstitution of Truncated M1Q/W2L-Viperin Purified from E. Coli. Reconstitution was performed with slight modification of the protocol described by Duschene and Broderick (13). All steps were performed in a Coy chamber (O2 <25 ppm) using anoxic buffers unless otherwise noted. The following protocol is for ~ 2 mg of purified truncated M1Q/W2L-viperin. The day prior to reconstitution, an 8.3 mL PD-10 desalting column was equilibrated with copious amounts (~50 column volumes) of reconstitution buffer (10 mM tris-HCl, 300 mM NaCl, 10% glycerol, pH 8.0) in order to make the column as oxygen free as possible. The column was left to equilibrate

overnight. The truncated M1Q/W2L-viperin stock solution was slowly thawed on a cold pack and the u.v.-visible spectrum recorded using an anaerobic cuvette as a prereconstitution control. The protein was incubated with DTT (Cf = 5mM) for 20 min on the cold pack with gentle magnetic stirring. $FeCl_3$ (Cf = 150 uM, 6 equivalents) was added drop-wise to the stirring solution and incubate an additional 20 min. Na_2S

(Cf = 150 uM, 6 equivalents) was added in one aliquot and stirred for 2 h on the cold pack. The cold pack was removed and stirred for an additional hour. EDTA (Cf = 2 mM) was added in one aliquot and stirred for 30 min to chelate any free iron and sulfide remaining in solution and solution diluted to 2.5 mL with reconstitution buffer (it is important not to exceed 2.5 mL as it is the limit for a PD-10 column). Load the reconstitution solution onto the PD-column and elute the protein. Elution aliquots were collected in 2 mL fractions. The first two fractions (dark reddish brown) were pooled and the u.v.-visible spectrum recorded using an anaerobic cuvette. The reconstituted protein was divided into 500 µL aliquots and stored at -80 °C. Since the desalting column exchanges the truncated M1Q/W2L-viperin into reconstitution buffer, the concentration can now be determined using a calculated extinction (averaging the fully reduced and fully oxidized states) of ε280 = 42,712.5 M-1cm-1. Reconstituted protein yielded was typically ~ 26 µM (1 mg/mL).

Purification of FPPS from BL21(DE3) E. coli cells. FPPS was purified as described for truncated M1Q/W2L-viperin without the use of anoxic buffers, DTT, or Coy chamber. Elution fractions containing FPPS were pooled, concentrated and dialyzed 4x into 1 L of 10 mM tris-HCl, pH 8, 10% glycerol at 4 °C. Using a calculated extinction coefficient (average between the enzyme's oxidized and reduced states) of ε280 = 56,458 M-1cm-1, the final concentration was adjusted to 15 mg/mL, aliquoted and stored at -80 °C. FPPS (Mr 42,925.8 Da) was determined to be to > 95% as judged by SDS-PAGE. Protein yield was ~ 50 mg/L culture.

In vitro SAM cleavage assay of Viperin in the presence of FPPS. The SAM cleavage assay was performed with slight modification of the protocol described by Duschene and Broderick (13).

Reagents were used in final concentrations of 78 μM reconstituted truncated M1Q/W2L-viperin, 5 mM DTT, 5 mM dithionite, 200 μM SAM, 10 mM tris-HCl at pH 8.0, 300 mM NaCl, and 10% glycerol in a total volume of 515 μL. The assay mixture was allowed to incubate at room temperature for 30 min prior to starting the reaction by the addition of SAM. The assay was allowed to age for 60 min at room temperature. The assay was quenched by heating at 95 °C for 10 min. The solution was chilled to 4 °C and precipitated proteins removed by centrifugation. The supernatant was decanted into a Microcon Ultracel YM30 spin column, and centrifuged at 13,000 rpm, 4 °C for 1 h to ensure all the solution passes through. The production of 5'-deoxyadenosine was then analyzed by reverse phase HPLC. 4.2.6.2. Detection of 5'-deoxyadenosine by HPLC. 5'-deoxyadenosine was analyzed by HPLC on a Vydac 201SP54 250 x 4.6 mm C18 reverse-phase column with a 5 μm particle size. 100 μL were injected onto the column (pre-equilibrated in Solvent A) using a 100 μL injection loop. 5'-deoxyadenosine was eluted using a gradient of 0 - 5 min, 0 - 15% B; 5 - 10 min, 15 - 75% B; 10 - 11 min, hold 75% B, 11 - 15 min, hold 100% B, 15 - 20 min, hold 0% B at a flow rate of 1 mL/min.

5'-deoxyadenosine was detected by monitoring its absorbance at 260 nm (RT = 7.50 min) and confirmed by ESI-MS in the positive ion mode ([M+H]+ = 252.1). The amount of 5'-deoxyadenosine produced was determined by peak integration and compared to a standard curve. L-tryptohan (40 ng/μL, RT = 9.95 min) was used as an internal standard. (Solvent A = 0.1% TFA in water, Solvent B = 0.1% TFA in acetonitrile).

Radioactive FPPS assay in the presence of purified viperin. Enzymatic activity was monitored through modification of a radioactivity-based assay described Kavanagh and coworkers (24). Reagents were used in final concentrations of 4.7 nM FPPS (0.4ng/μL), 20 μM GPP, 18 μM IPP, 0.2 μCi/mL [4-C14]-IPP (specific activity 10.8 Ci/mol), 5 μg/mL BSA, 2 mM DTT, 2 mM MaCl2, 10% glycerol, 50 mM tris-HCl at pH 8.0 in a final volume of 800 μL. All reagents except enzyme were combined into a 1.5 mL eppendorf tube and equilibrated to 37 °C over 5 min. The assay,

initiated by the addition of enzyme, was allowed to age and over the course of 15 min, 100 µL aliquots were quenched by addition into 200 µL of a 4:1 MeOH/HCl solution pre-equilibrated at 37 °C. The quenched solution was further incubated for 10 min at 37 °C, allowing for the selective hydrolysis of FPP to farnesol and nerolidol. The hydrolyzed FPP products were extracted into 400 µL ligroin and vortexed for 2 min. 200 µL of the ligroin layer was diluted into 4 mL scintillation cocktail and the absolute C14 content in decays per minute (DPM) of the extracted FPP hydrolysis products was then determined using the LS6500 Beckman liquid scintillation counter's factory installed quench curve.

Cloning of human viperin and FPPS. The genes encoding human viperin (GenBank: AAL50053.1) and farnesyl pyrophoshphate synthase (FPPS; GenBank: AAA52423.1) were purchased from GenScript. Both genes were subsequently amplified via polymerase chain reaction (PCR) and subcloned into the pcDNA3.1(+) vector (Invitrogen). The primers for the pcDNA3.1(+)-viperin construct introduced an N-terminal 3X-FLAG tag –(DYKDHDGDYKDHDIDYKDDDDK) and the Kozak consensus sequence (5'-GCCAAC-3') for downstream protein expression in eukaryotic cells.(25) Similarly, the primers for the pcDNA3.1(+)-FPPS construct introduced an N-terminal hexahistidine tag and the necessary Kozak sequence. Two additional N-terminal 3X-FLAG tagged variants of human viperin were also constructed using standard Gibson assembly cloning methods. The first variant, viperin-ΔN50, featured a deletion of the first 50 amino acids of the N-terminus. The second variant, NS5A-TN50, included a replacement of the native N-terminus by the first 30 amino acid residues from the hepatitis C virus non-structural 5A (NS5A) protein. The gene encoding the NS5A protein was obtained from AddGene as the pCMV-Tag1-NS5A plasmid. The point mutations described in this paper were introduced using the QuikChange site-directed mutagenesis method (Agilent Technologies, Mississauga, ON). DNA sequencing confirmed the presence of each gene and the absence of any PCR-induced errors for each construct.

Expression of human viperin and FPPS in HEK293T cells. Over-expression of the full-length recombinant human viperin and FPPS proteins was accomplished through transient transfection of HEK293T cells (cultivated in DMEM supplemented with 10% FBS and 1% antibiotics) with the pcDNA3.1(+)-viperin construct or the pcDNA3.1(+)-FPPS construct, respectively. In addition, co-transfection of both DNA constructs allowed for co-expression of viperin and FPPS within the HEK293T cells. The same transfection protocols were used for expression of each of the viperin variants. Briefly, 2.5 µg of the respective plasmid DNA construct was mixed with FuGENE HD reagent in a 3:1 ratio, incubated at room temperature for 15 min, and then added to HEK293T cells at 40% confluence on a 35-mm dish. The transfected cells were then grown for up to 48 h, gently pelleted, and stored at –80 °C until use. Expression of viperin and FPPS proteins was also examined following growth of HEK293T cells in the presence of cycloleucine, an inhibitor of S-adenosyl-L-methionine synthesis. Transfected HEK293T cells were grown for 48 h in the presence or absence of 20 mM or 50 mM cycloleucine. In all cases, protein expression was confirmed through western blotting with the appropriate anti-FLAG (Sigma-Aldrich) and/or anti-His (Thermo Scientific) monoclonal antibodies using GAPDH as a loading control. Chemiluminescent images were acquired on a Bio-Rad ChemiDoc Touch Imager. Where noted, rabbit anti-FPPS polyclonal antibodies (Proteintech) were also used to check for FPPS expression.

Immuno-blotting Cell lysates were subjected to electrophoresis and proteins transferred to PVDF membranes by standard methods.

Immunofluorescence and immuno-blotting. HEK293T cells were grown to 30% confluence on poly-L-lysine- coated coverslips and then transiently transfected with wild-type viperin, TN50, or NS5A-TN50 plasmid DNA. After 48 h the cells were fixed with 3% paraformaldehyde, permeabilized with 0.5% Triton X-100 diluted in PBS buffer, and stained with mouse monoclonal anti-viperin (Abcam) and rabbit polyclonal anti-calnexin (Abcam) antibodies. Protein localization

was visualized with Alexa Fluor 647-conjugated goat anti-mouse (Life Technologies) and Alexa Fluor 488-conjugated goat anti-rabbit (Abcam) antisera. Images were acquired on an Olympus IX-81 confocal microscope. Immuno-blotting and imaging of proteins was performed by standard methods using chemiluminescence to visualize proteins. Blots were visualized and band intensities quantified using a BioRad ChemiDoc Touch imaging system. Quantitative measurements of protein expression levels reported here represent the average of at least 3 independent biological replicates.

Cleavage of SAM by viperin in vivo*.* HEK293T cells over-expressing viperin were harvested from a 10 cm^2 dish, resuspended in 200 µL of anoxic Tris-buffered saline (50 mM Tris-Cl, pH 7.6, 150 mM NaCl) containing 1% Triton X-100, sonicated within an anaerobic glovebox (Coy Chamber), and centrifuged at 14,000 $\times$ g for 10 minutes. DTT (final concentration 5 mM) and dithionite (final concentration 5 mM) were added to the cell lysate. The assay mixture was incubated at room temperature for 30 min prior to starting the reaction by the addition of SAM (final concentration 200 µM). The assay was incubated for 60 min at room temperature after which the reaction stopped by heating at 95 °C for 10 min. The solution was chilled to 4 °C and precipitated proteins removed by centrifugation. The supernatant was then extracted with acetonitrile. Aliquots of 20 µL were subsequently derivatized with benzoyl chloride as described previously (14). The samples were analyzed in triplicate for the presence of 5'-deoxyadenosine by HPLC-tandem mass spectrometry, using an Acquity HSS T3 C18 chromatography column (1 mm x 100 mm, 1.8 um, 100 Å pore size) on a Waters nanoAcquity ultra performance liquid chromatograph interfaced to an Agilent 6410 triple quadrupole mass spectrometer. Mobile phase A was 100 mM ammonium acetate with 0.15% formic acid. Mobile phase B was acetonitrile. The flow rate was 100 µL/min, and the gradient was as follows: initial, 0% B; 0.01 min, 17% B; 0.5 min, 40% B; 2.99 min, 60% B; 3.00 min, 100% B; 3.99 min, 100% B; 4.00 min, 0% B; 5.00 min, 0% B. Internal standards included benzoylated adenosine, r.t. 3.33 min, 3'-deoxyadenosine, r.t. 3.85 min and 5'-

deoxyadenosine, r.t. 4.05 min. Peaks were integrated using Agilent MassHunter Workstation Quantitative Analysis for triple quadrupole, version B.05.00.

Purification of FPPS from HEK 293T cells. All purification steps were carried out at 4 °C. Cells overexpressing FPPS or FPPS and viperin (0.5 g, wet weight) were resuspended in 2 mL of Tris-buffered saline, 0.1% Tween-20, and 20 mM imidazole (pH 7.5) containing a mix of protease inhibitors (Sigma-Aldrich). The mixture was briefly sonicated followed by centrifugation at 14,000 rpm for 10 min. The supernatant was then mixed with 100 µL of Ni-NTA resin, pre-equilibrated with Tris-buffered saline and 20 mM imidazole (pH 7.5). Following a 1 h incubation period, the mix was washed twice with 1 mL Tris-buffered saline and 20 mM imidazole (pH 7.5) and then twice more with 1 mL Tris-buffered saline, 20 mM imidazole, and 10% glycerol. FPPS was eluted with 200 µL Tris-buffered saline, 250 mM imidazole, and 10% glycerol. The protein was concentrated and buffer-exchanged into 10 mM Tris-Cl (pH 8.0) containing 10% glycerol and frozen at –80 °C until use. The purity of the isolated FPPS protein was assessed by SDS PAGE (10 % gel). The Lowry assay method was used to determine the concentration of the protein.

Radiolabeled assays for FPPS activity. The catalytic activity of FPPS was monitored through the use of a previously described radiolabeled assay (24), with slight modification. Each 800 µL reaction mixture contained 50 mM Tris-Cl (pH 8.0), 10% glycerol, 2 mM $MgCl_2$, 2 mM DTT, 18 µM IPP, 10.8 Ci/mol [4-^{14}C-IPP], 20 µM GPP, and 4.7 nM FPPS. The reactions were initiated by the addition of FPPS and incubated at 37 ºC. Every 4 minutes a 100 µL aliquot was removed and quenched with 200 µL of a 4:1 MeOH/HCl solution, vortexed briefly, and incubated at 37 ºC for 10 minutes. Each quenched sample was subsequently extracted with 400 µL Ligroin and vortexed for 30 seconds. A 200 µL aliquot of the Ligroin layer was diluted in 4 mL of scintillation cocktail followed by scintillation counting on a Beckman LS 6500 Scintillation Counter. The experiment was repeated in triplicate and data were analyzed using Origin, version 8.5 (MicroCal Software, Inc.).

LC-MS Analysis of FPPS. Purified protein samples that were buffer exchanged into 10 mM Tris-Cl (pH 8.0) containing 10% glycerol were analyzed using an Agilent 6250 Accurate-Mass Q-TOF LC/MS system. Samples (3 µL) were injected into a Zorbax Eclipse Plus C18 column equilibrated with 4.75% acetonitrile and 0.1% formic acid. Proteins were eluted over a 6-minute gradient from 4.75% to 95% acetonitrile at a constant flow rate of 0.4 ml/min. Protein masses were obtained using ESI in positive ion mode and analyzed using Agilent MassHunter Quantitative Analysis software.

Pull-down assay of wild-type viperin and FPPS expressed in HEK293T cells. All steps were performed on ice or at 4 °C. Typically, HEK293T cells cotransfected with wild-type viperin and FPPS were resuspended in 500 µL lysis buffer containing tris-buffered saline, 1% Triton X-100, and 20 mM imidazole, pH 7.4 and lysed sonication. 25 µL Ni-NTA equilibrated in lysis buffer was added and the solution incubated for 10 - 15 min at room temperature with shaking to allow the HIS-tagged FPPS to bind to the resin. The solution was centrifuged to pellet the resin and the supernatant (flow-through) removed carefully by pipette. The resin was washed 3x with 500 µL lysis buffer (60x resin volume). Bound protein was eluted by incubating the resin with 50 µL lysis buffer (2x resin volume) containing 500 mM imidazole for 5 min. The resin was separated by centrifugation and the supernatant decanted (elution). Samples were analyzed by Western Blot.

References

1. Ono, A., and Freed, E. O. (2005) Role of Lipid Rafts in Virus Replication**This chapter was written by Akira Ono and Eric O. Freed in their personal capacity. The views expressed in this chapter do not necessarily reflect the views of the NIH, DHHS, or the United States. in *Advances in Virus Research*, Academic Press. pp 311-358
2. Mazzon, M., and Mercer, J. (2014) Lipid interactions during virus entry and infection. *Cell. Microbiol.* **16**, 1493-1502

3. Bajimaya, S., Frankl, T., Hayashi, T., and Takimoto, T. (2017) Cholesterol is required for stability and infectivity of influenza A and respiratory syncytial viruses. *Virology* **510**, 234-241

4. Gower, T. L., and Graham, B. S. (2001) Antiviral activity of lovastatin against respiratory syncytial virus in vivo and in vitro. *Antimicrob. Agents Chemother.* **45**, 1231-1237

5. Budd, A., Alleva, L., Alsharifi, M., Koskinen, A., Smythe, V., Müllbacher, A., Wood, J., and Clark, I. (2007) Increased Survival after Gemfibrozil Treatment of Severe Mouse Influenza. *Antimicrob. Agents Chemother.* **51**, 2965-2968

6. Wang, X., Hinson, E. R., and Cresswell, P. (2007) The Interferon-Inducible Protein Viperin Inhibits Influenza Virus Release by Perturbing Lipid Rafts. *Cell Host Microbe* **2**, 96-105

7. Seo, J.-Y., and Cresswell, P. (2013) Viperin Regulates Cellular Lipid Metabolism during Human Cytomegalovirus Infection. *PLoS Pathog.* **9**, e1003497

8. Nasr, N., Maddocks, S., Turville, S. G., Harman, A. N., Woolger, N., Helbig, K. J., Wilkinson, J., Bye, C. R., Wright, T. K., Rambukwelle, D., Donaghy, H., Beard, M. R., and Cunningham, A. L. (2012) HIV-1 infection of human macrophages directly induces viperin which inhibits viral production. *Blood* **120**, 778-788

9. Jumat, M. R., Huong, T. N., Ravi, L. I., Stanford, R., Tan, B. H., and Sugrue, R. J. (2015) Viperin protein expression inhibits the late stage of respiratory syncytial virus morphogenesis. *Antiviral Research* **114**, 11-20

10. Tang, H.-B., Lu, Z.-L., Wei, X.-K., Zhong, T.-Z., Zhong, Y.-Z., Ouyang, L.-X., Luo, Y., Xing, X.-W., Liao, F., Peng, K.-K., Deng, C.-Q., Minamoto, N., and Luo, T. R. (2016) Viperin inhibits rabies virus replication via reduced cholesterol and sphingomyelin and is regulated upstream by TLR4. *Sci. Rep.* **6**, 30529-30529

11. Park, J., Zielinski, M., Magder, A., Tsantrizos, Y. S., and Berghuis, A. M. (2017) Human farnesyl pyrophosphate synthase is allosterically inhibited by its own product. *Nat Commun* **8**, 14132-14132

12. Tsoumpra, M. K., Muniz, J. R., Barnett, B. L., Kwaasi, A. A., Pilka, E. S., Kavanagh, K. L., Evdokimov, A., Walter, R. L., Von Delft, F., Ebetino, F. H., Oppermann, U., Russell, R. G. G., and Dunford, J. E. (2015) The inhibition of human farnesyl pyrophosphate synthase by nitrogen-containing bisphosphonates. Elucidating the role of active site threonine 201 and tyrosine 204 residues using enzyme mutants. *Bone* **81**, 478-486

13. Duschene, K. S., and Broderick, J. B. (2010) The antiviral protein viperin is a radical SAM enzyme. *Febs Lett* **584**, 1263-1267

14. Wong, J. M. T., Malec, P. A., Mabrouk, O. S., Ro, J., Dus, M., and Kennedy, R. T. (2016) Benzoyl chloride derivatization with liquid chromatography-mass spectrometry for targeted metabolomics of neurochemicals in biological samples. *J. Chromatogr. A* **1446**, 78-90

15. Yang, H., Sadda, M. R., Li, M., Zeng, Y., Chen, L., Bae, W., Ou, X., Runnegar, M. T., Mato, J. M., and Lu, S. C. (2004) S-adenosylmethionine and its metabolite induce apoptosis in HepG2 cells: Role of protein phosphatase 1 and Bcl-x(S). *Hepatology* **40**, 221-231

16. Helbig, K. J., Eyre, N. S., Yip, E., Narayana, S., Li, K., Fiches, G., McCartney, E. M., Jangra, R. K., Lemon, S. M., and Beard, M. R. (2011) The antiviral protein viperin inhibits hepatitis C virus replication via interaction with nonstructural protein 5A. *Hepatology* **54**, 1506-1517

17. Bonissone, S., Gupta, N., Romine, M., Bradshaw, R. A., and Pevzner, P. A. (2013) N-terminal Protein Processing: A Comparative Proteogenomic Analysis. *Molecular & Cellular Proteomics* **12**, 14-28

18. Wang, X., Hinson, E. R., and Cresswell, P. (2007) The interferon-inducible protein viperin inhibits influenza virus release by perturbing lipid rafts. *Cell Host Microbe* **2**, 96-105

19. Helbig, K. J., Carr, J. M., Calvert, J. K., Wati, S., Clarke, J. N., Eyre, N. S., Narayana, S. K., Fiches, G. N., McCartney, E. M., and Beard, M. R. (2013) Viperin is induced following dengue virus type-2 (DENV-2) infection and has anti-viral actions requiring the C-terminal end of viperin. *PLoS Negl Trop Dis* **7**, e2178

20. Chin, K. C., and Cresswell, P. (2001) Viperin (cig5), an IFN-inducible antiviral protein directly induced by human cytomegalovirus. *Proc Natl Acad Sci U S A* **98**, 15125-15130

21. Panayiotou, C., Lindqvist, R., Kurhade, C., Vonderstein, K., Pasto, J., Edlund, K., Upadhyay, A. S., and Överby, A. K. (2018) Viperin Restricts Zika Virus and Tick-Borne Encephalitis Virus Replication by Targeting NS3 for Proteasomal Degradation. *J. Virol.* **92**, e02054-02017

22. Saitoh, T., Satoh, T., Yamamoto, N., Uematsu, S., Takeuchi, O., Kawai, T., and Akira, S. (2011) Antiviral protein Viperin promotes Toll-like receptor 7- and Toll-like receptor 9-mediated type I interferon production in plasmacytoid dendritic cells. *Immunity* **34**, 352-363

23. Upadhyay, A. S., Vonderstein, K., Pichlmair, A., Stehling, O., Bennett, K. L., Dobler, G., Guo, J. T., Superti-Furga, G., Lill, R., Overby, A. K., and Weber, F. (2014) Viperin is an iron-sulfur protein that inhibits genome synthesis of tick-borne encephalitis virus via radical SAM domain activity. *Cell Microbiol* **16**, 834-848

24. Kavanagh, K. L., Guo, K. D., Dunford, J. E., Wu, X. Q., Knapp, S., Ebetino, F. H., Rogers, M. J., Russell, R. G. G., and Oppermann, U. (2006) The molecular mechanism of nitrogen-containing bisphosphonates as anti osteoporosis drugs. *P Natl Acad Sci USA* **103**, 7829-7834

25. Kozak, M. (1987) An analysis of 5'-noncoding sequences from 699 vertebrate messenger RNAs. *Nucleic acids research* **15**, 8125-8148

Chapter 3

The Interaction of Viperin with Hepatitis C Virus Non-Structural Protein 5A Inhibits the Catalytic Activity of Viperin

(Works in this chapter are part of the manuscript submitted to *Biochemistry*)

3.1 Introduction In addition to regulation of cellular metabolic pathways, viperin appears to exert antiviral activity against a wide range of viruses by interacting with various viral proteins. Especially, it has been shown to inhibit several flaviviridae family viruses; including Hepatitis C Virus (HCV) (1-3), dengue virus (DENV) (4,5), tick-borne encephalitis virus (TBEV) (6-8), West Nile virus (WNV) (4), and Zika virus (ZIKV) (8-11).

Viral non-structural proteins, encoded by flaviviridae family viruses, are the primary innate immunity pathway antagonists in flavivirus/hepacivirus infection (12). These proteins are processed from viral polyprotein precursor through posttranslational modification and are essential for viral replication and assembly and modulating innate immunity of host cells (12,13).

The molecular basis of viperin's inhibitory effects against the viral proteins seems to be virus-specific. For HCV and DENV, it was shown to inhibit viral replication by interacting with the non-structural proteins (1,5,11,14), while for TBEV, it impedes the synthesis of positive-strand viral RNA (7). A recent study revealed that viperin can also inhibit ZIKV

and TBEV replication by interacting with both structural and non-structural viral proteins (8). The regulation of viral proteins by viperin unveils the mechanistic insights of its antiviral activity. However, the underlying unifying mechanism by which viperin targets a broad range of viruses is still under investigation.

Viperin was shown to catalyse the formation of a novel antiviral ribonucleotide by dehydration of CTP to 3'-deoxy-3', 4'-didehydro-CTP (ddhCTP) that acts as a chain terminator for the RNA-dependent RNA polymerases (RdRp) in flaviviruses. This may explain one facet of viperin's antiviral activity against flaviviruses (15). However, it is not yet clear whether and how viperin's ability to produce ddhCTP is regulated in the presence of viral structural and non-structural proteins.

In this study, we focus on viperin's interaction with the Non-structural protein 5 (NS5A) from the Hepatitis C virus and how this interaction leads to the modulation in ddhCTP production by viperin. NS5A is one of the major viral core proteins, playing an important role in HCV replication as an essential component of the viral replication complex (1,3). NS5A localizes at the cytoplasmic face of the endoplasmic reticulum and lipid droplets together with the RdRp, NS5B. Interaction of NS5A with the sterol regulatory host protein, vesicle-associated membrane protein-associated protein A (VAP-33), is also needed to support HCV replication (14,16). Through FRET analysis (3), confocal microscopy and co-immunoprecipitation studies (1), viperin was shown to interact with NS5A through VAP-33 at lipid droplets. This observation suggests that the interaction between viperin and VAP-33 may interfere with the association of NS5A and VAP-33, thereby perturbing the viral replication complex formation **[*Figure 3.1*]**. Mutagenic analysis showed that the

C-terminal domain of viperin is required for its interaction with NS5A through VAP-33 in HEK293T cells.

Here, collaboratively with Ayesha Patel and Timothy Grunkemeyer, we have investigated the interactions between viperin, NS5A and VAP-33 and their effect of virperin's catalytic activity to produce 5'-deoxyadenosine using proteins transiently expressed in HEK293T cells and with pure proteins *in vitro*. We show that full-length viperin interacts with NS5A in presence of host cell factor VAP-33 and leads to its degradation through the proteasomal degradation pathway. Concomitantly, NS5A and VAP-33 reduce the ddhCTP-forming activity of viperin. The formation of the complex between viperin, NS5A and VAP-33 is dependent on the membrane localization of all three proteins. The present study provides insight into the mechanism of regulation of a viral protein by viperin, coupled with its enzymatic activity.

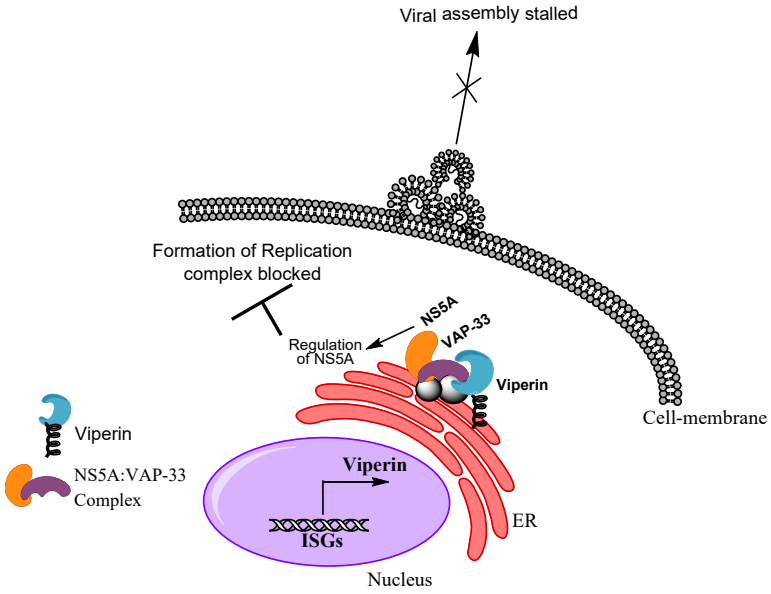

***Figure 3.1*: Overview of viperin's function in inhibiting Hepatitis C virus replication.** Role of viperin in restricting HCV replication complex formation by interacting with the HCV protein Non-structural 5A (NS5A) through vesicle-trafficking host protein VAP-33.

3.2 Results

3.2.1 Viperin interacts with NS5A at endoplasmic reticulum We first examined the interaction of viperin with NS5A and the c-terminal cytoplasmic domain of VAP-33 (VAP-33C; human homolog with amino acid residues 156-242), which previous studies (1) had shown is responsible for binding to NS5A. We conducted immunoprecipitation experiments using viperin or viperinΔ3C (viperin variant with iron-sulfur cluster-chelating cysteine residues mutated to alanine) as bait proteins and NS5A and/or VAP-33C as prey proteins.

NS5A was found to co-precipitate with viperin ***[Figure 3.2(a)]*****,** independent of the presence of VAP-33C. NS5A was also co-precipitated by the viperinΔ3C mutant ***[Figure 3.2(a)]***, suggesting that the presence of the iron-sulfur cluster is not an essential part of the viperin-NS5A interaction. Both viperin and viperinΔ3C mutant were found to precipitate VAP-33C individually. We further confirmed the co-localization of viperin, NS5A and VAP-33C by immuno-fluorescence microscopy of fixed HEK293T cells, where NS5A was observed to co-localize with viperin at endoplasmic reticulum in the presence and absence of VAP-33C ***[Figure 3.2(c)].***

We also assessed the importance of the N-terminal amphipathic helix of viperin for its interaction with NS5A and VAP-33C by co-immunoprecipitation using an N-terminal truncated viperin construct (viperin-ΔN50) that lacks the ER localizing amphipathic helix as the bait protein. In this case NS5A and VAP-33C showed a weaker interaction with viperin-ΔN50 ***[Figure 3.2(b)]*****,** indicating that the localization of viperin to the endoplasmic-reticulum is important for its interaction with the target proteins.

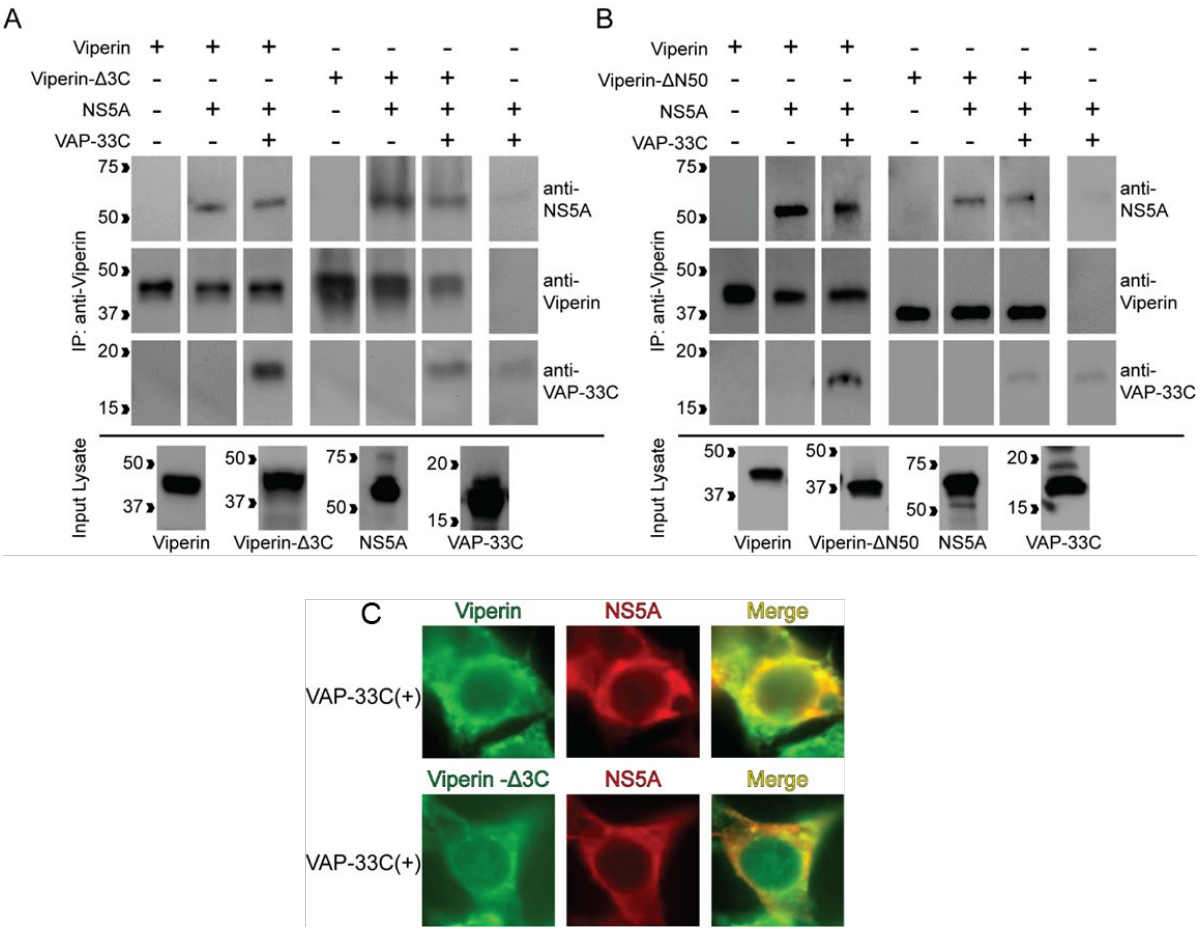

Figure 3.2. **Viperin interacts with NS5A and co-localizes at endoplasmic-reticulum.** (a) HEK293T cells transfected viperin or viperin-Δ3C (lacking the iron-sulfur cluster), NS5A and or FLAG-VAP-33C (c-terminal of VAP-33) were immunoprecipitated using anti-viperin antibody and blots probed with anti-NS5A monoclonal and anti-FLAG (for VAP-33C) antibody. The results demonstrate that viperin and viperin-Δ3C pull down both NS5A and VAP-33C and the iron-sulfur cluster is not required for viperin to bind NS5A and VAP-33C. (b) Co-immunoprecipitation using viperin or viperin-ΔN50 (lacking the N-terminal amphipathic helix) as bait and NS5A and VAP-33C as prey protein. The results demonstrate that the N-terminal amphipathic helix is important for viperin to bind NS5A and VAP-33C. (c) Immunofluorescence microscopy of HEK293T cells co-transfected with viperin (*upper panel*) or viperin-Δ3C (*lower panel*) and NS5A, in presence of VAP-33C. The cells were immobilized 30 hours post-transfection and stained for viperin (green) and NS5A (red). Both viperin and viperin-Δ3C co-localize (yellow in merged images) with NS5A.

3.2.2. Viperin leads to the degradation of NS5A through proteasomal degradation pathway Viperin has been found to alter the cellular expression levels of various proteins it interacts with (8,17). Therefore, we next examined how co-expression of viperin altered the cellular levels of NS5A and VAP-33C. Proteins were co-transfected into HEK293T cells and after 30 h the cells were harvested and protein expression analysed by immunoblotting. Co-expression with VAP-33C had no significant effect on NS5A expression, whereas co-expression with viperin resulted in a small decrease in NS5A levels. Co-expression of both VAP-33C and viperin led to the most significant decrease in intra-cellular expression level of NS5A, by ~2-fold, compared to NS5A expressed on its own ***[Figure 3.3(a)]***. No reduction of NS5A levels were observed in control experiments when empty vector (pcDNA3.1) was co-transfected with it. Similar reductions in NS5A levels were observed when NS5A was co-expressed with viperinΔ3C and VAP-33C, suggesting the iron-sulfur centre is not required for this effect.

To investigate the reason for the viperin-mediated reduction in NS5A expression, we examined the ability of the proteasomal inhibitor MG-132 to restore NS5A expression levels. The expression levels of NS5A co-expressed with viperin or viperinΔ3C were restored to levels comparable to those of the controls by treatment with MG-132 ***[Figure 3.3(b)]*****.** These results suggest that viperin promotes the degradation of NS5A through the proteosomal degradation pathway.

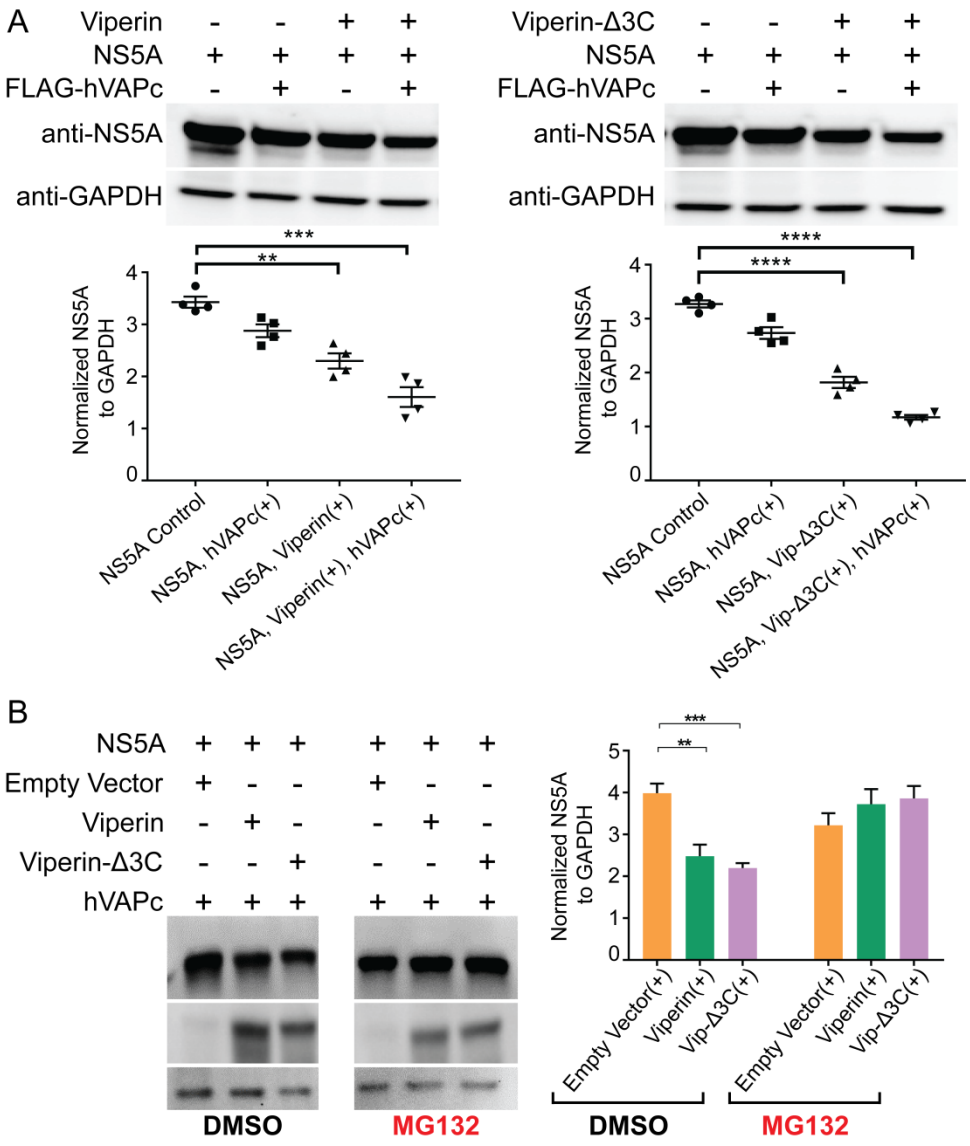

Figure 3.3: **Viperin promotes degradation of NS5A through the proteasomal degradation pathway.** (a) HEK293T cells were transfected with NS5A, FLAG-VAP-33C and either viperin or viperin-Δ3C. 30 hours post-transfection NS5A levels were visualized by immunoblotting. Co-expression of viperin or viperin-Δ3C and VAP-33C significantly decreases NS5A levels (*left panel* *** p = 0.0005, n = 4; *right panel* ****p = 0.0001, n = 4). (b) HEK293T cells were transfected with NS5A, VAP-33C and either viperin or viperin-Δ3C. 6 hours post transfection cells were treated with either 50 μM MG-132 (proteasome inhibitor) or DMSO control; 30 hours post-transfection NS5A levels were visualized by immunoblotting. MG-132 reverses the decrease in NS5A levels induced by co-expression of viperin or viperin-Δ3C (** p = 0.0019, n=6; *** p = 0.0002, n=6).

3.2.3.NS5A and VAP-33C together repress the reductive SAM cleavage activity of viperin to produce 5'-deoxyadenosine NS5A is known to antagonize the innate immune system by inactivating various ISGs (18). For example, NS5A was shown to disrupt dimerization and repress the enzymatic activity of Protein kinase R, a critical ISG in cellular antiviral response (19). Therefore, we investigated whether NS5A might alter the catalytic activity of viperin. To examine this possibility, we measured specific activity of viperin in HEK293T cell lysates when co-expressed with NS5A and/or VAP-33C. HEK293T cell-lysates were prepared under anaerobic conditions and viperin activity was quantified as described previously (20).

When expressed on its own, viperin showed a specific activity to produce 5'-deoxyadenosine, expressed as a turnover number, k_{obs} = 7.6 ± 0.6 h^{-1}. When co-expressed with VAP-33C, this activity increased slightly with k_{obs} = 13.1 ± 1.1 h^{-1}, whereas co-expression with NS5A did not change the specific activity of viperin, k_{obs} = 8.4 ± 0.7 h^{-1}. However, when viperin was co-expressed with both VAP-33C and NS5A, the specific activity of viperin was significantly lowered to k_{obs} = 4.0 ± 0.4 h^{-1}. ***[Figure 3.4(A), Appendix A.2]***. VAP-33 is a known interaction partner of viperin, therefore, it was not unexpected to see the increase in activity of viperin (about ~1.7- fold relative to single-expressed viperin) in its presence. However, a ~3.3-fold reduction in relative activity of viperin upon addition of NS5A (comparing viperin with VAP-33C alone and with both proteins) is quite remarkable; as this deactivation of radical SAM activity of viperin has not been previously observed.

Since the deletion of membrane –localizing domain of viperin abrogated its interaction with NS5A and VAP-33C, we conducted the radical SAM assay on HEK293T cell lysate

expressing viperin-ΔN50. As expected, viperin-ΔN50 did not show any change in its specific activity by its own (k_{obs} = 0.7 ± 0.04 h^{-1}), or when co-expressed with NS5A (k_{obs} = 0.5 ± 0.08 h^{-1}) and VAP-33C (k_{obs} = 0.7 ± 0.05 h^{-1}) or both (k_{obs} = 0.5 ± 0.06 h^{-1}) ***[Figure 3.4(b), Appendix A.2]***. However, viperin-ΔN50 showed a relatively slower turnover number than full length viperin, suggesting that disruption of the membrane associated structure of viperin actually have an impact on its catalytic efficiency.

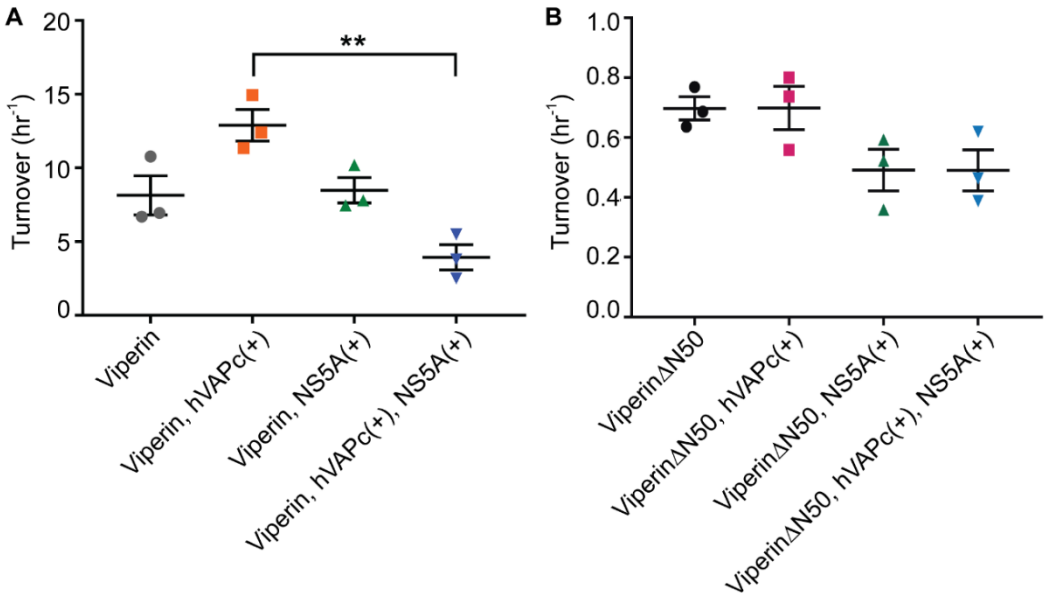

Figure 3.4: **Co-expression of NS5A and VAP-33C inhibits reductive SAM cleavage activity of Viperin in HEK293T cell-lysates.** (a) Activity of viperin in HEK293T cell-lysates co-expressing either NS5A and/or VAP-33C. The amount of 5'-dA produced was determined after 1 hour and normalized to the amount of viperin expressed in the cell extract; data presented as mean ± SEM n = 3. A significant (**p=0.0033) reduction in reductive SAM cleavage activity was observed when viperin was co-expressed with NS5A and VAP-33C. (b) Activity of viperin-ΔN50 in HEK293T cell-lysates co-expressing either NS5A and/or VAP-33C. The amount of 5'-dA produced was determined following the same method mentioned for viperin.

3.2.4 The membrane-localizing domains of viperin, NS5A and VAP-33 are required for complex formation To examine the changes in enzymatic activity in more detail we attempted to reconstitute the interactions between viperin, NS5A and VAP-33C using purified proteins obtained by over-expression in *E. coli.* However, this necessitated removing the membrane-binding domains of these proteins so that they could be produced in soluble form. A C-terminal His_6-tagged viperin lacking the first 50 membrane-associated amino acids (viperin-ΔN50), was purified under anaerobic conditions and the iron-sulfur cluster was reconstituted using procedures as described previously (21). NS5A lacking the first 39 amino acids comprising the membrane-binding amphipathic helix (NS5A-ΔN39), was expressed and purified as a fusion protein with maltose-binding protein (MBP), followed by TEV cleavage and size exclusion chromatography as described in the methods section. The N-terminal His_6-tagged VAP-33 construct lacking the last 20 amino acids of the trans-membrane domain on the C-terminus (VAP-33-ΔC20), was purchased commercially.

However, when the interactions between these three proteins we examined by immunoprecipitation using an anti-viperin antibody, no protein complexes could be detected ***[Figure 3.5(A)]***. Further experiments designed to detect the formation of protein complexes using the lysine-reactive covalent cross-linking reagent, bis(sulfosuccinimidyl)suberate (BS^3), similarly failed to detect any inter-protein crosslinking ***[Figure 3.5(B)]***. Consistent with this, and as observed in mammalian cell lysate radical SAM assay, the catalytic activity of viperin-ΔN50 was unaffected by the presence of NS5A-Δ39, or VAP-33-ΔC20. Under the conditions of the assay, k_{obs} for viperin-ΔN50 to produce 5'-deoxyadenosine was 4.1 ± 0.3 h^{-1}, with the lower activity

observed for the truncated construct being consistent with previous observations (20). When mixed with stoichiometric amounts of NS5A-ΔN39 or VAP-33-ΔC20, we measured rates of 2.7 ± 0.2 h^{-1} and 2.8 ± 0.1 h^{-1} respectively. Finally, combining all three proteins yielded a comparable result with k_{obs} = 2.8 ± 0.1 h^{-1} ***[Figure 3.6]***. These results suggest that removing the membrane-associated domains from these proteins effectively abolishes the ability of the proteins to form a complex.

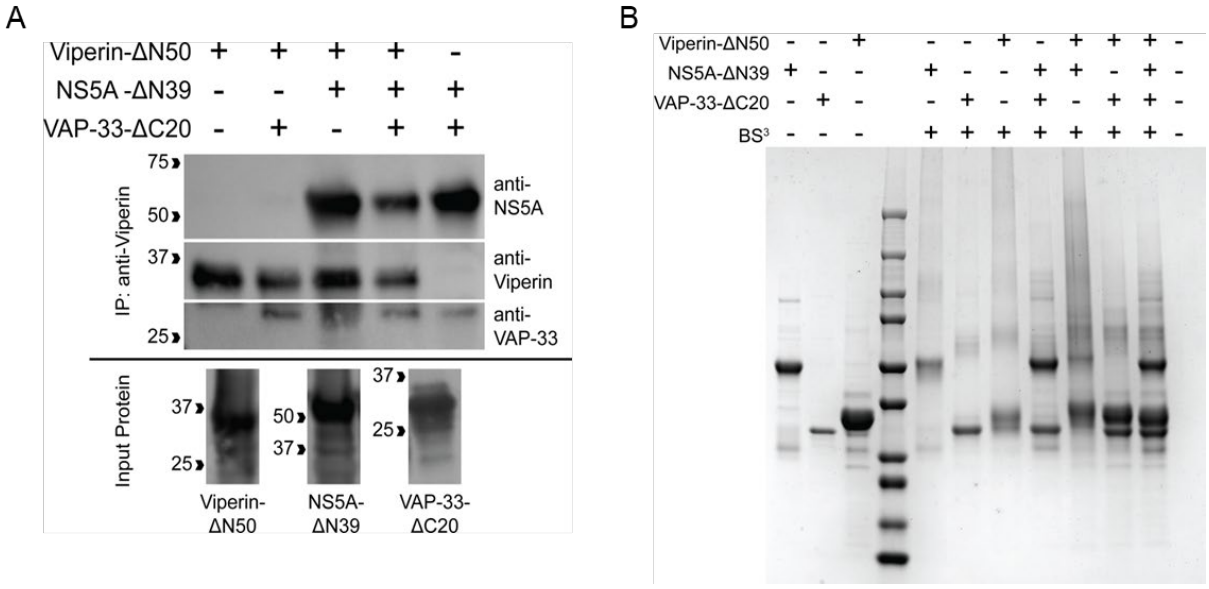

Figure 3.5: **Loss of interaction among recombinant NS5A-Δ39 and VAP-33-ΔC20 and viperin-ΔN50 (lacking the membrane associated sequence) *in vitro***: (A) Recombinant viperin was incubated with its possible prey protein recombinant NS5A-ΔN39 and VAP-33-ΔC20, followed by its immunoprecipitation, using anti-viperin antibody. The immunoprecipitated samples were immunoblotted with anti-his antibody to probe for the proteins. No specific interaction was observed between viperin and NS5A in presence and absence of VAP-33, suggesting that the membrane associated sequence of these interacting proteins are important for protein-complex formation. (B) Purified proteins were incubated with each other or by itself prior to the addition of chemical crosslinker BS^3. The three proteins individually formed dimers and showed non-specific oligomerization in the presence other partner protein. The protein complex among these three proteins was not observed.

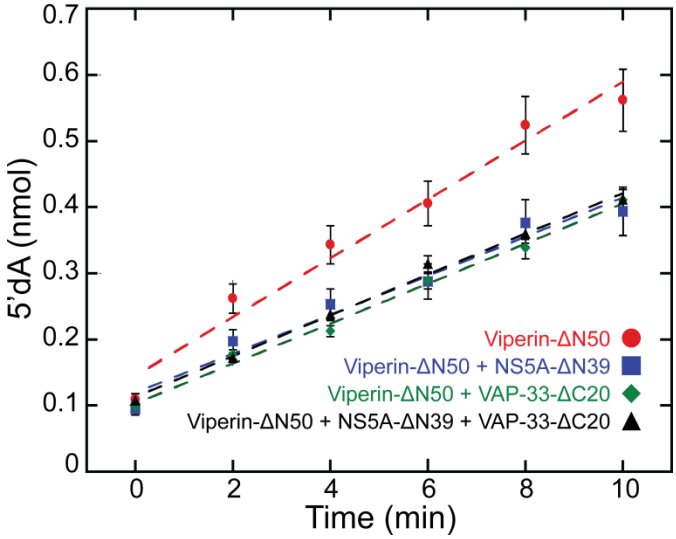

Figure 3.6: **Recombinant NS5A and VAP-33, lacking the membrane associated domain, did not change the reductive SAM cleavage activity of recombinant viperin *in vitro.*** Activity of purified viperin (viperin-ΔN50) was assessed by monitoring the rate of 5'-deoxyadenosine production. The turnover of 5'-deoxyadenosine by viperin was calculated from the linear fitting curve. Viperin showed the turnover of 4.1 ± 0.3 h^{-1} alone and 2.7 ± 0.2 h^{-1}, 2.8 ± 0.1 h^{-1}, 2.8 ± 0.1 h^{-1} when incubated with recombinant NS5A (NS5A-ΔN39), VAP-33 (VAP-33-ΔC20) or both, respectively. Overall, no significant change was observed in the activity of viperin, when combined with purified NS5A and VAP-33.

3.3 Discussion To date, most of the studies conducted on the antiviral activity of viperin against flaviviridae viruses have been focused on identifying physical interactions between viperin and viral core and non-structural proteins and correlating perturbations of these interactions with changes in viral replication or infectivity. Though the importance of domain-specific interactions between viperin and its target viral proteins has been shown through mutational analysis, no investigation of the effects of these interactions on the recently-revealed catalytic activity of viperin have been undertaken. The discovery that viperin catalyzes the formation of the antiviral nucleotide ddhCTP from CTP raises the question of whether the activity of viperin is modulated by the numerous proteins it

has been shown to interact with. Understanding the mechanism by which the synthesis of ddhCTP is viperin regulated by other proteins may open the way to the design of new antiviral therapeutics.

Non-structural protein NS5A from HCV is one of the viral proteins that interacts with viperin. NS5A interacts with the viral RNA-dependent RNA polymerase, NS5B, within the replication complex and is essential for genome replication (22,23). The reported interaction of NS5A and viperin could either be a mechanism by which viperin inhibits viral replication, or an adaptation of the virus to inhibit viperin. To investigate these possibilities we have examined the enzymatic activity of viperin in complex with NS5A and the cellular protein VAP-33, which is co-opted as part of the viral replication complex.

By reconstituting the complex between viperin, NS5A and VAP-33 in HEK293T cells, we were able to investigate how NS5A and VAP-33 alter viperin's catalytic activity. The most significant difference in viperin activity was apparent when comparing the complex of viperin and VAP-33 and the complex of viperin, VAP-33 and NS5A, with the addition of NS5A reducing the activity of viperin to produce 5'-deoxyadenosine by ~ 3 fold. This suggests that NS5A may have evolved, in part, to counteract the synthesis ddhCTP, thereby potentiating the infectivity HCV. The localization of these proteins to the ER membrane or lipid droplets appears to be crucial for the complex to form. This was evident from our *in vivo* radical SAM assay and *in vitro* studies using purified proteins, which necessitated the removal of the membrane associated domains from the proteins to facilitate their expression and purification. The N-terminal truncated viperin in HEK293T cells and the truncated proteins failed to associate with each other as evident from *in vitro* co-immunoprecipitation and chemical crosslinking experiments. This

observation is in agreement with previous studies on swine fever virus in which the N-terminal domain of viperin was shown to be crucial to co-localize with the replication complex at lipid droplets in HCV and interact with NS5A (24).

Although NS5A appears to inhibit viperin, our studies find support for the hypothesis that viperin exerts an antiviral effect by promoting the degradation of NS5A through the proteasomal degradation pathway. This presumably occurs by ubiquitination of NS5A. In this respect we note that viperin has been shown to activate the E3 ubiquitin ligase TRAF6 in the context of innate immune signalling. It seems plausible that viperin could act to recruit other E3 ligases that function in the endoplasmic reticulum-associated protein degradation (ERAD) pathway. Notably, this function of viperin does not appear to require the iron-sulfur cluster, as the viperinΔ3C variant was equally effective in reducing the cellular levels of NS5A. These findings are in accord with other studies showing that viperin promotes the degradation of non-structural protein NS3 in other flaviviruses through the proteasomal degradation pathway (8).

In conclusion, we find opposing effects on viral replication for the interaction between viperin and HCV NS5A ***[Figure 3.7].*** On one hand, NS5A appears to inhibit the activity of viperin to roduce 5'-deoxyadenosine, thereby reducing the potential for ddhCTP to interfere with replication of the viral genome. On the other hand, viperin appears to decrease the expression of NS5A to limit the formation of the replication complex. These studies point to complex interplay between viral proteins and cellular proteins they co-opt for their replication.

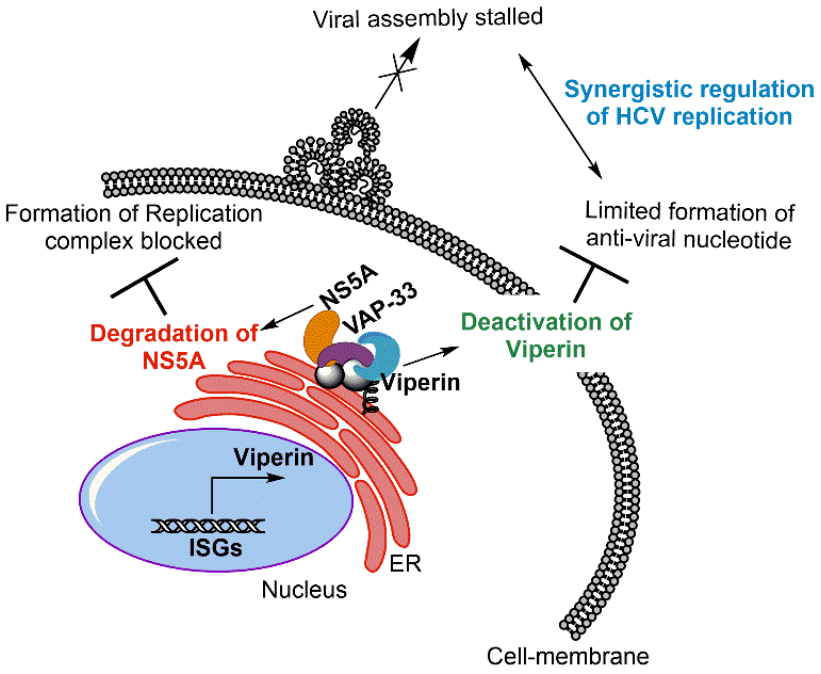

Figure 3.7: **Overview of the functional interactions between NS5A and viperin.** Viperin exerts anti-viral activity against Hepatitis C virus by promoting the degradation of NS5A in the replication complex. In contrast, NS5A reduces the catalytic activity of viperin, decreasing ddhCTP levels. Membrane localization of viperin, NS5A and proviral adaptor protein VAP-33 is crucial for the interactions between these proteins.

3.4 Experimental Procedure

Cell lines The HEK293T cell line was obtained from ATCC. *E. Coli* strain BL21(DE3) was acquired from New England Biolabs.

Plasmids Synthetic genes encoding human viperin (GenBank accession numbers AAL50053.1) were purchased from GenScript and sub-cloned into the pcDNA3.1(+) vector (Invitrogen). The primers for the pcDNA3.1(+)-viperin construct introduced an N-terminal 3x-FLAG tag (DYKDHDGDYKDHDIDYKDDDDK) and a Kozak consensus sequence (5'-GCCAAC-3') for downstream protein expression in eukaryotic cells. An additional construct of viperin, truncating the first 50 amino acids from the full length construct, was cloned into pcDNA3.1(+) between HindIII and EcoRI sites, using Gibson

Assembly (New England Biolabs). The point mutations described herein were introduced using the QuikChange site-directed mutagenesis kit (Agilent Technologies, Mississauga, ON). The gene encoding the NS5A (genotype 1b) protein was obtained from AddGene as the pCMV-Tag1-NS5A plasmid and was sub-cloned into the pcDNA3.1(+) vector with N-terminal Myc-tag (EQKLISEEDL) using Gibson Assembly. The VAP-33 construct (VAP-33C, VAP-33 residues 156-242) with N-terminal 3x-FLAG tag in pcDNA3.1(+) was a kind gift from professor Zhenghong Yuan, Fudan University, Shanghai, China(1).

For expression of vipeirn in E. coli, a codon-optimized gene encoding viperin in pET28a vector lacking the first 50 amino acids of the N-terminal amphipathic alpha helix (viperin-ΔN50, residues 50-361) was purchased from Genscript. Viperin-ΔN50 was sub-cloned into pRSFDuet-1 using the MfeI and HindIII restriction sites with a C-terminal 6x-His tag using Gibson Assembly. For expression of recombinant NS5A in E.Coli, a codon-optimized NS5A gene, lacking first 39 amino acids of N-terminal amphipathic helix (NS5A-ΔN39, residues 39-447), housed in pET52b(+) was purchased from Genscript. NS5A-ΔN39 was sub-cloned downstream of maltose binding protein (MBP) in pMALc5x between the NdeI and HindIII restriction sites, using Gibson Assembly. This added a tobacco etch virus (TEV)-cleavable MBP tag to the N-terminus with a non-cleavable 6x-His tag (encoded in the downstream primer) on the C-terminus of NS5A. The pMALc5x and pRSFDuet-1 vectors were obtained from GenScript. All sequences were confirmed at the University of Michigan Biomedical Research Core Facilities Advanced Genomics Core. Recombinant human VAP-33 protein (VAP-33-ΔC20, residues 1-227) with an N-terminal 6x-His tag was purchased from IBL America (catalog number IBATGP0471).

Cell Culture and Transfection The pcDNA3.1(+) encoded constructs were overexpressed in HEK293T cells (cultivated in DMEM supplemented with 10% FBS and 1% antibiotics) through transient transfection using polyethyleneimine transfecting agent. Co-transfection of two or more DNA constructs, allowing co-expression of viperin and its target proteins within the HEK293T cells, was performed using the same transfection protocol. Briefly, 20 µg of the respective plasmid DNA construct was mixed with polyethyleneimine at a 1:2 ratio, incubated at room temperature for 10 minutes, and then added to HEK293T cells at 50-60% confluence on a 100-mm dish. The transfected cells were then grown for up to 36 hours, gently pelleted, and stored at -80 °C until use.

Antibodies Rabbit polyclonal RSAD2/ viperin antibody (11833-1-AP) and mouse monoclonal viperin (MABF106) were obtained from Protein Tech and EMD Millipore respectively. Mouse monoclonal anti-NS5A antibody was purchased from Virogen (256-A). Goat anti-rabbit (170-6515) and anti-mouse (626520) Ig secondary antibodies were purchased from BioRad and Life Technologies respectively. Rabbit polyclonal GAPDH (10494-1-AP) was purchased from Proteintech and mouse monoclonal GAPDH antibody (6C5) was obtained from EMD Millipore. Mouse monoclonal anti-FLAG® M2 antibody (F1804) and 6x-His tag monoclonal antibody (MA1-135) were purchased from Sigma-Aldrich and ThermoFisher Scientific. Goat anti-mouse IgG (H+L)-HRP conjugate secondary antibody (catalog number 626520) and goat anti-rabbit IgG (H+L)-HRP conjugate secondary antibody (catalog number 1706515) were purchased from ThermoFisher Technologies and Bio-Rad, respectively.

Reagents S-(5′-Adenosyl)-L-methionine *p*-toluenesulfonate salt (≥80% (HPLC), 25 MG-A2408), 5’-deoxyadenosine (D1771-25MG) was purchased from Sigma-Aldrich. Sodium

Hydrosulfite (7775-14-6, 100g) and DTT (DSD11000-25 MG) were purchased from Fisher Scientific and DOT Scientific Inc. respectively. MG-132 10 mM solution in DMSO, 1 mL (A11043) was purchased from AdooQ Bioscience. Nucleotide substrates CTP (Cytidine 5'- triphosphate, disodium salt hydrate, 95%) were purchased from Acros Organics-226225000. Pierce™ protein A/G plus agarose resin and control agarose resin (Pierce classic IP kit 26146) were purchased from ThermoFisher Scientific. Transfection Grade Linear Polyethylenimine Hydrochloride (MW 40,000) (Catalog No. 24765-1) was purchased from Polysciences, Inc. for DNA transfection in HEK293T cells. For *in vitro* chemical crosslinking experiment, bis(sulfosuccinimidyl)suberate or (BS^3) (catalog number 21580) was purchased from Thermo Fisher Scientific.

Immunoblotting Cells were lysed in lysis buffer (20 mM Tris, pH 7.5, 1% NP-40, 150 mM NaCl, 1 mM EDTA, 1 mM Na_3VO_4, and 10 mM β-glycerophosphate with SIGMAFAST™ Protease Inhibitor Tablets, S8830; Sigma). Supernatants of lysates were collected and mixed with 4x Laemmli sample buffer and 2-mercaptoethanol. The total amount of protein in lysates was determined by DC™ Protein Assay (5000116, Biorad). The supernatants were separated on 10% SDS-PAGE gels and transferred to PVDF membrane. Membranes were blocked for 1 h at room temperature in TBST buffer (20 mM Tris, pH 7.5, 137 mM NaCl, and 0.1% Tween 20) containing 5% nonfat dry milk, followed by overnight incubation at 4°C in TBST buffer containing 5% nonfat dry milk and the appropriate primary antibody. Membranes were washed three times in TBST and then incubated for 1 h at room temperature with the secondary IgG-coupled horseradish peroxidase antibody. Primary antibodies were used at the following dilutions: viperin constructs - rabbit polyclonal diluted 1:2500, GAPDH - rabbit polyclonal diluted 1:5000,

NS5A - mouse monoclonal diluted 1:5000, anti-FLAG - mouse monoclonal diluted 1:3000, and anti-His - mouse monoclonal diluted 1:3000. Secondary antibodies were used at the following dilutions: goat anti-mouse diluted 1:5000 and goat anti-rabbit diluted 1:5000. The membranes were washed three times with TBST, and the signals were visualized with enhanced chemilluminescence reagent. Band intensities quantified using a Bio-Rad ChemiDoc Touch imaging system. Integrated density measurements were done using ImageJ software. Quantitative measurements of protein expression levels reported here represent the average of at least three independent biological replicates.

Co-immunoprecipitation Cells expressing viperin/ viperinΔ3C/viperin-ΔN50, NS5A and VAP-33C from 100 mm tissue culture plate were rinsed twice with ice-cold PBS, harvested in lysis buffer (20 mM Tris, pH 7.5, 1% NP-40, 150 mM NaCl, 1 mM EDTA, 1 mM Na_3VO_4, and 10 mM β-glycerophosphate with EDTA-free protease inhibitor cocktail from Sigma), incubated on ice for 20 minutes and briefly sonicated. Lysates were collected by centrifugation at 13,000 × g for 15 minutes at 4°C and pre-cleared with 20 µl Pierce Control Agarose Resin. Lysates containing bait protein viperin/ viperinΔ3C/TN50-vip were incubated with rabbit polyclonal anti-viperin antibody for 1 h at 4°C with end-to-end rotation. The protein-antibody-complexes were incubated with pre-equilibrated Pierce protein A/G plus agarose resin at the ratio of suspension to packed gel volume 4:1 for 1 h at 4°C by end-to-end rotation. Lysates containing prey protein NS5A and VAP-33C were incubated with bait proteins at 1:1:1 total protein ratio for 30 minutes at 4°C. Flow-through was collected by gravity flow using Pierce gravity –flow columns and washed three times with wash buffer (20 mM Tris, pH 7.5, 1% NP-40, 150 mM NaCl, 1 mM EDTA, 1 mM Na_3VO_4, and 10 mM β-glycerophosphate). Immuno-complexes were

eluted by boiling in 1x SDS-PAGE sample buffer and immunoblotted with the appropriate antibodies.

Immunofluorescence HEK293T cells were grown to 30% confluence on poly-L-lysine-coated coverslips and then transiently transfected with wild-type viperin, viperinΔ3C, NS5A and VAP-33C plasmid DNA. After 36 hours of transfection, the cells were fixed with 1% paraformaldehyde, permeabilized with 0.05% Triton X-100 dissolved in PBS, and washed three times with PBS containing 0.1% Tween20. The fixed cells were stained with the appropriate antibodies after blocking with 1% FBS in PBS. Primary antibodies were diluted in PBS containing, 1% FBS and stained with rabbit polyclonal anti-viperin (Proteintech) and mouse monoclonal anti-NS5A (Virogen) antibodies at 1:500 dilution. After incubation at 4°C overnight, the coverslips were washed with PBS containing 0.1% Tween20 and treated with Alexa Fluor 647-conjugated goat anti-mouse (Life Technologies) and Alexa Fluor 488-conjugated goat anti-rabbit (Abcam) secondary antibodies at a dilution of 1:500 at room temperature for 2 hours. The coverslips were washed three times with PBS containing 0.1% Tween20 and mounted in ProLong™ Gold Antifade Mountant (Molecular Probes). Images were acquired with an Olympus IX81 microscope with 60x objective. The images were processed with ImageJ software.

Reductive SAM assay of viperin HEK293T cells transfected with viperin or viperinΔN50, and/or NS5A and VAP-33C were harvested from one 100-mm diameter tissue culture plate each, re-suspended in 500 µl of anoxic Tris-buffered saline (50 mM Tris-Cl, pH 7.6, 150 mM NaCl) containing 1% Triton X-100, sonicated within an anaerobic glovebox (Coy Chamber), and centrifuged at 14,000 g for 10 min. Dithiothreitol (DTT; 5 mM) and dithionite (5 mM) were added to the cell lysate together with CTP (300 µM). The assay

mixture was incubated at room temperature for 30 min prior to starting the reaction by the addition of SAM (200 μM). The assay was incubated for 60 min at room temperature, after which the reaction stopped by heating at 95 °C for 10 min. The solution was chilled to 4 °C, and the precipitated proteins were removed by centrifugation at 14,000 rpm for 25 min. The supernatant was then extracted with acetonitrile. Samples were analysed in triplicate by UPLC-tandem mass spectrometry (25).

NS5A-ΔN39 in vitro expression and purification MBP_NS5A-ΔN39 was transformed into BL21(DE3) chemically competent cells and plated on ampicillin (AMP) supplemented LB-agar plates. The following day, a single colony was picked and added to 2-25mL fractions of AMP-supplemented LB media and shaken overnight at 37°C. The seed cultures were added to 2L of 2xYT media supplemented with AMP and 1% glycerol. The culture was shaken for approximately 3 hours, until mid-log was achieved ($O.D._{600} \approx 0.8$), then cold shocked by incubation at 4°C for one hour. 0.5 mM IPTG was added and the culture was grown at 16°C overnight. The cells were centrifuged and the pellet was harvested and stored at -80°C.

The cell pellet was re-suspended at a ratio of 30 mL/ 2L culture in NS5A lysis buffer (26)(50 mM Tris pH 8.0, 200 mM NaCl, 10 mM imidazole, 5% glycerol, 2 mM L-Cysteine – HCl, 2 mM 2-mercaptoethanol) supplemented with 1 cOmplete™ EDTA-free protease inhibitor cocktail tablet. The cell suspension was lysed on ice via sonication at amplitude 8 in 20 second intervals for a total process time of 4 minutes. The lysate was centrifuged for 45 min at 12,000 RPM. 1 mL of 100% Ni-NTA resin (pre-equilibrated with lysis buffer) was added to the supernatant and incubated at 4°C for 2 hr. The mixture was added to a 20 mL fritted column and the flow-through was collected and set aside. The column was

washed with 30 column volumes of lysis buffer supplemented with 25 mM imidazole. The protein was eluted from the Ni-NTA using three - 10 column volume washes of lysis buffer supplemented with 100, 200, or 300 mM imidazole. The lysate, pellet, supernatant, flow through, wash, and all elutions were analysed via reducing sodium dodecyl sulfate – polyacrylamide gel electrophoresis (SDS-PAGE).

NS5A-ΔN39 TEV cleavage and size exclusion chromatography Once presence and purity of the protein was confirmed, the appropriate elution fraction was subjected to TEV cleavage. The reaction contained approximately 10-15 mg of pure MBP_NS5A-ΔN39, 50 µg TEV, and 3 mM DTT, was carried out overnight (18-20 hours) at 4°C, and the cleaved protein was purified over a pre-packed 5 mL MBP-trap column (from GE). The reaction was circulated over the column via peristaltic pump at 0.5 mL/min three times and the flow through, which contained cleaved NS5A, was collected after a fourth pass. The column was washed with 10 column volumes of NS5A storage buffer (50 mM Tris pH 8.0, 150 mM NaCl, 10% glycerol). Any un-cleaved protein was eluted with 5 column volumes of NS5A storage buffer supplemented with 10 mM maltose.

Next, a size exclusion step was added in order to remove any soluble aggregate and additional protein contaminants not removed by the post-TEV cleavage purification. Cleaved NS5A-ΔN39 was concentrated down to approximately 3 mL and injected onto a pre-equilibrated prep-grade Superdex-200 size exclusion column. The column was washed with NS5A storage buffer without glycerol at 1 mL/min. Elution fractions were compared against a 15-600 kDa protein standard (Millipore Sigma) and analysed via SDS-PAGE for purity and presence of soluble, cleaved NS5A-ΔN39. These fractions were concentrated and buffer exchanged using a PD-10 desalting column into NS5A

storage buffer. This was concentrated further to 500 µL (final concentration ~ 38 µM), aliquoted, and flash frozen for future use. Protein concentration was estimated via Abs_{280} and confirmed with gel quantification.

Viperin-ΔN50 in vitro expression and purification Viperin-ΔN50 was expressed in the same manner as described above with small differences. pRSFDuet-1 is kanamycin (KAN) resistant, so all antibiotic selection steps were done with KAN. Once the culture entered mid-log phase, it was equilibrated to 18°C after which 0.2 mM $Na_2S \cdot 9H_20$ was added. After 20 additional minutes of equilibration, 0.2 mM $FeCl_3$ and 0.1 mM IPTG were added and the culture was shaken overnight at 16°C. Cells were harvested by centrifugation the following day and stored at -80°C.

The purification was carried out in the same manner as above, with small differences. All purification steps were done in an anaerobic environment (Coy chamber) using anoxic (nitrogen flushed) buffers (viperin-ΔN50 lysis buffer contained 50 mM HEPES pH 7.5, 300mM NaCl, and 5% glycerol). Once the lysate had been cleared via centrifugation it was added to a pre-packed 5 mL His-Trap column (from GE) via peristaltic pump. The solution was flowed over the column 3x at 0.5 mL/min and the flow through was collected on the fourth pass. The column was washed with 10 column volumes of viperin-ΔN50 lysis buffer supplemented with 50mM imidazole. viperin-ΔN50 was eluted with three 15 mL washes of lysis buffer supplemented with 200 mM imidazole. Protein presence and purity was analysed in the same manner as above. Once confirmed, the appropriate elution fraction was concentrated, buffer exchanged into viperin storage buffer (50mM Tris pH 8.0, 150 mM NaCl, 10% glycerol) with a PD-10 desalting column, and stored on ice before reconstitution.

Reconstitution of viperin-ΔN50 [4Fe-4S] cluster The reconstitution of the [4Fe-4S] cluster in the purified viperin-ΔN50 was performed in an anaerobic environment (Coy chamber, O_2 levels kept below 20 ppm)(21). Purified protein was incubated with 5 mM DTT for 20 min on cold beads. The stock solution of 0.1 M $FeCl_3$ and 0.1 M Na_2S was added drop-wise, incubating for 10 min after each addition until the protein turned dark brown in color. A 10 mL PD-10 desalting column was equilibrated with 2 column volumes of viperin storage buffer. The reconstituted protein (2.5 mL) was then added to the equilibrated PD-10 column and eluted with 3.5 mL of viperin storage buffer. The elution was then concentrated again using vivapore concentrators to the final volume of 1 mL. The concentrated protein (final concentration~ 68 μM) was aliquoted, flash frozen in liquid nitrogen, and stored at -80°C.

Co-immunoprecipitation of recombinant NS5A and VAP-33 using recombinant viperin All steps were performed inside anaerobic Coy chamber. Recombinant human viperin-ΔN50, purified from BL21 (DE3) *E. Coli*, was incubated with rabbit polyclonal anti-viperin antibody for 1h at 4°C, at final concentration 0.5 μM, in the presence of dithiothritol (5 mM) and CTP (300 μM). The protein-antibody complex was incubated with pre-equilibrated protein A/G beads (pre-blocked with 2mg/ml Bovine Serum albumin protein overnight at 4°C) for 1h at 4°C. Recombinant prey proteins NS5A-ΔN39 and VAP-33-ΔC20 were incubated with viperin-antibody-bead-complex at a final concentration of 1μM for 30 minutes at 4°C. Flow-through was collected using Pierce gravity columns and washed three times with 50 mM Tris, pH 7.5, 150 mM NaCl, 10% glycerol, 1.0% Tween-20. Immuno-complexes were eluted by boiling in 1x SDS-PAGE sample buffer outside Coy chamber and immunoblotted with appropriate antibodies.

In vitro SAM cleavage assay The reaction containing purified 5 uM viperin-ΔN50, 7.5 uM NS5A-ΔN39 or VAP-33-ΔC20 or both in 50 mM tris-HCl pH 8.0, 150 mM NaCl, 10% glycerol, 5 mM DTT, 100 uM L-tryptophan (internal standard), and 300 uM CTP were incubated on cold beads for 2 hours under anaerobic conditions to allow for complex formation. The reactions were then incubated at 37°C for 5 minutes after the addition of 5 mM dithionite. Finally, 200 uM SAM was added to each reaction and 20 uL aliquots were taken at various time intervals (0, 2, 4, 6, 8, and 10 minutes). Each sample was quenched with 20 uL of 50 mM H_2SO_4 solution. The samples were centrifuged at 14,000 rpm for 10 minutes to precipitate protein before loading it on to a Vydac 201TP 10 µm C18 column (250 X 4.6 mm, 10 µm particle size). Buffer A was 0.01% TFA in DI water and buffer B was 0.01% TFA in acetonitrile. The flow rate was 1.0 ml/min and the following gradient was applied: 0% B for 0.01 minutes, 0-5% B from 0.01-5.01 minutes, 5% B from 5.01-5.31 minutes, 5-75% B from 5.31-25.31 minutes, 75% B from 25.31-26.31 minutes, 75-100% B from 26.31-27.01 minutes, 100% B from 27.01-32.01 minutes, 100-0% B from 32.01-32.31 minutes, 0% B from 32.31-36.31 minutes. The internal standard peak (L-tryptophan) was observed at 13.25 minutes and the 5'deoxyadenosine (5'dA) peak was observed at 10.10 minutes. The peaks were integrated using LCSolution software.

In vitro chemical crosslinking To determine presence of a TN50-NS5A-VAP33 protein complex, chemical crosslinking via bis(sulfosuccinimidyl)suberate (BS^3) was employed. This would allow for covalent tethering of nearby proteins with an 8-carbon spacer via exposed lysine residues using N-hydroxysulfosuccinimide (NHS) ester chemistry. Purified TN50, NS5A, and VAP33 were buffer exchanged in to crosslinking buffer (50 mM HEPES pH 7.5, 150 mM NaCl) and used at 10 uM (each) with a 35x molar excess of BS^3

reagent. The proteins were incubated at 4°C for one hour before the addition of crosslinker. The reaction was allowed to proceed for two hours at 4°C before they were quenched with 100mM Tris pH 7.5. The reactions were analyzed via SDS-PAGE and Western Blot.

References

1. Wang, S., Wu, X., Pan, T., Song, W., Wang, Y., Zhang, F., and Yuan, Z. (2012) Viperin inhibits hepatitis C virus replication by interfering with binding of NS5A to host protein hVAP-33. *J. Gen. Virol.* **93**, 83-92
2. Jiang, D., Guo, H., Xu, C., Chang, J., Gu, B., Wang, L., Block, T. M., and Guo, J.-T. (2008) Identification of Three Interferon-Inducible Cellular Enzymes That Inhibit the Replication of Hepatitis C Virus. *J. Virol.* **82**, 1665-1678
3. Helbig, K. J., Eyre, N. S., Yip, E., Narayana, S., Li, K., Fiches, G., McCartney, E. M., Jangra, R. K., Lemon, S. M., and Beard, M. R. (2011) The antiviral protein viperin inhibits hepatitis C virus replication via interaction with nonstructural protein 5A. *Hepatology* **54**, 1506-1517
4. Jiang, D., Weidner, J. M., Qing, M., Pan, X.-B., Guo, H., Xu, C., Zhang, X., Birk, A., Chang, J., Shi, P.-Y., Block, T. M., and Guo, J.-T. (2010) Identification of Five Interferon-Induced Cellular Proteins That Inhibit West Nile Virus and Dengue Virus Infections. *J. Virol.* **84**, 8332-8341
5. Helbig, K. J., Carr, J. M., Calvert, J. K., Wati, S., Clarke, J. N., Eyre, N. S., Narayana, S. K., Fiches, G. N., McCartney, E. M., and Beard, M. R. (2013) Viperin Is Induced following Dengue Virus Type-2 (DENV-2) Infection and Has Anti-viral Actions Requiring the C-terminal End of Viperin. *PLoS Negl. Trop. Dis.* **7**, e2178
6. Vonderstein, K., Nilsson, E., Hubel, P., Nygård Skalman, L., Upadhyay, A., Pasto, J., Pichlmair, A., Lundmark, R., and Överby, A. K. (2018) Viperin Targets Flavivirus Virulence by Inducing Assembly of Noninfectious Capsid Particles. *J. Virol.* **92**, e01751-01717
7. Upadhyay, A. S., Vonderstein, K., Pichlmair, A., Stehling, O., Bennett, K. L., Dobler, G., Guo, J.-T., Superti-Furga, G., Lill, R., Överby, A. K., and Weber, F. (2014) Viperin is an iron-sulfur protein that inhibits genome synthesis of tick-borne encephalitis virus via radical SAM domain activity. *Cell. Microbiol.* **16**, 834-848
8. Panayiotou, C., Lindqvist, R., Kurhade, C., Vonderstein, K., Pasto, J., Edlund, K., Upadhyay, A. S., and Överby, A. K. (2018) Viperin Restricts Zika Virus and Tick-Borne Encephalitis Virus Replication by Targeting NS3 for Proteasomal Degradation. *J. Virol.* **92**, e02054-02017
9. Vanwalscappel, B., Tada, T., and Landau, N. R. (2018) Toll-like receptor agonist R848 blocks Zika virus replication by inducing the antiviral protein viperin. *Virology* **522**, 199-208
10. Van der Hoek, K. H., Eyre, N. S., Shue, B., Khantisitthiporn, O., Glab-Ampi, K., Carr, J. M., Gartner, M. J., Jolly, L. A., Thomas, P. Q., Adikusuma, F., Jankovic-

Karasoulos, T., Roberts, C. T., Helbig, K. J., and Beard, M. R. (2017) Viperin is an important host restriction factor in control of Zika virus infection. *Sci. Rep.* **7**, 4475
11. Richard, L., and K., Ö. A. (2018) The Role of Viperin in Antiflavivirus Responses. *DNA Cell Biol.* **37**, 725-730
12. Chen, S., Wu, Z., Wang, M., and Cheng, A. (2017) Innate Immune Evasion Mediated by Flaviviridae Non-Structural Proteins. *Viruses* **9**, 291
13. Cedillo-Barrón, L., García-Cordero, J., Shrivastava, G., Carrillo-Halfon, S., León-Juárez, M., Bustos Arriaga, J., León Valenzuela, P., and Gutiérrez Castañeda, B. (2018) The Role of Flaviviral Proteins in the Induction of Innate Immunity. in *Virus Protein and Nucleoprotein Complexes* (Harris, J. R., and Bhella, D. eds.), Springer Singapore, Singapore. pp 407-442
14. Reyes, G. R. (2002) The nonstructural NS5A protein of hepatitis C virus: An expanding, multifunctional role in enhancing hepatitis C virus pathogenesis. *J. Biomed. Sci.* **9**, 187-197
15. Gizzi, A. S., Grove, T. L., Arnold, J. J., Jose, J., Jangra, R. K., Garforth, S. J., Du, Q., Cahill, S. M., Dulyaninova, N. G., Love, J. D., Chandran, K., Bresnick, A. R., Cameron, C. E., and Almo, S. C. (2018) A naturally occurring antiviral ribonucleotide encoded by the human genome. *Nature* **558**, 610-614
16. Wyles, J. P., McMaster, C. R., and Ridgway, N. D. (2002) Vesicle-associated Membrane Protein-associated Protein-A (VAP-A) Interacts with the Oxysterol-binding Protein to Modify Export from the Endoplasmic Reticulum. *J. Biol. Chem.* **277**, 29908-29918
17. Makins, C., Ghosh, S., Román-Meléndez, G. D., Malec, P. A., Kennedy, R. T., and Marsh, E. N. G. (2016) Does Viperin Function as a Radical S-adenosyl-L-methionine-dependent Enzyme in Regulating Farnesylpyrophosphate Synthase Expression and Activity? *J. Biol. Chem.*
18. Kriegs, M., Bürckstümmer, T., Himmelsbach, K., Bruns, M., Frelin, L., Ahlén, G., Sällberg, M., and Hildt, E. (2009) The hepatitis C virus non-structural NS5A protein impairs both the innate and adaptive hepatic immune response in vivo. *The Journal of biological chemistry* **284**, 28343-28351
19. Gale, M., Jr., Blakely, C. M., Kwieciszewski, B., Tan, S. L., Dossett, M., Tang, N. M., Korth, M. J., Polyak, S. J., Gretch, D. R., and Katze, M. G. (1998) Control of PKR protein kinase by hepatitis C virus nonstructural 5A protein: molecular mechanisms of kinase regulation. *Mol. Cell. Biol.* **18**, 5208-5218
20. Dumbrepatil, A. B., Ghosh, S., Zegalia, K. A., Malec, P. A., Hoff, J. D., Kennedy, R. T., and Marsh, E. N. G. (2019) Viperin interacts with the kinase IRAK1 and the E3 ubiquitin ligase TRAF6, coupling innate immune signaling to antiviral ribonucleotide synthesis. *J. Biol. Chem.*
21. Duschene, K. S., and Broderick, J. B. (2010) The antiviral protein viperin is a radical SAM enzyme. *FEBS Lett.* **584**, 1263-1267
22. Shimakami, T., Hijikata, M., Luo, H., Ma, Y. Y., Kaneko, S., Shimotohno, K., and Murakami, S. (2004) Effect of Interaction between Hepatitis C Virus NS5A and NS5B on Hepatitis C Virus RNA Replication with the Hepatitis C Virus Replicon. *J. Virol.* **78**, 2738-2748
23. Shirota, Y., Luo, H., Qin, W., Kaneko, S., Yamashita, T., Kobayashi, K., and Murakami, S. (2002) Hepatitis C Virus (HCV) NS5A Binds RNA-dependent RNA

Polymerase (RdRP) NS5B and Modulates RNA-dependent RNA Polymerase Activity. *J. Biol. Chem.* **277**, 11149-11155
24. Xu, C., Feng, L., Chen, P., Li, A., Guo, S., Jiao, X., Zhang, C., Zhao, Y., Jin, X., Zhong, K., Guo, Y., Zhu, H., Han, L., Yang, G., Li, H., and Wang, Y. Viperin inhibits classical swine fever virus replication by interacting with viral nonstructural 5A protein. *J. Med. Virol.* **0**
25. Wong, J.-M. T., Malec, P. A., Mabrouk, O. S., Ro, J., Dus, M., and Kennedy, R. T. (2016) Benzoyl chloride derivatization with liquid chromatography-mass spectrometry for targeted metabolomics of neurochemicals in biological samples. *Journal of chromatography. A* **1446**, 78-90
26. Foster, T. L., Belyaeva, T., Stonehouse, N. J., Pearson, A. R., and Harris, M. (2010) All three domains of the hepatitis C virus nonstructural NS5A protein contribute to RNA binding. *J. Virol.* **84**, 9267-9277

Chapter 4

Activation of the Radical SAM Activity of Viperin through the Interplay of Innate-immune Signalling Proteins Kinase IRAK1 and Ubiquitin Ligase TRAF6

(Work in this chapter is published in *J. Biol. Chem*. (2019), 294, 6888-6898)

4.1 Introduction In addition to exerting antiviral activity against a diverse range of pathogens, viperin has also been found to directly modulate innate immunity signalling (1,2). Stimulation of T cells from viperin knockout mice resulted in a decrease in inflammatory cytokine production, ultimately affecting the viral DNA binding activity of NF-kB signaling. This indicates that viperin plays a role in T cell activation (3). Viperin was also found to be involved in the Toll-like receptor signalling pathways (TLR7/9) to upregulate interferons, thereby, promoting the host defense response (4). As a part of innate immunity, Toll-like receptor 7 (TLR7) and TLR9 are among various pattern recognition receptors that sense viral nucleic acids and induce the production of type I interferons by plasmacytoid dendritic cells (pDCs) to protect the host from viral infection(5-7). The TLR7/9 signaling pathways were stimulated in these cells with either dsRNA or lipopolysaccharides to induce viperin expression (2,4,8). As a component of this pathway, viperin was shown to interact with two signal mediator proteins: interleukin-1 receptor-associated kinase (IRAK1) and the E3 ubiquitin ligase, TRAF6. Viperin recruits IRAK1 and TRAF6 to lipid bodies and stimulates the K63-linked poly-ubiquitination of IRAK1 by the E3 ubiquitin ligase, TRAF6 (1,9). K63-linked poly-

ubiquitination, in turn, activates IRAK1 to phosphorylate interferon regulatory factor 7 (IRF7), causing IRF7 to migrate to the nucleus where it activates transcription of type 1 interferons (9,10) ***[Figure. 4.1].***

Another adaptor protein, mitochondrial antiviral signaling protein (MAVS), involved in cytosolic RNA receptors RIG-I (retinoic acid-inducible gene I) and MDA5 (melanoma differentiation-associated protein 5), was also identified as a potential interacting partner of viperin (11,12). As a result of this interaction, viperin was observed to suppress the MAVS-dependent signaling pathway and act as a negative effector in IFNβ production.

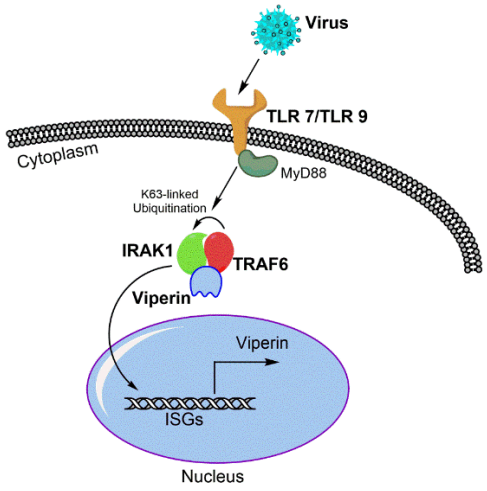

Figure 4.1: **Interaction of viperin with kinase IRAK1 and E3 Ubiquitin ligase TRAF6 in Toll-like receptor 7/9 pathway**. Viperin facilitates the K63-linked ubiquitination of IRAK1 by TRAF6, thereby promoting IRAK1 activation.

As viperin functions differently in controlling various signaling pathways, it proved difficult to provide a possible explanation for the molecular mechanism of viperin. Progress was made by the finding that the enzymatic activity of viperin involves producing the antiviral nucleotide ddhCTP from CTP (13). We anticipated that its enzymatic activity might be regulated by interactions with its partner proteins. To examine this possibility, we

reconstituted the interactions between viperin, IRAK1, and TRAF6 that lead to poly-ubiquitination of IRAK1 in HEK293T cells. Our experiments demonstrate that IRAK1 and TRAF6 activate viperin towards reductive cleavage of SAM and the production of ddhCTP. At the same time, viperin stimulates the poly-ubiquitination of IRAK1 by TRAF6, in a manner that is SAM-dependent. The synergistic activation of these enzymes provides a mechanism to couple innate immune signaling to the production of antiviral ribonucleotides. The work was described this chapter was done collaboratively with Arti Dumbrepatil and published in *J. Biol. Chem*. (2019) , **294,** 6888-6898.

4.2 Results As full length viperin was unable to be expressed in *E. coli*, we decided to study the interactions between viperin, TRAF6 and IRAK1 in a cellular context. Expression of viperin, IRAK1 and TRAF6 in eukaryotic cells allowed viperin to localize to the endoplasmic-reticulum membrane and lipid droplets, and allowed the effect of viperin on the poly-ubiquitination of IRAK1 by TRAF6 to be examined.

4.2.1 IRAK1 mediates interactions between Viperin and TRAF6. To examine whether viperin, IRAK1 and TRAF6 form a complex, immunoprecipitation experiments were conducted using either FLAG-tagged viperin as bait and HA-tagged TRAF6 and Myc-tagged IRAK1 as prey proteins. Immunoprecipitation experiments were conducted on HEK 293T cells transfected with all three proteins and with extracts of cells singly transfected with viperin, IRAK1 or TRAF6. For singly transfected cell extracts these were combined in a 1:1:1 ratio and incubated for 30 min at 4^{o} C before being subjected to immunoprecipitation. The bait protein was then immunoprecipitated with the appropriate antibody. Both sets of experiments yielded similar results ***[Figure. 4.2]***.

With viperin as bait, IRAK1 co-precipitated independently of TRAF6; however, TRAF6 only co-precipitated in presence of both viperin and IRAK1 ***[Figure. 4.2]***. These observations imply that IRAK1 binds to both TRAF6 and viperin to mediate complex formation, whereas viperin and TRAF6 do not independently associate with each other. Similar results were obtained when viperinΔ3C was used as the bait protein, which suggests that the iron-sulfur cluster is not crucial for IRAK1 to bind viperin.

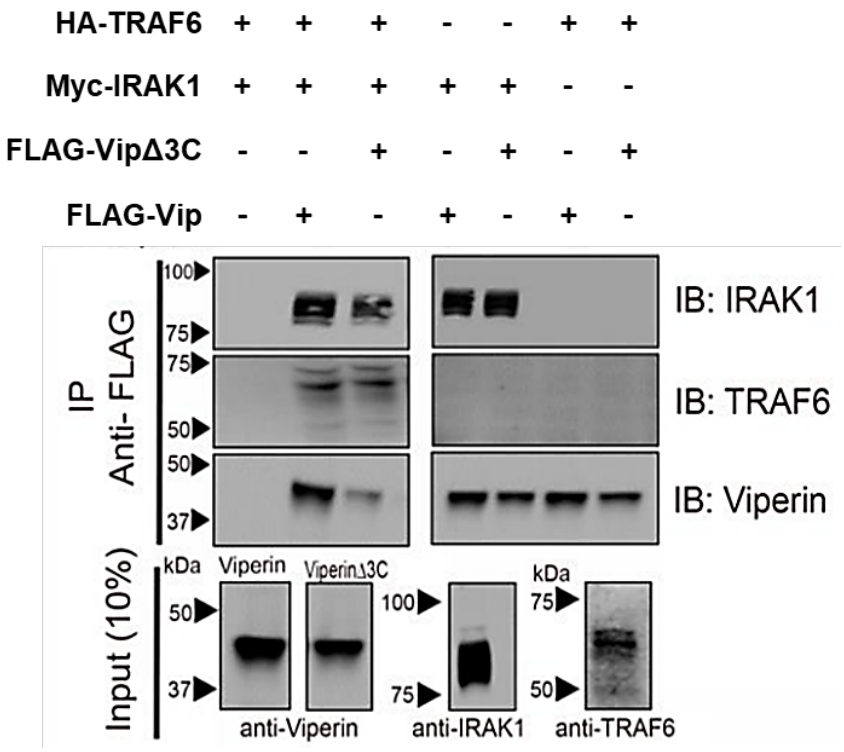

Figure 4.2: **IRAK1 mediates formation of the complex between viperin, IRAK1 and TRAF6.** Immuno-tagged genes were expressed into HEK 293T cells and viperin was immunoprecipitated with anti-FLAG antibody after incubating with IRAK1 or TRAF6 or both. Immunoblotting against IRAK1 and TRAF6 showed the complex formation among these proteins. Mutations in the radical SAM domain (viperinΔ3C) do not affect ability of viperin to interact with IRAK1. The figure is reproduced from *J.Biol. Chem*. (2019) **294**, 6888-6898.

The N-terminal domain of viperin serves to localize the enzyme to the cytoplasmic face of lipid droplets and the ER (14), whereas TRAF6 and IRAK1 are cytosolic enzymes (15).

Consistent with the immunoprecipitation results, we observed that co-expression of viperin with TRAF6 and IRAK1 caused these enzymes to re-localize to the ER membrane as determined by immuno-fluorescence microscopy of fixed and immuno-stained cells ***[Figure. 4.3].***

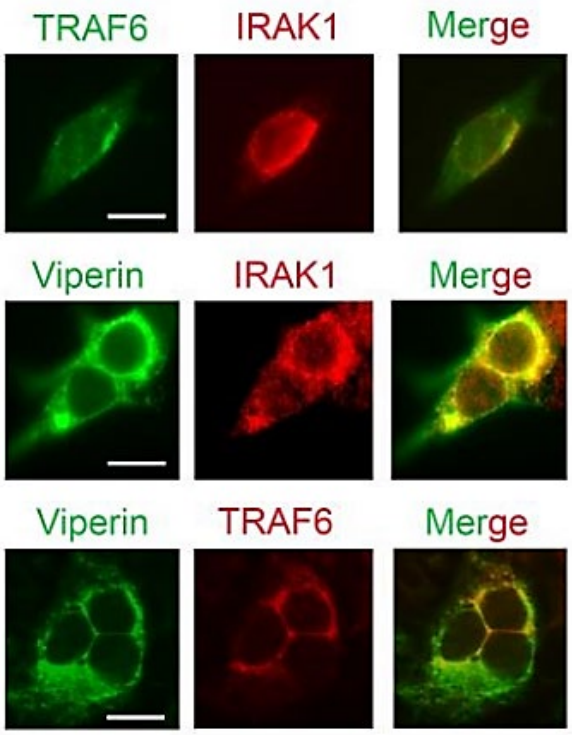

Figure 4.3: **Relocalization of IRAK1 and TRAF6 to the endoplasmic reticulum by viperin.** HEK293T cells were transfected with viperin, IRAK1 and TRAF6 and immune-stained for the proteins. *Top panels:* cells co-transfected with IRAK1 (red) and TRAF6 (green) show diffuse expression throughout the cell. *Middle panels:* cells were co-transfected with IRAK1, TRAF6 and viperin. Staining for viperin (green) and IRAK1 (red) demonstrates co-localization (yellow) of viperin and IRAK1. *Bottom panels:* cells were co-transfected with IRAK1, TRAF6 and viperin. Staining for viperin (green) and TRAF6 (red) demonstrates co-localization (yellow) of viperin and TRAF6. Co-expression of IRAK with viperin appears to result in IRAK1 also forming punctate structures that do not co-localize (middle panels). Scale bar = 5 μm. The figure is reproduced from *J.Biol. Chem*. (2019) **294**, 6888-6898.

4.2.2 IRAK1 and TRAF6 synergistically activate viperin. As enzymes in signaling pathways typically function by activating or repressing the activity of other enzymes, the involvement of viperin in the TLR7/9 signaling pathways suggested that the enzymatic

activity of viperin may be regulated by IRAK1 and/or TRAF6. Therefore, as viperin was confirmed to form a complex with these Toll-like receptor signalling enzymes, we examined the effects of IRAK1 and TRAF6 co-expression on the enzymatic activity of viperin to produce 5'-deoxyadenosine. Cell extracts were prepared under anaerobic conditions (due to the *in vitro* oxygen-sensitivity of radical SAM enzymes) from HEK 293T cells co-transfected with viperin, IRAK1 and TRAF6. The enzymatic activity of viperin was quantified by measuring the formation of 5'-dA, and the specific activity was measured based on the amount of viperin present in the cell extracts, quantified by immunoblotting ***[Fig. 4.4(A)].***

When assayed in the absence of exogenous CTP, cell extracts expressing only viperin exhibited low levels of activity to produce 5'-deoxyadenosine, with an apparent turnover number, k_{obs} = 0.94 ± 0.05 h^{-1} ***[Figure. 4(B), Appendix A.3]***. This basal activity is likely due to low concentrations endogenous CTP in the cell extract. Negligible amounts of 5'-dA were formed in cell extracts lacking viperin or in cells expressing viperinΔ3C. Surprisingly, when the co-substrate CTP (300 μM) was added to the assay, only a modest 2.4-fold increase in activity (k_{obs} = 2.38 ± 0.05 h^{-1}) was observed. In contrast, when lysates prepared from cells co-expressing IRAK1 and TRAF6 were assayed, viperin activity with CTP as substrate increased ~10-fold ***(Fig. 4.4B)***. Under these conditions k_{obs} = 21.4 ± 1.6 h^{-1}, which is 2-fold higher than the apparent k_{cat} reported for truncated rat viperin (13). In the absence of exogenous CTP, the basal level of viperin activity was increased 4-fold (k_{obs} = 4.30 ± 0.21 h^{-1}) by co-expression with IRAK1 and TRAF6, consistent with these proteins activating viperin. Expression of viperin with IRAK1 alone resulted in lower levels of activation, whereas co-expression of viperin with TRAF6 alone

had no effect on viperin activity. These results suggested that IRAK1 and TRAF6 synergistically activate viperin to produce 5'-deoxyadenosine, and concommitently formation of ddhCTP from CTP, through radical SAM cleavage activity.

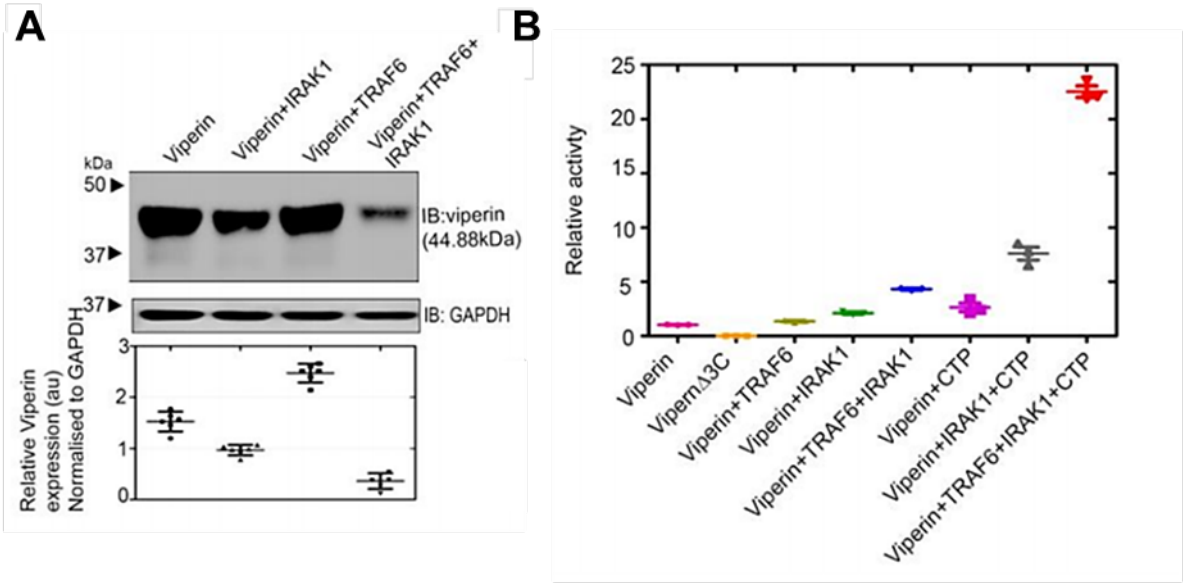

Figure 4.4: **IRAK1 and TRAF6 synergistically activate viperin.** Reductive SAM cleaving activity of viperin, expressing in HEK293T cells viperin with IRAK1 and TRAF6, was measured by monitoring the amount of 5'-deoxyadenosine produced over 1 h. *(A)* Immunoblot showing the expression level of viperin, co-expressed with IRAK1 and/or TRAF6. The relative expression levels were determined by normalizing to GAPDH, used as the internal loading control. *(B)* The amount of 5'-dA formed in 1 h, normalized for the amount of viperin present in the cell extracts, is plotted relative to the viperin-only sample = 1.0. The data represent the mean and standard deviation of three independent biological replicates with three technical replicates of each measurement. The figure is reproduced from *J.Biol. Chem*. (2019) **294**, 6888-6898.

4.2.3 Ubiquitination of IRAK1 requires viperin. Given that IRAK1 and TRAF6 appeared to activate viperin towards the production of ddhCTP, we were interested to know whether, conversely, viperin stimulated the ubiquitination of IRAK1 by TRAF6.

To identify the ubiquitinated isoforms of IRAK1, it was immune-precipitated from HEK293T cell extracts and the recovered protein then analyzed by immunoblotting with anti-ubiquitin antibodies. High molecular weight isoforms of IRAK1 were observed in the

immunoblots, especially in both situation when IRAK1 was transfected with viperin and TRAF6 or viperin only ***[Figure. 4.5]***. This result confirmed that viperin specifically stimulates IRAK1 ubiquitination. In contrast, the inactive viperinΔ3C mutant failed to stimulate ubiquitination of IRAK1 ***[Figure. 4.5]***.

Interestingly, co-expression of TRAF6 with viperin did not change the level of IRAK1 ubiquitination significantly ***[Figure. 4.5]***. This suggests that the complex of viperin with IRAK1 either recruits endogenous TRAF6 and/or other E3 ubiquitin ligases to ubiquitinate IRAK1 (4,10). Overall, the fraction of over-expressed IRAK1 converted to high molecular weight isoforms remained relatively small. This observation reflects the fact that ubiquitination is dynamic processes in which de-ubiquitination pathways also operate; furthermore, the high, non-physiological concentrations of IRAK1 produced by transfection may exceed the capacity of the cellular ubiquitination machinery.

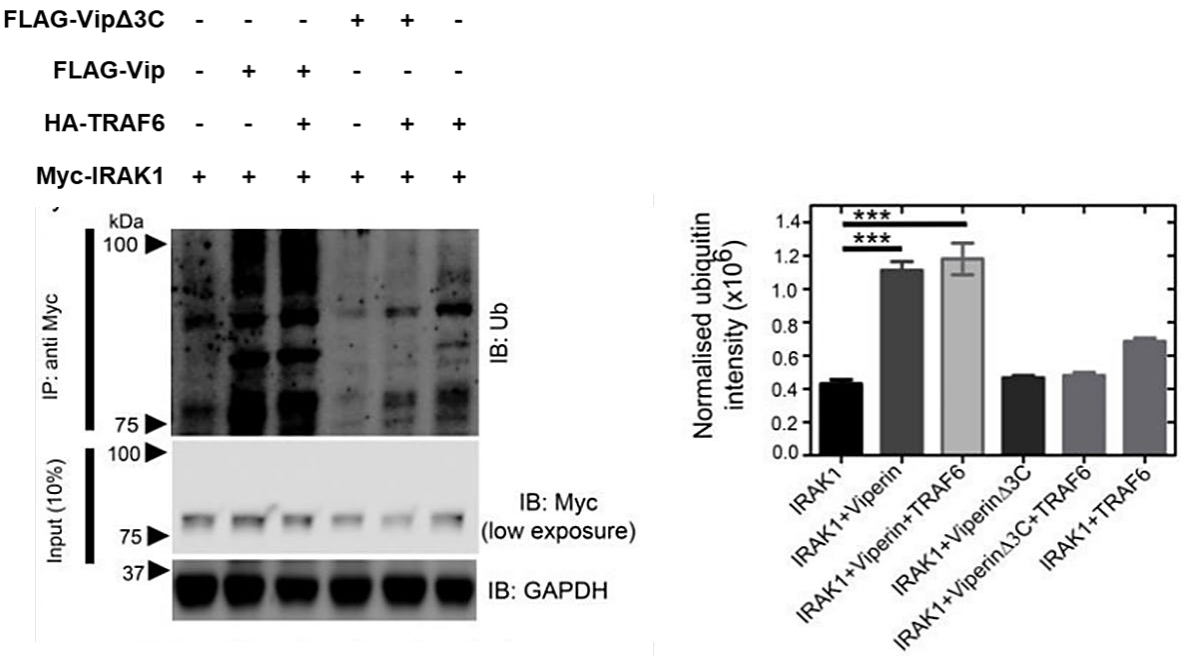

Figure 4.5: **Viperin stimulates ubiquitination of IRAK1.** HEK293T cells were transfected with genes encoding IRAK1, TRAF6, viperin or viperinΔ3C as indicated. *Left panel:* IRAK1 was immunoprecipitated as bait protein and immunoblotted with anti-ubiquitin antibody. GAPDH was used as a loading control. *Right panel:* Quantification of ubiquitination of IRAK1 using ImageJ software, normalized to GAPDH. Statistical analyses were presented as mean +/− S.E.M. (n=3) with *** indicating $p < 0.001$, (Student's t-test for independent samples). The figure is reproduced from *J.Biol. Chem*. (2019) **294**, 6888-6898.

4.3 Discussion A number of studies suggest that interactions between viperin and a variety of host and viral proteins are important for its antiviral effects (16,17) (18) (19) (20) (21) (22), although the evidence has tended to rely on indirect measures of viperin's activity such as the reduction of viral titre or viral RNA levels. Furthermore, in several cases the radical SAM activity of viperin appears to be dispensable for its antiviral activity (17,19,23). The discovery that viperin catalyzes the synthesis of ddhCTP (13) provided an important advance in our understanding of the mechanism by which viperin exerts its antiviral effects. Therefore, we took an enzymatic approach to decipher the mechanism how viperin interact with its target-proteins to impart antiviral activity. By reconstituting the interactions between viperin, IRAK1 and TRAF6 in HEK 293T cells, we have been able to examine a specific, biochemically well-defined function of viperin: the activation of IRAK1 by poly-ubiquitination. This finding underscores the necessity of the interaction between viperin, IRAK1 and TRAF6 for ubiquitination of IRAK1 to occur.

Given viperin's role as a component of the TLR7/9 signaling pathways, it might be expected that other proteins in the pathway would regulate its enzymatic activity. Our studies show that the enzymatic activity of viperin to produce 5'-deoxyadenosine is increased by ~10-fold by co-expression with IRAK1 and TRAF6, whereas IRAK1 is not efficiently ubiquitinated *in vivo* unless viperin is also co-expressed. Thus, the activities of

viperin and IRAK1 appear to be synergistically regulated activities, mediated through protein-protein interactions between viperin, IRAK1 and TRAF6. The Fe-S cluster is required for viperin to catalyze the formation of ddhCTP; however, we have shown that the radical-SAM activity is *not* critically required for viperin to stimulate IRAK1 ubiquitination, as the poly-ubiquitinated IRAK1 isoforms were observed when co-expressed with viperinΔ3C. Also, IRAK1 and TRAF6 formed the protein-complex in the presence of the radical SAM domain-mutant viperin.

Based on these observations we suggest that the reductive cleavage of SAM, and concomitant formation of ddhCTP, may serve as a mechanism by which viperin could regulate the ubiquitination of IRAK. We propose that in the absence of SAM, viperin adopts a conformation that is unable to stimulate ubiquitination of IRAK1. Upon binding SAM, viperin undergoes a conformational change to an active state that stimulates K63-linked poly-ubiquitination of IRAK1 by TRAF6 (or other E3 ligases), eventually leading to transcription of type I interferons (4). Once the complex between IRAK1, TRAF6 and viperin is formed, viperin is activated to cleave SAM, thereby initiating the catalytic cycle leading to the formation of ddhCTP and 5'-dA. Completion of the catalytic cycle returns viperin to its inactive state, preventing further poly-ubiquitination of IRAK1.

Our measurements of viperin activity to produce 5'-deoxyadenosine in cell extracts indicate that viperin converts CTP to ddhCTP with k_{obs}, = 21.4 ± 1.6 h^{-1}, which is about twice as fast as *in vitro* kinetic data reported previously (13), but still rather slow by comparison with most enzyme reactions. However, the slow kinetics of viperin make this reaction well suited to regulate a signaling pathway in a manner analogous to signal regulation by hetero-trimeric G proteins (24,25). We note that; although consistent with

our data, further studies with purified enzymes will be needed to validate this mechanistic proposal, which would constitute a new mode of regulating cellular protein activity by radical-SAM enzymes.

In conclusion, our experiments provide evidence for a regulatory mechanism that links the production of the newly identified antiviral nucleotide, ddhCTP, by viperin to transduction of innate immune signaling through K63-linked polyubiquitination of IRAK1 by TRAF6. In this manner, the up-regulation of various proteins that constitute the cellular antiviral response is coordinated with the production of a small molecule inhibitor of viral replication. Protein ubiquitination plays multiple roles in cellular proteostasis and signal transduction (26,27). We suggest that the wide-ranging roles that viperin plays in the antiviral response may, in part, result from the ability of the enzyme to recruit and activate a subset of the many E3 ubiquitin ligases present in the cell to ubiquitinate target proteins, thereby regulating their cellular levels in response to viral infection.

4.4 Experimental Procedures

Cell lines The HEK293T cell line was obtained from ATCC.

Antibodies Rabbit polyclonal RSAD2/ Viperin antibody (11833-1-AP) was obtained from Protein Tech. Rabbit polyclonal IRAK1 antibody (PA5-17490) was obtained from Thermo Scientific. Rabbit polyclonal Ubiquitin antibody (sc-9133) and mouse monoclonal TRAF6 antibody (sc-8409) were purchased from Santa Cruz. Goat anti-rabbit (170-6515) and anti-mouse (626520) Ig secondary Abs were purchased from BioRad and Life Technologies respectively. Rabbit polyclonal GAPDH (TAB1001) was purchased from

Thermo Scientific and Mouse monoclonal GAPDH antibody (6C5) was obtained from EMD Millipore.

Plasmids Synthetic genes encoding human viperin, IRAK1 and TRAF6 (GenBank accession numbers AAL50053.1, NM145803, NM001569 respectively) were purchased from GenScript. For details see supplementary information.

Reagents The sources of other reagents were as described previously (17).. Nucleotide substrates: Cytidine 5'-triphosphate, disodium salt hydrate, 95%; were purchased from Acros Organics (226225000). Pierce™ Anti-c-Myc Magnetic Beads (88842) were purchased from ThermoFisher Scientific.

Transfection HEK 293T cells, cultured as described above, were transiently transfected using FuGENE® HD (Promega) following the manufacturer's instructions.

Immunofluorescence analyses Cells were grown on poly-L-lysine-coated coverslips to 30–40% confluence, transfected with plasmids expressing Viperin, IRAK1 and/or TRAF6 and incubated for 30 h. Cells were fixed with 4% paraformaldehyde, permeabilized with 0.05% Triton X-100 dissolved in PBS, and washed three times with PBS containing 0.1% Tween20. The fixed cells were stained with the appropriate antibodies. Primary antibodies were diluted in PBS containing, 1% FBS and 0.1% Tween 20. Viperin was detected by using mouse monoclonal anti-viperin (Abcam) diluted 1:250, and calnexin was detected with rabbit polyclonal antibody (Abcam) diluted 1:250. IRAK1 was detected by using rabbit polyclonal IRAK1 antibody (Thermo Scientific) diluted 1:250 and mouse monoclonal c-Myc Tag antibody (Thermo Scientific) diluted 1:100. TRAF6 was detected by using mouse monoclonal TRAF6 antibody (Santa Cruz) diluted 1:100. After incubation at room temperature for 1 h or overnight at 4°C, the coverslips were washed with PBS

containing 0.1% Tween20 and treated with Alexa Fluor 647-conjugated goat anti-mouse (Life Technologies) and Alexa Fluor 488-conjugated goat anti-rabbit (Abcam) secondary antibodies at a dilution of 1:400 at room temperature for 2 h. The coverslips were washed three times with PBS containing 0.1% Tween20 and mounted in ProLong™ Gold Antifade Mountant (Molecular Probes). Images were acquired with an Olympus IX81 microscope with a 60× 1.49NA objective on an Andor iXON Ultra EMCCD camera. 488 nm (Coherent Cube 488-50) and 640 nm (Coherent Cube 640–100) laser excitation was aligned in HILO imaging mode for axial sectioning using an Olympus cell^TIRF module.

Immunoblotting Cells were lysed in TBST buffer (20 mM Tris (pH 7.5), 500 mM NaCl, 0.05% Tween-20) containing protease inhibitors (SIGMAFAST™ Protease Inhibitor Tablets, S8830; Sigma). Supernatants of lysates were collected and mixed with reducing sample buffer. The supernatants were separated on 10% SDS-PAGE gels. The bicinchoninic acid (BCA) assay (Thermo Scientific) was used to determine the total amount of protein in the lysates. Immunoblotting was performed as describes previously (17). Primary antibodies used were directed against viperin (rabbit polyclonal diluted 1:2500), GAPDH (rabbit polyclonal diluted 1:5000), IRAK1 (rabbit polyclonal diluted 1:4000), TRAF6 (mouse monoclonal diluted 1:500) and GAPDH (mouse monoclonal diluted 1:5000). Rabbit polyclonal ubiquitin antibody was used at a dilution of 1:1000. Blots were visualized, and band intensities quantified using a Bio-Rad ChemiDoc Touch imaging system. Integrated density measurements were done using ImageJ software. Quantitative measurements of protein expression levels reported here represent the average of at least three independent biological replicates.

Immunoprecipitation Assays Cells were rinsed twice with ice-cold PBS, harvested in P40 lysis buffer (50 mM Tris, pH 7.4, 1% Triton X-100, 150 mM NaCl, 10% glycerol, 1 mM EDTA, 10 mM NaF, and 0.2 mM phenylmethylsulfonyl fluoride with protease inhibitor cocktail from Sigma), and briefly sonicated. Lysates were collected by centrifugation at 12,000 × *g* for 15 minutes at 4°C. For immunoprecipitation, ratio of suspension to packed gel volume was 2:1. Resin pre-equilibration was done as per the manufacturer's protocol. Three hundred microliters of a 1:1:1 ratio of cell lysates was added and incubated for 16 hours at 4°C with gentle rotation. Beads were pelleted by centrifugation at 5,000 × *g* for 30 seconds at 4°C and washed three times with washing buffer (50 mM Tris, pH 7.4,150 mM NaCl, 10% glycerol, 1 mM EDTA, 10 mM NaF, and 0.2 mM phenylmethylsulfonyl fluoride with protease inhibitor cocktail from Sigma). Immunocomplexes were eluted by boiling in SDS-PAGE sample buffer, separated by SDS-PAGE, and transferred to a nitrocellulose membrane. Immunoprecipitation using Protein A beads or anti Myc-tagged magnetic beads was performed as per the manufacturers protocol. Membranes were blocked for 2 h at room temperature in TBST buffer (20 mM Tris, pH 7.5, 137 mM NaCl, and 0.1% Tween 20) containing 5% nonfat dry milk, followed by overnight incubation at 4°C in TBST buffer containing 3% nonfat dry milk and the appropriate primary antibody. Membranes were washed three times in TBST and then incubated for 2 h at room temperature with the secondary IgG-coupled horseradish peroxidase antibody. The membranes were washed three times with TBST, and the signals were visualized with enhanced chemiluminescence reagent as described in immunoblotting.

Statistical analyses Results from all studies were compared with unpaired two-tailed Student's t test using GraphPad Prism 5 software. P values less than 0.05 were considered significant.

Assay of viperin in HEK 293T cell lysates HEK 293T cells transfected with viperin, and/or IRAK1 and TRAF6 were harvested from one 10 cm diameter tissue culture plate each, resuspended in 500 µl of anoxic Tris-buffered saline (50 mM Tris-Cl, pH 7.6, 150 mM NaCl) containing 1% Triton X-100, sonicated within an anaerobic glovebox (Coy Chamber), and centrifuged at 14,000 g for 10 min. Dithiothreitol (DTT; 5 mM) and dithionite (5 mM) were added to the cell lysate together with CTP (300 µM). The assay mixture was incubated at room temperature for 30 min prior to starting the reaction by the addition of SAM (200 µM). The assay was incubated for 60 min at room temperature, after which the reaction stopped by heating at 95 °C for 10 min. The solution was chilled to 4 °C, and the precipitated proteins were removed by centrifugation at 14,000 rpm for 25 min. The supernatant was then extracted with acetonitrile. Samples were analyzed in triplicate by UPLC-tandem mass spectrometry as described previously (17). For details of standard curve construction and calculations refer to Supporting Information.

References

1. Saitoh, T., Satoh, T., Yamamoto, N., Uematsu, S., Takeuchi, O., Kawai, T., and Akira, S. (2011) Antiviral Protein Viperin Promotes Toll-like Receptor 7- and Toll-like Receptor 9-Mediated Type I Interferon Production in Plasmacytoid Dendritic Cells. *Immunity* **34**, 352-363
2. Jiang, X., and Chen, Z. J. (2011) Viperin links lipid bodies to immune defense. *Immunity* **34**, 285-287

3. Qiu, L.-Q., Cresswell, P., and Chin, K.-C. (2009) Viperin is required for optimal Th2 responses and T-cell receptor–mediated activation of NF-κB and AP-1. *Blood* **113**, 3520-3529
4. Saitoh, T., Satoh, T., Yamamoto, N., Uematsu, S., Takeuchi, O., Kawai, T., and Akira, S. (2011) Antiviral protein Viperin promotes Toll-like receptor 7- and Toll-like receptor 9-mediated type I interferon production in plasmacytoid dendritic cells. *Immunity* **34**, 352-363
5. Blasius, A. L., Arnold, C. N., Georgel, P., Rutschmann, S., Xia, Y., Lin, P., Ross, C., Li, X., Smart, N. G., and Beutler, B. (2010) Slc15a4, AP-3, and Hermansky-Pudlak syndrome proteins are required for Toll-like receptor signaling in plasmacytoid dendritic cells. *Proc Natl Acad Sci U S A* **107**, 19973-19978
6. Honda, K., Ohba, Y., Yanai, H., Negishi, H., Mizutani, T., Takaoka, A., Taya, C., and Taniguchi, T. (2005) Spatiotemporal regulation of MyD88–IRF-7 signalling for robust type-I interferon induction. *Nature* **434**, 1035-1040
7. Sasai, M., Linehan, M. M., and Iwasaki, A. (2010) Bifurcation of Toll-like receptor 9 signaling by adaptor protein 3. *Science (New York, N.Y.)* **329**, 1530-1534
8. Fitzgerald, K. A. (2011) The interferon inducible gene: Viperin. *Journal of interferon & cytokine research : the official journal of the International Society for Interferon and Cytokine Research* **31**, 131-135
9. Conze, D. B., Wu, C.-J., Thomas, J. A., Landstrom, A., and Ashwell, J. D. (2008) Lys63-linked polyubiquitination of IRAK-1 is required for interleukin-1 receptor- and toll-like receptor-mediated NF-kappaB activation. *Mol. Cell. Biol.* **28**, 3538-3547
10. Ordureau, A., Smith, H., Windheim, M., Peggie, M., Carrick, E., Morrice, N., and Cohen, P. (2008) The IRAK-catalysed activation of the E3 ligase function of Pellino isoforms induces the Lys63-linked polyubiquitination of IRAK1. *Biochem J* **409**, 43-52
11. Hee, J. S., and Cresswell, P. (2017) Viperin interaction with mitochondrial antiviral signaling protein (MAVS) limits viperin-mediated inhibition of the interferon response in macrophages. *PLoS One* **12**, e0172236
12. Severa, M., Coccia, E. M., and Fitzgerald, K. A. (2006) Toll-like Receptor-dependent and -independent Viperin Gene Expression and Counter-regulation by PRDI-binding Factor-1/BLIMP1. *J. Biol. Chem.* **281**, 26188-26195
13. Gizzi, A. S., Grove, T. L., Arnold, J. J., Jose, J., Jangra, R. K., Garforth, S. J., Du, Q., Cahill, S. M., Dulyaninova, N. G., Love, J. D., Chandran, K., Bresnick, A. R., Cameron, C. E., and Almo, S. C. (2018) A naturally occurring antiviral ribonucleotide encoded by the human genome. *Nature* **558**, 610-+
14. Hinson, E. R., and Cresswell, P. (2009) The N-terminal amphipathic alpha-helix of viperin mediates localization to the cytosolic face of the endoplasmic reticulum and inhibits protein secretion. *J Biol Chem* **284**, 4705-4712
15. Blasius, A. L., and Beutler, B. (2010) Intracellular toll-like receptors. *Immunity* **32**, 305-315
16. Wang, X., Hinson, E. R., and Cresswell, P. (2007) The interferon-inducible protein viperin inhibits influenza virus release by perturbing lipid rafts. *Cell Host Microbe* **2**, 96-105
17. Makins, C., Ghosh, S., Roman-Melendez, G. D., Malec, P. A., Kennedy, R. T., and Marsh, E. N. (2016) Does Viperin Function as a Radical S-Adenosyl-l-methionine-

dependent Enzyme in Regulating Farnesylpyrophosphate Synthase Expression and Activity? *J Biol Chem* **291**, 26806-26815
18. Seo, J. Y., Yaneva, R., Hinson, E. R., and Cresswell, P. (2011) Human cytomegalovirus directly induces the antiviral protein viperin to enhance infectivity. *Science* **332**, 1093-1097
19. Vonderstein, K., Nilsson, E., Hubel, P., Nygard Skalman, L., Upadhyay, A., Pasto, J., Pichlmair, A., Lundmark, R., and Overby, A. K. (2017) Viperin targets flavivirus virulence by inducing assembly of non-infectious capsid particles. *J Virol* **92**, e01751-01717
20. Panayiotou, C., Lindqvist, R., Kurhade, C., Vonderstein, K., Pasto, J., Edlund, K., Upadhyay, A. S., and Overby, A. K. (2018) Viperin Restricts Zika Virus and Tick-Borne Encephalitis Virus Replication by Targeting NS3 for Proteasomal Degradation. *Journal of Virology* **92**, e02054-02017
21. Helbig, K. J., Eyre, N. S., Yip, E., Narayana, S., Li, K., Fiches, G., McCartney, E. M., Jangra, R. K., Lemon, S. M., and Beard, M. R. (2011) The antiviral protein viperin inhibits hepatitis C virus replication via interaction with nonstructural protein 5A. *Hepatology* **54**, 1506-1517
22. Wang, S., Wu, X., Pan, T., Song, W., Wang, Y., Zhang, F., and Yuan, Z. (2012) Viperin inhibits hepatitis C virus replication by interfering with binding of NS5A to host protein hVAP-33. *J Gen Virol* **93**, 83-92
23. Helbig, K. J., Carr, J. M., Calvert, J. K., Wati, S., Clarke, J. N., Eyre, N. S., Narayana, S. K., Fiches, G. N., McCartney, E. M., and Beard, M. R. (2013) Viperin is induced following dengue virus type-2 (DENV-2) infection and has anti-viral actions requiring the C-terminal end of viperin. *PLoS Negl Trop Dis* **7**, e2178
24. Neer, E. J. (1995) Heterotrimeric G-proteins - Organizers of Transmembrane Signals *Cell* **80**, 249-257
25. Dohlman, H. G., and Thorner, J. (1997) RGS proteins and signaling by heterotrimeric G proteins. *J. Biol. Chem.* **272**, 3871-3874
26. Bhoj, V. G., and Chen, Z. J. (2009) Ubiquitylation in innate and adaptive immunity. *Nature* **458**, 430-437
27. Hu, H., and Sun, S. C. (2016) Ubiquitin signaling in immune responses. *Cell Res* **26**, 457-483

Chapter 5

Proteomics Analysis of Viperin and Identification of its *Interactome*

5.1 Introduction. The Eukaryotic cells undergo various spatial and temporal changes in organelle morphology and protein distribution upon viral infection. Viruses exploit the host proteome organization at different stages of viral replication, from viral entry to egress. With advances in microscopy and mass-spectrometric techniques, viruses have been shown to rely on the organization and morphology of host cell organelles and induce changes in the abundance of cellular proteins (1). The endoplasmic reticulum is one of the crucial membranous networks that has been co-opted by viruses to facilitate viral repication (2). Viruses manipulate the cellular protein folding and misfolding machinary, emerging from the ER and causing ER stress. In response to this ER stress, multiple proteins are activated as a part of stress-responsive pathways, some of are shared with interferon-regulated pathways. For example, the ER stress mediator RNA dependent protein kinase-like ER kinase (PERK), an ER-resident membrane protein, is directly activated during viral infection (3). Overall, the ER acts as a platform to support infection-induced change in proteome distribution and proteins translocation between ER to different organelles e.g. mitochondrial-associated ER membrane (MAM) (4).

Viperin is one such ER-associated protein that has been shown to be up-regulated during viral infection and translocate from the ER to mitochondria, specifically during

human cytomegalovirus pathogenesis (5,6). Viperin has been identified to participate in a diverse range of antiviral functions, including modulating immune signalling, metabolic and secretory pathways (7-16). The seemingly broad spectrum functions attributed to viperin appear to be dependent on the identity of the infecting viruses, as it is observed to interact with different protein targets dependent upon the virus. However, we hypothesized that there is a unifying mechanism that may explain viperin's aooarantly diverse modes of action. In our study, we have investigated viperin's interaction with various host and viral proteins, involved in multiple metabolic and signaling pathways. Viperin was shown to directly interact with the innate immune signaling proteins IRAK1 and TRAF6, and stimulate the K-63 linked ubiquitination of IRAK1 by the ubiquitin ligase TRAF6 (Chapter 4) (17). It was also shown to interact with the viral protein NS5A and target it for degradation through proteasome-mediated degradation, especially in the presence of the sterol-binding protein, VAP-33 (Chapter 3). Although no direct interaction between viperin and the cholesterol biosynthesis protein farnesyl pyrophosphate synthase (FPPS) to be established, it seemed that the intracellular level of FPPS is down-regulated by viperin, probably through proteosomal or lysosomal degradation pathway (Chapter 2) (18). This observation indicates that viperin may interact with other proteins and indirectly regulate FPPS.

Previous studies have shown that overexpression of viperin in BSR cells reduced the cholesterol and sphingomyelin levels in cell membranes (19). Label-free mass spectrometric study on the ATDC5 cultures overexpressing viperin showed differential expression of C-X-C motif chemokine 10 (CXCL10), a pro-inflammatory cytokine involved in chemotaxis, differentiation, and activation of peripheral immune cells (20). Using similar

mass spectrometric studies, viperin was found to interact with and inhibit the function of the cellular secretory protein Golgi brefeldin A-resistant guanine nucleotide exchange factor 1 (GBF1) (16). Cumulatively, the results from previous studies by other laboratories together with our present investigations suggest that viperin may associate with one or multiple cellular pathways involved in the viral replication process.

A comprehensive identification and understanding of the protein-protein interaction network of viperin can be obtained through mass spectrometry-based proteomics analysis (21). This is a quantitative approach to identify the alteration in protein abundances and post-translational modifications in various cellular processes, including viral infection and activation of the innate immune system (4,22). To this end, a proteomics study of viperin's interaction partners was undertaken, using co-immunoprecipitation of viperin, followed by mass spectrometric analysis. Collaborating with the University of Michigan bioinformatics and proteomics core, and Prof. Alexey Nesvizhskii's laboratory in the Department of Pathology, University of Michigan, we tried to determine the "interactome" of viperin through proteomic analysis with the objective of detecting unknown cellular interaction partners of viperin and the pathways they are involved in. This study may also highlight the common features of its target proteins.

We identified multiple cholesterol biosynthesis proteins, as the most enriched hits in the *interactome* of viperin. These proteins are mostly involved in the formation of lanosterol from farnesylpyrophosphate ***[Figure 5.1]***, suggesting that this is the major cellular pathway that viperin modulates. This observation also explains viperin's ability to block the viral budding process of several enveloped viruses by reducing cellular cholesterol levels. This study also identifies a few ubiquitin-conjugating proteins,

indicating that viperin may also be a part of the ubiquitin-dependent degradation pathway, through which it promotes the degradation of its target proteins (e.g. NS5A, FPPS). Taken together, our study explored several unique targets of viperin.

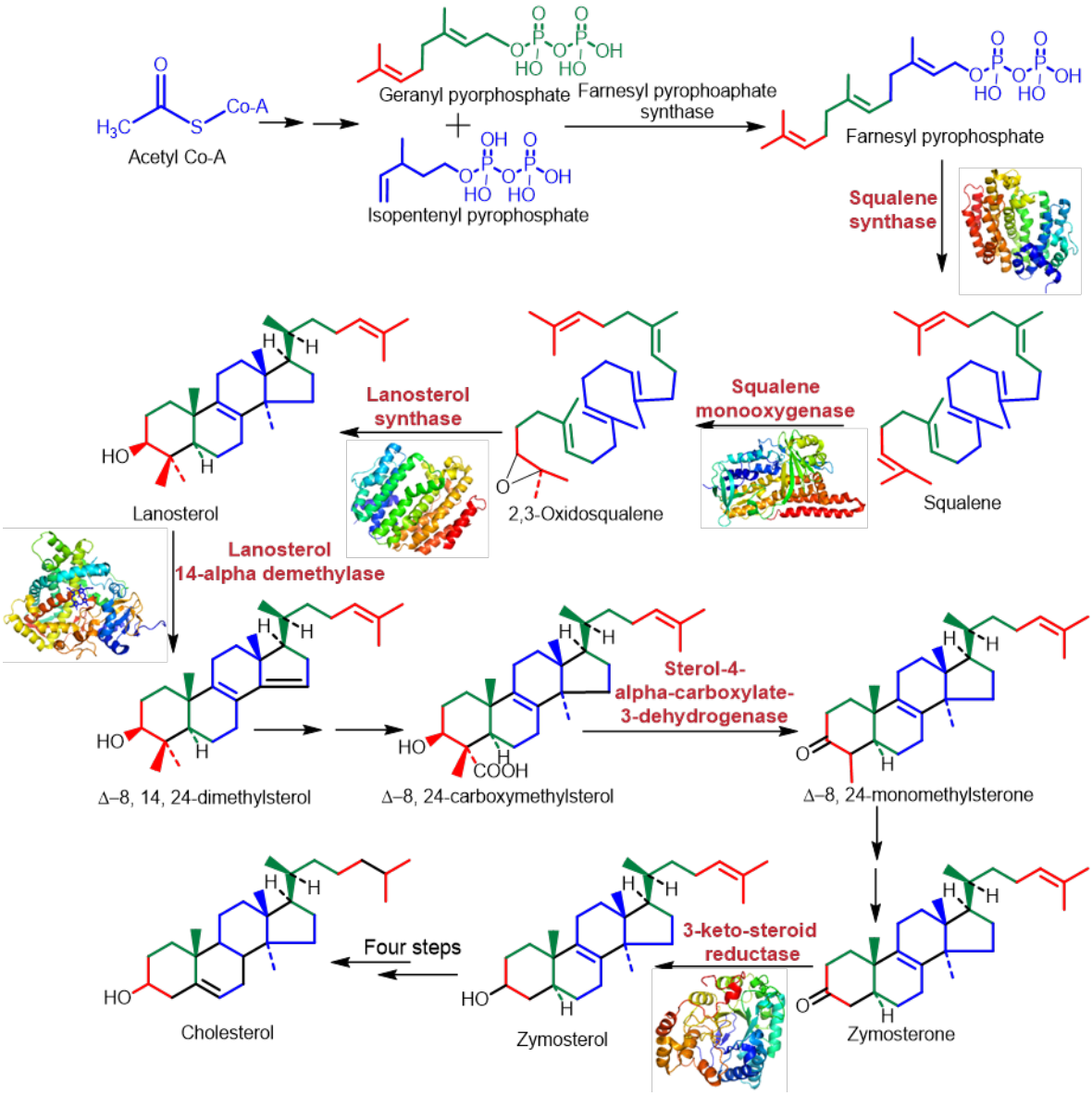

Figure 5.1: **A schematic diagram, showing different steps in cholesterol biosynthesis.** Steps catalysed by various cholesterol biosynthetic enzymes, observed to be interacting with viperin, as detected in affinity purified mass spectrometry (see Table 5.1 in *Results* section), are shown in red.

5.2 Results In order to identify the proteins interacting with viperin, we performed immunoprecipitation of viperin, overexpressed in HEK293T cells, followed by tryptic digestion and mass spectrometric analysis of the immunoprecipitated samples. To obtain a consistent expression level of viperin, a Tet-on HEK293T cell-line, stably expressing viperin under the control of a tetracycline inducible promoter was generated as described in ***Appendix A.5***. This cell line was used for initial screening of the interaction partners of viperin. However, transient transfection of viperin in HEK293T cells allowed us to achieve higher peptide counts compared to stably expressing viperin in tetracycline-induced cells. Therefore, the final interactome study was conducted using transiently transfected viperin in HEK293T cells.

5.2.1 Immunoprecipitation of viperin using epitope tagged beads and MS analysis on the immunoprecipitated protein complex. A 3x-FLAG-tagged construct of viperin in pcDNA3.1(+), was transfected into HEK293T cells, and expressed for 42 hours post transfection. This protein was immunoprecipitated using anti-FLAG magnetic beads. An empty 3x-FLAG tagged pcDNA3.1(+) construct was transfected in HEK293T cells as the empty vector control (Refer to the experimental procedure section for details). To recover immunoprecipitated proteins from the beads, on-bead tryptic-digestion was performed by the University of Michigan proteomics core using sequential reduction, alkylation and trypsin digestion of the proteins. Mass spectrometry of the peptides was performed using an Orbitrap Fusion Tribrid mass spectrometer (Thermo Fisher). The dataset was analysed by Proteome Discoverer™ (v2.1Thermo Fisher) and queried against UniProt *Homo Sapiens* database. The MS analysis was performed on three biological replicates for both viperin and control samples.

5.2.2 Screening of the protein dataset and pathway analysis. The initial protein list, containing over 4000 hits ***[Appendix A.4],*** was screened by setting the cut off for the fold change of the peptide-to-spectrum matches (PSMs) of viperin samples over the controls as ≥3. The shortened list was then screened through the Contaminant Repository for Affinity Purification (CRAPome) database to exclude the non-specific background proteins (i.e contaminants). A confidence score was assigned to the remaining proteins in the list by Significance Analysis of INTeractome (SAINT) software, which was used to predict the probability of a true interaction between a particular protein hit and viperin. By setting the SAINT probability cut off as >0.9, we obtained a list of 100 possible hits. We next performed a pathway enrichment analysis on these hits using DAVID, v6.8 (The Database for Annotation, Visualization and Integrated Discovery) software. Functional annotation of these proteins through KEGG pathway analysis showed the highest enrichment scores for cholesterol and sterol biosynthesis processes, suggesting that the cholesterol biosynthesis proteins are the top hits in the *interactome* of viperin (Enrichment score 3.59 in DAVID at high stringency). The following cholesterol biosynthesis enzymes were observed in the proteomics analysis, as good candidates for interacting with viperin:

Protein	Gene Name	Fold Change	Function
Lanosterol synthase	LSS	33.4	Epoxysqualene to lanosterin
Squalene monooxygenase	SQLE	25.2	Squalene to Epoxysqualene

Sterol-4-alpha-carboxylate 3-dehydrogenase, decarboxylating	NSDHL	15.2	Lanosterol to Zymosterol
Lanosterol 14-alpha demethylase	CYP51A1	10.3	C-14 demethylation of lanosterol
3-keto-steroid reductase	HSD17B7	10	reduction of the keto group on the C-3 of sterols
Squalene synthase	FDFT1	5.5	FPP to Squalene synthesis

Table 5.1: *List of cholesterol biosynthesis proteins enriched in the bait-protein complex, co-immunoprecipitated with viperin at endogenous level.*

Besides cholesterol biosynthesis proteins, we also observed iron-sulfur cluster installing proteins and E3-Ubiquitin ligase associated proteins in the top 100 proteins hits, though they were not the most enriched pathways in DAVID analysis. The following proteins were observed:

Iron-Sulfur cluster installing proteins:

Protein Name	Gene name	Fold Change	Function
Probable cytosolic iron-sulfur protein assembly protein CIAO1 (WD repeat-containing protein 39)	CIAO1	5.75	Facilitates the assembly of most cytosolic-nuclear Fe/S proteins
MMS19 nucleotide excision repair protein homolog (MMS19-like protein)	MMS19	4.7	Acts as an adapter between different protein components in cytosolic Fe-S cluster assembly complex

Table 5.2: *List of iron-sulfur cluster installing proteins observed in the bait-protein complex, co-immunoprecipitated with viperin at endogenous level.*

E3 Ubiquitin ligase/ Ubiquitin associated proteins:

Protein	Gene name	Fold Change	Function
UBX domain-containing protein 4	UBXN4	8.3	Involved in ubiquitin-dependent endoplasmic

			reticulum-associated protein degradation (ERAD)
Cullin-associated NEDD8-dissociated protein 2	CAND2	5.1	Assembly factor of SCF (SKP1-CUL1-F-box protein) E3 ubiquitin ligase complexes that promotes the exchange of the substrate-recognition F-box subunit in SCF complexes

Table 5.3: *List of ubiquitin ligase or ubiquitin associated proteins observed in the bait-protein complex, co-immunoprecipitated with viperin at endogenous level.*

Several sphingolipid biosynthesis and metabolic proteins were also observed, although with a lower enrichment score in pathway analysis. Viperin was shown to regulate intracellular level of sphingomyelin (19), therefore it may be possible that by regulating these proteins viperin is modulating the levels of cellular sphingolipids.

Protein	Gene name	Fold Change	Function
Sphingosine-1-phosphate lyase 1	SGPL1	21.6	Dephosphorylation of sphingoid bases (PSBs), such as sphingosine-1-phosphate, into fatty aldehydes and phosphoethanolamine
serine palmitoyltransferase long chain base subunit 1 and 2	SPTLC1 SPTLC2	9.6 and 13.7 respectively	Formation of 3-oxasphinganine from hexadecanoyl-CoA
Aldehyde dehydrogenase 3 family member A2	ALDH3A2	3.8	Conversion of the sphingosine 1-phosphate (S1P) degradation product hexadecenal to hexadecenoic acid

Table 5.4: *List of sphingolipid metabolic proteins observed in the bait-protein complex, co-immunoprecipitated with viperin at endogenous level.*

5.3 Discussion Viperin seems to be involved in various cellualr pathways (e.g. the innate immune signaling pathway and lipid biosynthesis); however very few studies have been focused on obtaining a comprehensive list of proteins belonging to the *interactome* of

viperin. To date, most investigations of viperin's antiviral effects have used cell-culture based experiments in which the antiviral activity of the enzyme was assayed either by measuring decreases in viral titer or viral RNA levels. Consequently, it seems that the mechanism by which viperin exerts its anti-viral activity differs in different viral strains. However, viperin's ability to target a broad range of viruses implies a unifying underlying mechanism, possibly by regulating a few specific biochemical pathways important to viral infection. Therefore, we focused on biochemical and proteomics approaches to identify the proteins that viperin interacts with at endogenous level.

In this study, we identified several cholesterol biosynthesis proteins as interacting with viperin at endogenous levels of expression. The two most enriched proteins in the viperin interactome are lanosterol synthase (LSS) and squalene monooxygenase (SQLE), involved in the formation of lanosterol from squalene (23). As the sterol biosynthetic proteins interact with each-other in a functional complex, it is possible that most of the proteins are being enriched through indirect interactions, rather than binding directly to viperin. Notably, the cholesterol biosynthetic enzymes detected in this study are ER-resident proteins and probably their subcellular localization is important for the interaction with viperin. Interestingly, consistent with the results obtained previously (Chapter 2), viperin was not observed to directly interact with the cytosolic protein farnesylpyrophospahte synthase (FPPS) at endogenous level.

Previous studies have demonstrated that lanosterol synthase (LSS) and squalene synthase (FDFT1) are essential for viral replication and potential targets for antiviral drugs. Inhibition of LSS and FDFT1 with small molecule inhibitors reduced the infection of Human rhino virus and hepatitis C virus, respectively and modulated the innate immune

system (24),(25). Therefore, by interacting with these proteins, viperin may retard or stall the cholesterol biosynthesis and thereby, inhibit the viral budding process.

In addition to regulating cholesterol, viperin may also exert its anti-viral activity by interacting with and inhibiting the sphingolipid biosynthesis associated proteins, identified in the analysis. Sphingolipids and their metabolites are potential key regulators in viral replication, assembly and release of several viruses, e.g. HIV (26). Prevention of *in vivo* sphingolipid synthesis by serine palmitoyltransferase disrupted the infection of HCV in human hepatocytes (27), suggesting that viperin may use similar mechanism to exhibit viral regulation by inhibiting serine palmitoyltransferase.

The presence of ubiquitin-conjugating enzymes (E3 ubiquitin ligases) in the viperin bait-protein complex strengthened the idea the fact that viperin is involved in ubiquitin-mediated signaling pathways and degradation pathways. We did not find any specific K63-linked ubiquitin ligase in the analysis. However, intriguingly, the occurrence of ubiquitin-dependent endoplasmic reticulum-associated degradation (ERAD) proteins in the interactome support our observation that viperin promotes the degradation of its target proteins (e.g. FPPS and NS5A) through the proteosomal degradation pathway (refer to chapter 2 and 3). In fact, several of the cholesterol biosynthetic enzymes, present in the immunoprecipitated protein complex, are also known to be controlled through proteosomal degradation (28).

The identification of the key enzymes involved in cholesterol synthesis as the interaction partners of viperin provides new insights into viperin's anti-viral activity. Our observations provide evidence to support viperin's ability to regulate cholesterol and lipid metabolism and stall the viral budding process for enveloped viruses. Further biochemical studies

will be needed to validate the interaction of the individual proteins identified in this analysis with vipeirn. This will then set the stage to identify common structural and functional motifs that viperin recognizes and binds to.

5. 4 Experimental Procedure

Cell line HEK293T cells were obtained from ATCC.

Reagents Transfection agent Fugene ^{HD} was purchased from Promega (E2311). Anti-FLAG® M2 Magnetic Beads, bound with anti-FLAG mouse monoclonal antibody, was purchased from Sigma-Aldrich (M8823). Reagents for on-bead tryptic digestion of viperin peptides were provided by the proteomics core, Department of pathology, University of Michigan. Anti-viperin rabbit polyclonal and mouse monoclonal antibodies are purchased from ProteinTech and EMD Millipore, respectively.

Cloning and Expression of viperin in HEK293T cells Full length 3x-FLAG tagged viperin in pcDNA3.1(+) was cloned as described in the experimental section of Chapter 2. The 3x-FLAG tagged pcDNA3.1(+), used as an empty vector control, was a kind gift from Dr. Brent Martin Lab, Department of Chemistry, University of Michigan. Expression of viperin or empty vector construct was achieved through transient transfection method in HEK293T cells (cultivated in DMEM supplemented with 10% FBS and 1% antibiotics). Briefly, 17 µg of the respective plasmid DNA construct was mixed with FuGENE HD reagent in a 3:1 ratio, incubated at room temperature for 15 min, and then added to HEK293T cells at 40% confluence on a 100-mm dish. The transfected cells were then grown for up to 48 h, gently pelleted, and stored at –80 °C until use.

Immunoprecipitation of viperin with anti-FLAG magnetic beads HEK293T cells over-expressing 3x-FLAG-viperin or 3x-FLAG-tagged empty vectors (3x-FLAG-pcDNA3.1) as a control were harvested in PBS from 100 mm plates. Each biological replicate was pooled from 3x 100 mm plates to maximize the protein concentration in the lysate. The cells were lysed one ice with lysis buffer (Tris-buffer saline with 0.1% Tween 20, 10% glycerol and protease inhibitors) and centrifuged for 20 minutes at 14,000 RPM at 4˚C. Total protein concentration of the supernatant was measured by Protein DC Assay (Bio-Rad) and subjected to immunoprecipitation using Anti-Flag M2 magnetic beads (Sigma-Aldrich). Supernatant with total protein concentration ~ 7ug/ul was incubated with the anti-FLAG magnetic beads (pre-equilibrated with lysis buffer) at 50:1 (w/v) ratio for two hours at room temperature. Beads were washed thrice with 20x bead volume of TBS and submitted to bioinformatics and proteomics core, Department of Pathology, University of Michigan. The efficiency of immunoprecipitation was determined through SDS gel electrophoresis, followed by Coomasie blue staining and immunoblotting technique ***[Figure 5.2]***.

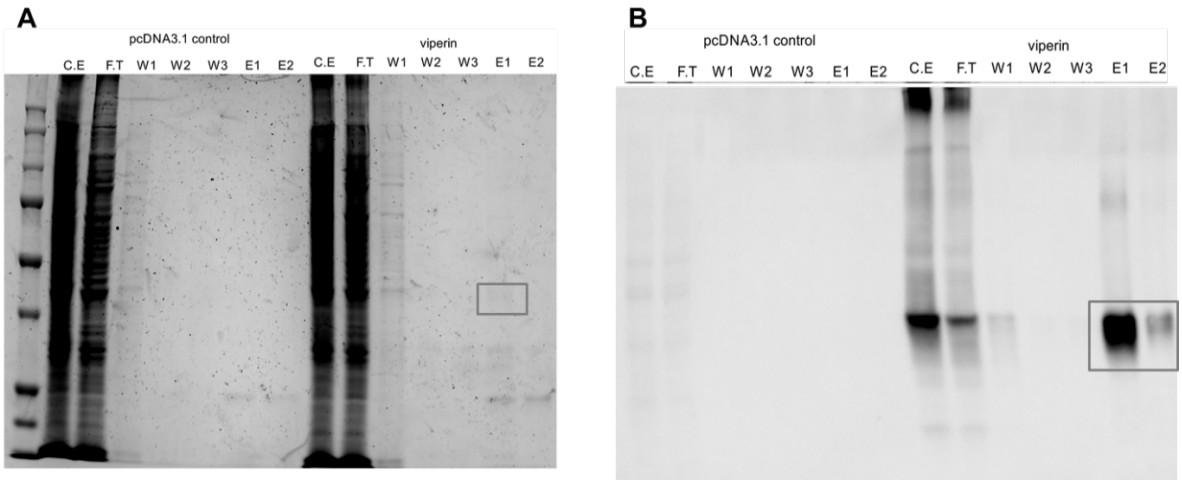

Figure 5.2: Determination of immunoprecipitated viperin using anti-FLAG tagged magnetic beads by (A) coomasie staining of the samples, analysed by SDS PAGE and (B) immunoblotting with anti-viperin antibody. The abbreviation used in the image are crude extract (C.E); flow-through (F.T); first, second and third wash (W1, 2, 3 respectively); first and second elution (E1 and 2 respectively).

In solution digestion and Mass spectrometric analysis At the proteomics core, the beads were re-suspended in 50 µl of 0.1M ammonium bicarbonate buffer (pH~8). Cysteines were reduced by adding 50 µl of 10 mM DTT and incubating at 45° C for 30 min. Samples were cooled to room temperature and alkylation of cysteines was achieved by incubating with 65 mM 2-Chloroacetamide, under darkness, for 30 min at room temperature. An overnight digestion with 1 ug sequencing grade, modified trypsin was carried out at 37° C with constant shaking in a Thermomixer. Digestion was stopped by acidification and peptides were desalted using SepPak C18 cartridges using manufacturer's protocol (Waters). Samples were completely dried using vacufuge. Resulting peptides were dissolved in 8 µl of 0.1% formic acid/2% acetonitrile solution and 2 µls of the peptide solution were resolved on a nano-capillary reverse phase column (Acclaim PepMap C18, 2 micron, 50 cm, ThermoScientific) using a 0.1% formic acid/2% acetonitrile (Buffer A) and 0.1% formic acid/95% acetonitrile (Buffer B) gradient at 300

nl/min over a period of 180 min (2-22% buffer B in 110 min, 22-40% in 25 min, 40-90% in 5 min followed by holding at 90% buffer B for 5 min and re-quilibration with Buffer A for 25 min). Eluent was directly introduced into Orbitrap Fusion tribrid mass spectrometer (Thermo Scientific, San Jose CA) using an EasySpray source. MS1 scans were acquired at 120K resolution (AGC target=$1x10^6$; max IT=50 ms). Data-dependent collision induced dissociation MS/MS spectra were acquired using Top speed method (3 seconds) following each MS1 scan (NCE ~32%; AGC target $1x10^5$; max IT 45 ms).

Proteins were identified by searching the MS/MS data against *Homo sapiens* protein database (UniProt; 42054 entries, 2016-11-30) using Proteome Discoverer (v2.1, Thermo Scientific). Search parameters included MS1 mass tolerance of 10 ppm and fragment tolerance of 0.2 Da; two missed cleavages were allowed; carbamidimethylation of cysteine was considered fixed modification and oxidation of methionine, deamidation of aspergine and glutamine, phosphorylation of serine, threonine and tyrosine, ubiquitination of lysine (diglycine signature) were considered as potential modifications. False discovery rate (FDR) was determined using Percolator and proteins/peptides with a FDR of ≤1% were retained for further analysis.

References

1. Jean Beltran, P. M., Cook, K. C., and Cristea, I. M. (2017) Exploring and Exploiting Proteome Organization during Viral Infection. *J. Virol.* **91**, e00268-00217
2. Inoue, T., and Tsai, B. (2013) How viruses use the endoplasmic reticulum for entry, replication, and assembly. *Cold Spring Harb. Perspect. Biol.* **5**, a013250-a013250
3. He, B. (2006) Viruses, endoplasmic reticulum stress, and interferon responses. *Cell Death Differ.* **13**, 393-403
4. Horner, S. M., Wilkins, C., Badil, S., Iskarpatyoti, J., and Gale, M., Jr. (2015) Proteomic analysis of mitochondrial-associated ER membranes (MAM) during

RNA virus infection reveals dynamic changes in protein and organelle trafficking. *PLoS One* **10**, e0117963-e0117963
5. Chin, K. C., and Cresswell, P. (2001) Viperin (cig5), an IFN-inducible antiviral protein directly induced by human cytomegalovirus. *Proc. Natl. Acad. Sci. U. S. A.* **98**, 15125-15130
6. Seo, J.-Y., Yaneva, R., Hinson, E. R., and Cresswell, P. (2011) Human Cytomegalovirus Directly Induces the Antiviral Protein Viperin to Enhance Infectivity. *Science* **332**, 1093
7. Hinson, E. R., and Cresswell, P. (2009) The N-terminal amphipathic alpha-helix of viperin mediates localization to the cytosolic face of the endoplasmic reticulum and inhibits protein secretion. *The Journal of biological chemistry* **284**, 4705-4712
8. Eom, J., Kim, J. J., Yoon, S. G., Jeong, H., Son, S., Lee, J. B., Yoo, J., Seo, H. J., Cho, Y., Kim, K. S., Choi, K. M., Kim, I. Y., Lee, H.-Y., Nam, K. T., Cresswell, P., Seong, J. K., and Seo, J.-Y. (2019) Intrinsic expression of viperin regulates thermogenesis in adipose tissues. *Proceedings of the National Academy of Sciences* **116**, 17419
9. Hee, J. S., and Cresswell, P. (2017) Viperin interaction with mitochondrial antiviral signaling protein (MAVS) limits viperin-mediated inhibition of the interferon response in macrophages. *PLoS One* **12**, e0172236
10. Nasr, N., Maddocks, S., Turville, S. G., Harman, A. N., Woolger, N., Helbig, K. J., Wilkinson, J., Bye, C. R., Wright, T. K., Rambukwelle, D., Donaghy, H., Beard, M. R., and Cunningham, A. L. (2012) HIV-1 infection of human macrophages directly induces viperin which inhibits viral production. *Blood* **120**, 778-788
11. Nelp, M. T., Young, A. P., Stepanski, B. M., and Bandarian, V. (2017) Human Viperin Causes Radical SAM-Dependent Elongation of Escherichia coli, Hinting at Its Physiological Role. *Biochemistry* **56**, 3874-3876
12. Saitoh, T., Satoh, T., Yamamoto, N., Uematsu, S., Takeuchi, O., Kawai, T., and Akira, S. (2011) Antiviral Protein Viperin Promotes Toll-like Receptor 7- and Toll-like Receptor 9-Mediated Type I Interferon Production in Plasmacytoid Dendritic Cells. *Immunity* **34**, 352-363
13. Seo, J.-Y., and Cresswell, P. (2013) Viperin Regulates Cellular Lipid Metabolism during Human Cytomegalovirus Infection. *PLoS Pathog.* **9**, e1003497
14. Severa, M., Coccia, E. M., and Fitzgerald, K. A. (2006) Toll-like Receptor-dependent and -independent Viperin Gene Expression and Counter-regulation by PRDI-binding Factor-1/BLIMP1. *J. Biol. Chem.* **281**, 26188-26195
15. Wang, X., Hinson, E. R., and Cresswell, P. (2007) The Interferon-Inducible Protein Viperin Inhibits Influenza Virus Release by Perturbing Lipid Rafts. *Cell Host Microbe* **2**, 96-105
16. Vonderstein, K., Nilsson, E., Hubel, P., Nygård Skalman, L., Upadhyay, A., Pasto, J., Pichlmair, A., Lundmark, R., and Överby, A. K. (2018) Viperin Targets Flavivirus Virulence by Inducing Assembly of Noninfectious Capsid Particles. *J. Virol.* **92**, e01751-01717
17. Dumbrepatil, A. B., Ghosh, S., Zegalia, K. A., Malec, P. A., Hoff, J. D., Kennedy, R. T., and Marsh, E. N. G. (2019) Viperin interacts with the kinase IRAK1 and the E3 ubiquitin ligase TRAF6, coupling innate immune signaling to antiviral ribonucleotide synthesis. *J. Biol. Chem.*

18. Makins, C., Ghosh, S., Román-Meléndez, G. D., Malec, P. A., Kennedy, R. T., and Marsh, E. N. G. (2016) Does Viperin Function as a Radical S-Adenosyl-l-methionine-dependent Enzyme in Regulating Farnesylpyrophosphate Synthase Expression and Activity? *J. Biol. Chem.* **291**, 26806-26815
19. Tang, H.-B., Lu, Z.-L., Wei, X.-K., Zhong, T.-Z., Zhong, Y.-Z., Ouyang, L.-X., Luo, Y., Xing, X.-W., Liao, F., Peng, K.-K., Deng, C.-Q., Minamoto, N., and Luo, T. R. (2016) Viperin inhibits rabies virus replication via reduced cholesterol and sphingomyelin and is regulated upstream by TLR4. *Sci. Rep.* **6**, 30529-30529
20. Steinbusch, M. M. F., Caron, M. M. J., Surtel, D. A. M., van den Akker, G. G. H., van Dijk, P. J., Friedrich, F., Zabel, B., van Rhijn, L. W., Peffers, M. J., and Welting, T. J. M. (2019) The antiviral protein viperin regulates chondrogenic differentiation via CXCL10 protein secretion. *The Journal of biological chemistry* **294**, 5121-5136
21. Geiger, T., Wehner, A., Schaab, C., Cox, J., and Mann, M. (2012) Comparative proteomic analysis of eleven common cell lines reveals ubiquitous but varying expression of most proteins. *Molecular & cellular proteomics : MCP* **11**, M111.014050-M014111.014050
22. Munk, C., Sommer, A. F. R., and Konig, R. (2011) Systems-Biology Approaches to Discover Anti-Viral Effectors of the Human Innate Immune Response. *Viruses-Basel* **3**, 1112-1130
23. Cerqueira, N. M. F. S. A., Oliveira, E. F., Gesto, D. S., Santos-Martins, D., Moreira, C., Moorthy, H. N., Ramos, M. J., and Fernandes, P. A. (2016) Cholesterol Biosynthesis: A Mechanistic Overview. *Biochemistry* **55**, 5483-5506
24. Saito, K., Shirasago, Y., Suzuki, T., Aizaki, H., Hanada, K., Wakita, T., Nishijima, M., and Fukasawa, M. (2015) Targeting cellular squalene synthase, an enzyme essential for cholesterol biosynthesis, is a potential antiviral strategy against hepatitis C virus. *J. Virol.* **89**, 2220-2232
25. McCrae, C., Dzgoev, A., Ståhlman, M., Horndahl, J., Svärd, R., Große, A., Großkopf, T., Skujat, M.-A., Williams, N., Schubert, S., Echeverri, C., Jackson, C., Guedán, A., Solari, R., Vaarala, O., Kraan, M., and Rådinger, M. (2018) Lanosterol Synthase Regulates Human Rhinovirus Replication in Human Bronchial Epithelial Cells. *Am. J. Respir. Cell Mol. Biol.* **59**, 713-722
26. Schneider-Schaulies, J., and Schneider-Schaulies, S. (2013) Viral Infections and Sphingolipids. in *Sphingolipids in Disease* (Gulbins, E., and Petrache, I. eds.), Springer Vienna, Vienna. pp 321-340
27. Katsume, A., Tokunaga, Y., Hirata, Y., Munakata, T., Saito, M., Hayashi, H., Okamoto, K., Ohmori, Y., Kusanagi, I., Fujiwara, S., Tsukuda, T., Aoki, Y., Klumpp, K., Tsukiyama–Kohara, K., El–Gohary, A., Sudoh, M., and Kohara, M. (2013) A Serine Palmitoyltransferase Inhibitor Blocks Hepatitis C Virus Replication in Human Hepatocytes. *Gastroenterology* **145**, 865-873
28. Zelcer, N., Sharpe, L. J., Loregger, A., Kristiana, I., Cook, E. C. L., Phan, L., Stevenson, J., and Brown, A. J. (2014) The E3 Ubiquitin Ligase MARCH6 Degrades Squalene Monooxygenase and Affects 3-Hydroxy-3-Methyl-Glutaryl Coenzyme A Reductase and the Cholesterol Synthesis Pathway. *Mol. Cell. Biol.* **34**, 1262

Chapter 6

Significance of the Study in Probing Viperin's Anti-viral activity and Future Outlooks

A better understanding of viral infection presents major opportunities for the improvement of public health and further mechanistic studies are required for the development of antiviral therapeutics. The development of anti-viral drugs lags behind anti-bacterial drugs; therefore, a better understanding of the mechanism of action of natural antiviral agents could lead to the design of new antiviral therapeutics.

By exploring the mechanism of action of viperin we aim to establish a better understanding of the mechanisms by which eukaryotic cells inhibit viruses. To date, most studies have employed cell culture-based experiments in which the antiviral activity of the enzyme was assayed either by measuring decreases in viral titer or viral RNA levels. Consequently, it seems that the mechanism of viperin's antiviral activity differs in different viral strains. However, viperin's ability to target a broad range of viruses implies a unifying underlying mechanism. Therefore, I focused on enzymatic and biochemical approaches to address the mechanism of viperin's antiviral action at the molecular level. The involvement of radical SAM chemistry in the mammalian antiviral responsive system was unexpected and sets viperin apart from other radical SAM enzymes. My dissertation project is unique in residing at the interface of immunology and enzymology and aims to break new ground in our understanding of the innate immune system.

With the recent finding that viperin's enzymatic reaction involves the radical-mediated dehydration of CTP, the goal of my project was to find out how viperin regulates its target proteins and the relationship of this regulatory function, if any to its enzymatic activity. Here, collaborating with other Marsh laboratory members and Prof. Robert Kennedy's laboratory at the Department of Chemistry, University of Michigan, I have shown that viperin regulates cellular and viral proteins *in vivo,* clearly indicating that it may have a role in controlling metabolic and signaling pathways, along with producing antiviral ribonucleotides (ddhCTP). However, further studies must be pursued to achieve a complete insight into the mechanism of viperin in regulating various cellular pathways.

6.1 Regulation of intracellular expression of FPPS by Viperin: Following the work of Wang *et al* (2), the regulation of FPPS by viperin (3) was the starting point for our research on viperin. We demonstrated that over-expression of viperin in human embryonic kidney cells (HEK293T), reduces the intracellular accumulation of FPPS, but does not inhibit or inactivate FPPS. These results suggested that the reduction in activity of FPPS in cell lysates, as shown by Wang *et al*, is due to increased degradation of FPPS by viperin, and not because of a direct interaction between these two proteins. Mutagenesis studies on the radical SAM domain and reductive SAM cleaving activity of viperin implied that *viperin in this case may not act as a radical SAM enzyme in regulating FPPS.* However, the enzymatic activity of viperin was only measured based on the 5'-deoxyadenosine produced from the uncoupled reaction of SAM, as CTP was known to be the co-substrate of viperin at the time. Therefore, in the light of new information regarding the catalytic activity of viperin, it would be profitably to re-explore whether FPPS acts as a regulator of viperin's activity in producing the antiviral nucleotide ddhCTP.

As the localization of viperin to the endoplasmic reticulum was crucial for its inhibitory activity against FPPS, it seems that FPPS might be localized to a membrane structure in the presence of viperin. Therefore, it would be interesting investigate the cellular localization of FPPS changes when co-expressed with viperin. Moreover, the *in vivo* degradation of FPPS by viperin, as suggested by our studies, could be investigated in more detail in light of the results obtained from our proteomics study that found that viperin interactd with several ERAD-associated ubiquitin ligases.

6.2 Inactivation of viperin's enzymatic activity to produce 5'-deoxyadenosine through the interaction with viral protein NS5A and VAP-33. Although the involvement of radical chemistry in the regulation of FPPS by viperin was ruled out, it is still possible that radical SAM chemistry plays a role in viperin's regulation of other protein targets. The viral protein NS5A, a potential protein target of viperin (4,5), is known for its importance in regulating viral replication of hepatitis C virus (HCV) (6-9). As viperin was shown to limit viral replication by producing the antiviral nucleotide ddhCTP, we undertook experiments to investigate how viperin's catalytic activity is altered when interacting with NS5A. We showed that the interaction between viperin and NS5A in the presence of an adaptor protein VAP33 leads to the degradation of NS5A through proteosomal degradation pathway. However, interestingly, co-expression of NS5A and VAP-33 with viperin reduced the enzyme's activity, suggesting that NS5A may have evolved to bind viperin as a strategy to reduce ddhCTP synthesis and thereby reduce the possibility of the replication complex introducing this chain-terminating nucleotide during genome synthesis.

These results pose new questions regarding whether viperin regulates the interaction of NS5A with viral polymerase NS5B within the HCV replication complex to control the viral replication process. Re-constitution of the protein-complex between viperin, NS5A and other components in the replication complex *in vivo* may reveal insights of the regulatory features of viperin on NS5A.

Because the membrane localization of viperin, NS5A and VAP-33 is important for the interaction of these proteins and the inhibition of viperin's activity, the expression and purification of these proteins using a nanodisc system would greatly facilitate their study. Formation of the nanodiscs of viperin can be achieved by slowly removing detergent from the solution while incubating cell lysate expressing viperin with membrane scaffolding proteins and phospholipids. This method can be applied to cell lysate co-expressing viperin with its interacting proteins, especially membrane bound protein partners NS5A and VAP-33, enabling the formation of the protein complex within the nanodiscs. In this way, the biologically significant complex between viperin, NS5A and VAP-33 could be isolated *in vitro* and the enzymatic activity of viperin investigated.

6.3 Activation of viperin's activity by Toll-like receptor signaling proteins IRAK1 and TRAF6. Following the work of Saitoh *et al* (10), we investigated how viperin's enzymatic activity is regulated by the innate immune signaling protein partners, IRAK1 and TRAF6. Reconstituting the interactions between viperin, IRAK1 and TRAF6 by transiently expressing these enzymes in HEK 293T cells, we showed that IRAK1 and TRAF6 increase viperin activity by ~10-fold to efficiently catalyze the radical-mediated dehydration of CTP to ddhCTP. Furthermore, we found that TRAF6-mediated ubiquitination of IRAK1 requires the association of viperin with both IRAK1 and TRAF6.

However, to exclude the possibilities that the change in viperin's activity by IRAK1 and TRFA6 is not aided by other proteins in HEK293T cells, further studies with purified enzymes will be needed to validate this mechanistic proposal. The modification of ubiquitination level of IRAK1 by TRFA6 in the presence of viperin may be also investigated further with the purified proteins. As IRAK1 and TRAF6 are known interaction partners of viperin, structural studies on viperin with CTP, in the presence of these purified signaling proteins may reveal the binding site conformation of the biologically significant protein-small molecule complex.

6.4 Interactome analysis of viperin and identification of cholesterol biosynthesis proteins. It is clear from the results from Chapter 2 that viperin does not directly interact with or inactivate FPPS. We hypothesize that viperin may recruit additional proteins in degrading FPPS. To this end, the pathway analysis of viperin and obtaining a complete inventory of interacting protein partners through proteomics methods assumes new importance. This was achieved by the proteomics study on the immunoprecipitated viperin.

The initial proteomic analysis of viperin interaction partners indicates that it interacts with various proteins involved in cholesterol and lipid biosynthesis and in regulatory pathways. Enrichment of cholesterol biosynthesis proteins in the *interactome* indicated that viperin might exert its antiviral activity by controlling cellular cholesterol levels and thereby retardi the viral assembly and budding process. Various ubiquitin-conjugating enzymes were also found in the "interactome" of viperin, strengthening the idea that viperin is involved in ubiquitin-mediated signaling or degradation pathway.

The interaction between viperin and the cholesterol biosynthesis enzymes may be further validated by co-expressing these proteins with viperin *in vivo* and monitoring how viperin alters their cellular expression and localization. For example, the two most highly enriched cholesterol biosynthetic enzymes, lanosterol synthase and squalene monooxygenase may be considered as two potential targets of viperin. It would be valuable to see if viperin reduces the enzymatic activity of these enzymes in catalyzing various steps in the cholesterol synthesis. Changes in the activity of these enzymes as a result of their interaction with viperin might also be investigated in a cell free environment using purified enzymes. Simultaneously, the changes to the catalytic activity of viperin while bound to the cholesterol biosynthetic enzymes, can be also explored.

Apart from the functional annotation of the proteins observed in the interactome of viperin, a further extensive analysis of the sequence and the structure of the proteins may reveal a common structural motif that viperin binds to or common post-translational modification performed by viperin on its protein targets. This may provide important structural insights of the binding site of viperin while forming complex with the interacting.

Considering previous studies by other groups and the results obtained in our studies on viperin, it seems viperin exerts its antiviral activity in two ways. Firstly, viperin likely directly inhibits the viral genomic replication by producing antiviral nucleotide ddhCTP. Additionally, viperin acts as a regulatory protein in cellular pathways involved in viral pathogenesis, by interacting with cellular or viral proteins. However, our study also suggested that these two functions are inter-related and equally contribute towards potentiating viperin’s antiviral activity.

The interplay between these two functions of viperin may be explored further by investigating the biological effects of antiviral nucleotide ddhCTP more broadly. It might be possible that viperin modifies ddhCTP further to an epoxy-containing nucleotide which may act as an antiviral nucleotide analog against a broader range of viruses beyond flaviviruses ***[Figure 6.1].*** Alternatively, viperin could also employ this epoxy-nucleotide to covalently modify nucleophilic protein sidechains through Michael addition to the electrophilic epoxide. To this end, identification, characterization and isolation of the modified nucleotide (ddhCTP or the epoxy-analog of ddhCTP) is required.

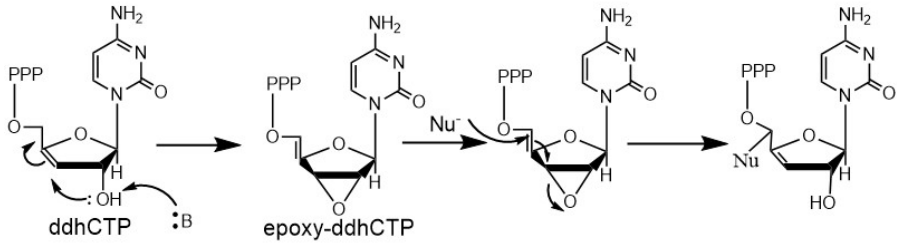

Figure 6.1: Schematic diagram of conversion of ddhCTP to epoxy-ddhCTP and Michael addition of nucleophilic side chain residues of protein

Native mass spectrometry could be used to identify the complex formed between viperin and its product. Furthermore, the kinetics of ddhCTP formation (or its analogs) catalyzed by viperin in the presence of its interacting proteins would be informative to investigate. Such studies are essential to understand the regulation of viperin by its interacting proteins. Ultimately, structural studies on viperin with the modified nucleotides, co-crystalized with its interacting protein partner, may provide insights of the binding conformation of protein-protein and enzyme-substrate or enzyme-product complex.

Taking these approaches, we may advance the prospect of establishing a unifying mechanism underlying the role of viperin in regulating the antiviral response. Furthermore, this may lead to developing the antiviral therapeutics, mimicking the modified nucleotide, generated by viperin.

References

1. Gizzi, A. S., Grove, T. L., Arnold, J. J., Jose, J., Jangra, R. K., Garforth, S. J., Du, Q., Cahill, S. M., Dulyaninova, N. G., Love, J. D., Chandran, K., Bresnick, A. R., Cameron, C. E., and Almo, S. C. (2018) A naturally occurring antiviral ribonucleotide encoded by the human genome. *Nature* **558**, 610-614

2. Wang, X., Hinson, E. R., and Cresswell, P. (2007) The Interferon-Inducible Protein Viperin Inhibits Influenza Virus Release by Perturbing Lipid Rafts. *Cell Host Microbe* **2**, 96-105

3. Makins, C., Ghosh, S., Román-Meléndez, G. D., Malec, P. A., Kennedy, R. T., and Marsh, E. N. G. (2016) Does Viperin Function as a Radical S-Adenosyl-l-methionine-dependent Enzyme in Regulating Farnesylpyrophosphate Synthase Expression and Activity? *J. Biol. Chem.* **291**, 26806-26815

4. Helbig, K. J., Eyre, N. S., Yip, E., Narayana, S., Li, K., Fiches, G., McCartney, E. M., Jangra, R. K., Lemon, S. M., and Beard, M. R. (2011) The antiviral protein viperin inhibits hepatitis C virus replication via interaction with nonstructural protein 5A. *Hepatology* **54**, 1506-1517

5. Wang, S., Wu, X., Pan, T., Song, W., Wang, Y., Zhang, F., and Yuan, Z. (2012) Viperin inhibits hepatitis C virus replication by interfering with binding of NS5A to host protein hVAP-33. *J. Gen. Virol.* **93**, 83-92

6. Foster, T. L., Belyaeva, T., Stonehouse, N. J., Pearson, A. R., and Harris, M. (2010) All three domains of the hepatitis C virus nonstructural NS5A protein contribute to RNA binding. *J. Virol.* **84**, 9267-9277

7. Reyes, G. R. (2002) The nonstructural NS5A protein of hepatitis C virus: An expanding, multifunctional role in enhancing hepatitis C virus pathogenesis. *J. Biomed. Sci.* **9**, 187-197

8. Shimakami, T., Hijikata, M., Luo, H., Ma, Y. Y., Kaneko, S., Shimotohno, K., and Murakami, S. (2004) Effect of Interaction between Hepatitis C Virus NS5A and NS5B on Hepatitis C Virus RNA Replication with the Hepatitis C Virus Replicon. *J. Virol.* **78**, 2738-2748

9. Shirota, Y., Luo, H., Qin, W., Kaneko, S., Yamashita, T., Kobayashi, K., and Murakami, S. (2002) Hepatitis C Virus (HCV) NS5A Binds RNA-dependent RNA Polymerase (RdRP) NS5B and Modulates RNA-dependent RNA Polymerase Activity. *J. Biol. Chem.* **277**, 11149-11155

10. Saitoh, T., Satoh, T., Yamamoto, N., Uematsu, S., Takeuchi, O., Kawai, T., and Akira, S. (2011) Antiviral Protein Viperin Promotes Toll-like Receptor 7- and Toll-like Receptor 9-Mediated Type I Interferon Production in Plasmacytoid Dendritic Cells. *Immunity* **34**, 352-363

APPENDICES

Appendix A1: Gene sequences of proteins used in this study

A1.1 Viperin:

ATGTGGGTGCTTACACCTGCTGCTTTTGCTGGGAAGCTCTTGAGTGTGTTCAGGCA
ACCTCTGAGCTCTCTGTGGAGGAGCCTGGTCCCGCTGTTCTGCTGGCTGAGGGCA
ACCTTCTGGCTGCTAGCTACCAAGAGGAGAAAGCAGCAGCTGGTCCTGAGAGGGC
CAGATGAGACCAAAGAGGAGGAAGAGGACCCTCCTCTGCCCACCACCCCAACCA
GCGTCAACTATCACTTCACTCGCCAGTGCAACTACAAATGCGGCTTCTGTTTCCAC
ACAGCCAAAACATCCTTTGTGCTGCCCCTTGAGGAAGCAAAGAGAGGATTGCTTTT
GCTTAAGGAAGCTGGTATGGAGAAGATCAACTTTTCAGGTGGAGAGCCATTTCTTC
AAGACCGGGGAGAATACCTGGGCAAGTTGGTGAGGTTCTGCAAAGTAGAGTTGCG
GCTGCCCAGCGTGAGCATCGTGAGCAATGGAAGCCTGATCCGGGAGAGGTGGTT
CCAGAATTATGGTGAGTATTTGGACATTCTCGCTATCTCCTGTGACAGCTTTGACG
AGGAAGTCAATGTCCTTATTGGCCGTGGCCAAGGAAAGAAGAACCATGTGGAAAA
CCTTCAAAAGCTGAGGAGGTGGTGTAGGGATTATAGAGTCGCTTTCAAGATAAATT
CTGTCATTAATCGTTTCAACGTGGAAGAGGACATGACGGAACAGATCAAAGCACTA
AACCCTGTCCGCTGGAAAGTGTTCCAGTGCCTCTTAATTGAGGGTGAGAATTGTGG
AGAAGATGCTCTAAGAGAAGCAGAAAGATTTGTTATTGGTGATGAAGAATTTGAAA
GATTCTTGGAGCGCCACAAAGAAGTGTCCTGCTTGGTGCCTGAATCTAACCAGAA
GATGAAAGACTCCTACCTTATTCTGGATGAATATATGCGCTTTCTGAACTGTAGAAA
GGGACGGAAGGACCCTTCCAAGTCCATCCTGGATGTTGGTGTAGAAGAAGCTATA
AAATTCAGTGGATTTGATGAAAAGATGTTTCTGAAGCGAGGAGGAAAATACATATG
GAGTAAGGCTGATCTGAAGCTGGATTGGTAG

A1.2 Viperin-ΔN50:

CTAGTGCTGCGCGGTCCGGATGAAACCAAAGAAGAAGAAGAAGATCCGCCGCTGC
CGACCACGCCGACCTCAGTTAACTATCATTTTACGCGTCAGTGTAATTACAAATGC
GGCTTTTGTTTCCACACCGCGAAAACGTCGTTCGTGCTGCCGCTGGAAGAAGCGA
AACGTGGTCTGCTGCTGCTGAAAGAAGCCGGCATGGAAAAAATTAACTTTTCAGGC
GGTGAACCGTTCCTGCAGGATCGCGGTGAATATCTGGGCAAACTGGTTCGTTTTTG
CAAAGTCGAACTGCGCCTGCCGAGCGTTTCTATTGTCTCAAACGGTTCGCTGATCC
GTGAACGCTGGTTTCAAAATTATGGCGAATACCTGGATATTCTGGCCATCAGCTGC
GATTCTTTCGACGAAGAAGTGAACGTTCTGATCGGCCGCGGTCAGGGCAAGAAAA
ACCATGTCGAAAATCTGCAAAAACTGCGTCGCTGGTGTCGTGATTACCGCGTTGCA
TTCAAAATCAACTCCGTGATCAACCGTTTCAATGTTGAAGAAGACATGACCGAACA

GATTAAAGCTCTGAACCCGGTGCGCTGGAAAGTTTTTCAATGCCTGCTGATCGAAG
GTGAAAATTGTGGCGAAGATGCGCTGCGTGAAGCCGAACGCTTCGTGATTGGTGA
CGAAGAATTTGAACGTTTCCTGGAACGCCACAAAGAAGTCAGTTGCCTGGTGCCG
GAATCCAACCAGAAAATGAAAGATAGCTATCTGATCCTGGACGAATACATGCGTTT
TCTGAATTGTCGTAAAGGCCGCAAAGATCCGAGTAAATCCATTCTGGACGTCGGTG
TGGAAGAAGCGATCAAATTTTCTGGCTTCGATGAAAAAATGTTCCTGAAACGTGGT
GGCAAATACATCTGGAGCAAAGCCGACCTGAAACTGGATTGGTGA

A1.3 FPPS:

ATGAACGGAGACCAGAATTCAGATGTTTATGCCCAAGAAAAGCAGGATTTCGTTCA
GCACTTCTCCCAGATCGTTAGGGTGCTGACTGAGGATGAGATGGGGCACCCAGAG
ATAGGAGATGCTATTGCCCGGCTCAAGGAGGTCCTGGAGTACAATGCCATTGGAG
GCAAGTATAACCGGGGTTTGACGGTGGTAGTAGCATTCCGGGAGCTGGTGGAGC
CAAGGAAACAGGATGCTGATAGTCTCCAGCGGGCCTGGACTGTGGGCTGGTGTGT
GGAACTGCTGCAAGCTTTCTTCCTGGTGGCAGATGACATCATGGATTCATCCCTTA
CCCGCCGGGGACAGACCTGCTGGTATCAGAAGCCGGGCGTGGGTTTGGATGCCA
TCAATGATGCTAACCTCCTGGAAGCATGTATCTACCGCCTGCTGAAGCTCTATTGC
CGGGAGCAGCCCTATTACCTGAACCTGATCGAGCTCTTCCTGCAGAGTTCCTATCA
GACTGAGATTGGGCAGACCCTGGACCTCCTCACAGCCCCCCAGGGCAATGTGGAT
CTTGTCAGATTCACTGAAAAGAGGTACAAATCTATTGTCAAGTACAAGACAGCTTTC
TACTCCTTCTACCTTCCTATAGCTGCAGCCATGTACATGGCAGGAATTGATGGCGA
GAAGGAGCACGCCAATGCCAAGAAGATCCTGCTGGAGATGGGGGAGTTCTTTCAG
ATTCAGGATGATTACCTTGACCTCTTTGGGGACCCCAGTGTGACCGGCAAAATTGG
CACTGACATCCAGGACAACAAATGCAGCTGGCTGGTGGTTCAGTGTCTGCAACGG
GCCACTCCAGAACAGTACCAGATCCTGAAGGAAAATTACGGGCAGAAGGAGGCTG
AGAAAGTGGCCCGGGTGAAGGCGCTATATGAGGAGCTGGATCTGCCAGCAGTGTT
CTTGCAATATGAGGAAGACAGTTACAGCCACATTATGGCTCTCATTGAACAGTACG
CAGCACCCCTGCCCCCAGCCGTCTTTCTGGGGCTTGCGCGCAAAATCTACAAGCG
GAGAAAGTGA

A.1.4 NS5A:

ATCTTGTCCGGCTCGTGGCTAAGGGATGTTTGGGATTGGATATGCACGGTGTTGA
CTGACTTCAAGACCTGGCTCCAGTCCAAACTCCTGCCGCGGTTACCGGGAGTCCC
TTTCCTGTCATGCCAACGCGGGTACAAGGGAGTCTGGCGGGGGGGACGGCATCAT
GCAAACCACCTGCCCATGCGGAGCACAGATCGCCGGACATGTCAAAAACGGTTCC
ATGAGGATCGTAGGGCCTAGAACCTGCAGCAACACGTGGCACGGAACGTTCCCCA
TCAACGCATACACCACGGGACCTTGCACACCCTCCCCGGCGCCCAACTATTCCAG
GGCGCTATGGCGGGTGGCTGCTGAGGAGTACGTGGAGGTTACGCGTGTGGGGGA
TTTCCACTACGTGACGGGCATGACCACTGACAACGTAAAGTGCCCATGCCAGGTT
CCGGCCCCCGAATTCTTCACGGAGGTGGATGGAGTGCGGTTGCACAGGTACGCT
CCGGCGTGCAAACCTCTTCTACGGGAGGACGTCACGTTCCAGGTCGGGCTCAACC

AATACTTGGTCGGGTCGCAGCTCCCATGCGAGCCCGAACCGGACGTAACAGTGCT
TACTTCCATGCTCACCGATCCCTCCCACATTACAGCAGAGACGGCTAAGCGTAGG
CTGGCTAGAGGGTCTCCCCCCTCTTTAGCCAGCTCATCAGCTAGCCAGTTGTCTG
CGCCTTCTTTGAAGGCGACATGCACTACCCACCATGACTCCCCGGACGCTGACCT
CATCGAGGCCAACCTCTTGTGGCGGCAGGAGATGGGCGGAAACATCACTCGCGT
GGAGTCAGAGAATAAGGTAGTAATTCTGGACTCTTTCGAACCGCTTCACGCGGAG
GGGGATGAGAGGGAGATATCCGTCGCGGCGGAGATCCTGCGAAAATCCAGGAAG
TTCCCCTCAGCGTTGCCCATATGGGCACGCCCGGACTACAATCCTCCACTGCTAG
AGTCCTGGAAGGACCCGGACTACGTCCCTCCGGTGGTACACGGATGCCCATTGCC
ACCTACCAAGGCTCCTCCAATACCACCTCCACGGAGAAAGAGGACGGTTGTCCTG
ACAGAATCCAATGTGTCTTCTGCCTTGGCGGAGCTCGCCACTAAGACCTTCGGTAG
CTCCGGATCGTCGGCCGTTGATAGCGGCACGGCGACCGCCCTTCCTGACCTGGC
CTCCGACGACGGTGACAAAGGATCCGACGTTGAGTCGTACTCCTCCATGCCCCCC
CTTGAAGGGGAGCCGGGGGACCCCGATCTCAGCGACGGGTCTTGGTCTACCGTG
AGTGAGGAGGCTAGTGAGGATGTCGTCTGCTGCTAG

A 1.5 VAP-33 (from China):

CNCNNCTGTAGCTGGTNCGAGCTCGGATCCCATGGACTACAAAGACCATGACGGT
GATTATAAAGATCATGACATCGATTACAAGGATGACGATGACAAGCTTGAATTCATG
GCGAAGCACGAGCAGATCCTGGTCCTCGATCCGCCCACAGACCTCAAATTCAAAG
GCCCCTTCACAGATGTAGTCACTACAAATCTTAAATTGCGAAATCCATCGGATAGA
AAAGTGTGTTTCAAAGTGAAGACTACAGCACCTCGCCGGTACTGTGTGAGGCCCA
ACAGTGGAATTATTGACCCAGGGTCAACTGTGACTGTTTCAGTAATGCTACAGCCC
TTTGACTATGATCCGAATGAAAAGAGTAAACACAAGTTTATGGTACAGACAATTTTT
GCTCCACCAAACACTTCAGATATGGAAGCTGTGTGGAAAGAGGCAAAACCTGATG
AATTAATGGATTCCAAATTGAGATGCGTATTTGAAATGCCCAATGAAAATGATAAAT
TGAATGATATGGAACCTAGCAAAGCTGTTCCACTGAATGCATCTAAGCAAGATGGA
CCTATGCCAAAACCACACAGTGTTTCACTTAATGATACCGAAACAAGGAAACTAAT
GGAAGAGTGTAAAAGACTTCAGGGAGAAATGATGAAGCTATCAGAAGAAAATCGG
CACCTGAGAGATGAAGGTTTAAGGCTCAGAAAGGTAGCACATTCGGATAAACCTG
GATCAACCTCAACTGCATCCTTCAGAGATAATGTCACCAGTCCTCTTCCTTCACTTC
TTGTTGTAATTGCAGCCATTTTCATTGGATTCTTTCTAGGGAAATTCATCTTGTAGCT
CGAGTCTAGAGGGCCCTTCGAACAAAAACTCATCTCAGAAGAGGATCTGAATATGC
ATACCGGTCATCATCACCATCACCATTGAGTTTAAACCCCGCTGATCAGCCTCGAC
TGTGCCTTCTAGTTGCCAGCCATCTGTTGGTTNGCCCCCTCCCCCGGGNCCTTCC
TTGACCCCTGGAANGGNGCCACTCCCCCTGGCCCTTTCCTAAATAAAATNGAGGA
AATTGCCCTCCCCATTGNTCTGAAGTAGGGNNTCATTCTATTTTTGGGGGGGGNG
GGGGGGGGNCAGGACACCCANGGGGGGAGGAATTGGGAAAAANAAAAANCAGN
CNTNCNTGGGGAATGNGGNGGGCCTNT

A 1.6 TRAF6:

GAATTCATGAGTCTGCTAAACTGTGAAAACAGCTGTGGATCCAGCCAGTCTGAAAG
TGACTGCTGTGTGGCCATGGCCAGCTCCTGTAGCGCTGTAACAAAAGATGATAGT

GTGGGTGGAACTGCCAGCACGGGGAACCTCTCCAGCTCATTTATGGAGGAGATCC
AGGGATATGATGTAGAGTTTGACCCACCCCTGGAAAGCAAGTATGAATGCCCCATC
TGCTTGATGGCATTACGAGAAGCAGTGCAAACGCCATGCGGCCATAGGTTCTGCA
AAGCCTGCATCATAAAATCAATAAGGGATGCAGGTCACAAATGTCCAGTTGACAAT
GAAATACTGCTGGAAAATCAACTATTTCCAGACAATTTTGCAAAACGTGAGATTCTT
TCTCTGATGGTGAAATGTCCAAATGAAGGTTGTTTGCACAAGATGGAACTGAGACA
TCTTGAGGATCATCAAGCACATTGTGAGTTTGCTCTTATGGATTGTCCCCAATGCCA
GCGTCCCTTCCAAAAATTCCATATTAATATTCACATTCTGAAGGATTGTCCAAGGAG
ACAGGTTTCTTGTGACAACTGTGCTGCATCAATGGCATTTGAAGATAAAGAGATCC
ATGACCAGAACTGTCCTTTGGCAAATGTCATCTGTGAATACTGCAATACTATACTCA
TCAGAGAACAGATGCCTAATCATTATGATCTAGACTGCCCTACAGCCCCAATTCCA
TGCACATTCAGTACTTTTGGTTGCCATGAAAAGATGCAGAGGAATCACTTGGCACG
CCACCTACAAGAGAACACCCAGTCACACATGAGAATGTTGGCCCAGGCTGTTCATA
GTTTGAGCGTTATACCCGACTCTGGGTATATCTCAGAGGTCCGGAATTTCCAGGAA
ACTATTCACCAGTTAGAGGGTCGCCTTGTAAGACAAGACCATCAAATCCGGGAGCT
GACTGCTAAAATGGAAACTCAGAGTATGTATGTAAGTGAGCTCAAACGAACCATTC
GAACCCTTGAGGACAAAGTTGCTGAAATCGAAGCACAGCAGTGCAATGGAATTTAT
ATTTGGAAGATTGGCAACTTTGGAATGCATTTGAAATGTCAAGAAGAGGAGAAACC
TGTTGTGATTCATAGCCCTGGATTCTACACTGGCAAACCCGGGTACAAACTGTGCA
TGCGCTTGCACCTTCAGTTACCGACTGCTCAGCGCTGTGCAAACTATATATCCCTT
TTTGTCCACACAATGCAAGGAGAATATGACAGCCACCTCCCTTGGCCCTTCCAGG
GTACAATACGCCTTACAATTCTTGATCAGTCTGAAGCACCTGTAAGGCAAAACCAC
GAAGAGATAATGGATGCCAAACCAGAGCTGCTTGCTTTCCAGCGACCCACAATCC
CACGGAACCCAAAAGGTTTTGGCTATGTAACTTTTATGCATCTGGAAGCCCTAAGA
CAAAGAACTTTCATTAAGGATGACACATTATTAGTGCGCTGTGAGGTCTCCACCCG
CTTTGACATGGGTAGCCTTCGGAGGGAGGGTTTTCAGCCACGAAGTACTGATGCA
GGGGTATAGCTCGAG

A 1.7 IRAK1:

GAATTCATGGCCGGGGGGCCGGGCCCGGGGGAGCCCGCAGCCCCCGGCGCCCA
GCACTTCTTGTACGAGGTGCCGCCCTGGGTCATGTGCCGCTTCTACAAAGTGATG
GACGCCCTGGAGCCCGCCGACTGGTGCCAGTTCGCCGCCCTGATCGTGCGCGAC
CAGACCGAGCTGCGGCTGTGCGAGCGCTCCGGGCAGCGCACGGCCAGCGTCCT
GTGGCCCTGGATCAACCGCAACGCCCGTGTGGCCGACCTCGTGCACATCCTCAC
GCACCTGCAGCTGCTCCGTGCGCGGGACATCATCACAGCCTGGCACCCTCCCGC
CCCGCTTCCGTCCCCAGGCACCACTGCCCCGAGGCCCAGCAGCATCCCTGCACC
CGCCGAGGCCGAGGCCTGGAGCCCCCGGAAGTTGCCATCCTCAGCCTCCACCTT
CCTCTCCCCAGCTTTTCCAGGCTCCCAGACCCATTCAGGGCCTGAGCTCGGCCTG
GTCCCAAGCCCTGCTTCCCTGTGGCCTCCACCGCCATCTCCAGCCCCTTCTTCTAC
CAAGCCAGGCCCAGAGAGCTCAGTGTCCCTCCTGCAGGGAGCCCGCCCCTTTCC
GTTTTGCTGGCCCCTCTGTGAGATTTCCCGGGGCACCCACAACTTCTCGGAGGAG

CTCAAGATCGGGGAGGGTGGCTTTGGGTGCGTGTACCGGGCGGTGATGAGGAAC
ACGGTGTATGCTGTGAAGAGGCTGAAGGAGAACGCTGACCTGGAGTGGACTGCA
GTGAAGCAGAGCTTCCTGACCGAGGTGGAGCAGCTGTCCAGGTTTCGTCACCCAA
ACATTGTGGACTTTGCTGGCTACTGTGCTCAGAACGGCTTCTACTGCCTGGTGTAC
GGCTTCCTGCCCAACGGCTCCCTGGAGGACCGTCTCCACTGCCAGACCCAGGCC
TGCCCACCTCTCTCCTGGCCTCAGCGACTGGACATCCTTCTGGGTACAGCCCGGG
CAATTCAGTTTCTACATCAGGACAGCCCCAGCCTCATCCATGGAGACATCAAGAGT
TCCAACGTCCTTCTGGATGAGAGGCTGACACCCAAGCTGGGAGACTTTGGCCTGG
CCCGGTTCAGCCGCTTTGCCGGGTCCAGCCCCAGCCAGAGCAGCATGGTGGCCC
GGACACAGACAGTGCGGGGCACCCTGGCCTACCTGCCCGAGGAGTACATCAAGA
CGGGAAGGCTGGCTGTGGACACGGACACCTTCAGCTTTGGGGTGGTAGTGCTAG
AGACCTTGGCTGGTCAGAGGGCTGTGAAGACGCACGGTGCCAGGACCAAGTATCT
GAAAGACCTGGTGGAAGAGGAGGCTGAGGAGGCTGGAGTGGCTTTGAGAAGCAC
CCAGAGCACACTGCAAGCAGGTCTGGCTGCAGATGCCTGGGCTGCTCCCATCGC
CATGCAGATCTACAAGAAGCACCTGGACCCCAGGCCCGGGCCCTGCCCACCTGA
GCTGGGCCTGGGCCTGGGCCAGCTGGCCTGCTGCTGCCTGCACCGCCGGGCCA
AAAGGAGGCCTCCTATGACCCAGGTGTACGAGAGGCTAGAGAAGCTGCAGGCAG
TGGTGGCGGGGGTGCCCGGGCATTCGGAGGCCGCCAGCTGCATCCCCCCTTCCC
CGCAGGAGAACTCCTACGTGTCCAGCACTGGCAGAGCCCACAGTGGGGCTGCTC
CATGGCAGCCCCTGGCAGCGCCATCAGGAGCCAGTGCCCAGGCAGCAGAGCAGC
TGCAGAGAGGCCCCAACCAGCCCGTGGAGAGTGACGAGAGCCTAGGCGGCCTCT
CTGCTGCCCTGCGCTCCTGGCACTTGACTCCAAGCTGCCCTCTGGACCCAGCACC
CCTCAGGGAGGCCGGCTGTCCTCAGGGGGACACGGCAGGAGAATCGAGCTGGG
GGAGTGGCCCAGGATCCCGGCCCACAGCCGTGGAAGGACTGGCCCTTGGCAGCT
CTGCATCATCGTCGTCAGAGCCACCGCAGATTATCATCAACCCTGCCCGACAGAA
GATGGTCCAGAAGCTGGCCCTGTACGAGGATGGGGCCCTGGACAGCCTGCAGCT
GCTGTCGTCCAGCTCCCTCCCAGGCTTGGGCCTGGAACAGGACAGGCAGGGGCC
CGAAGAAAGTGATGAATTTCAGAGCTGACTCGAG

Appendix A2: Generation of standard curve to measure the amount of viperin present in the HEK293T cell lysate for reductive SAM assay

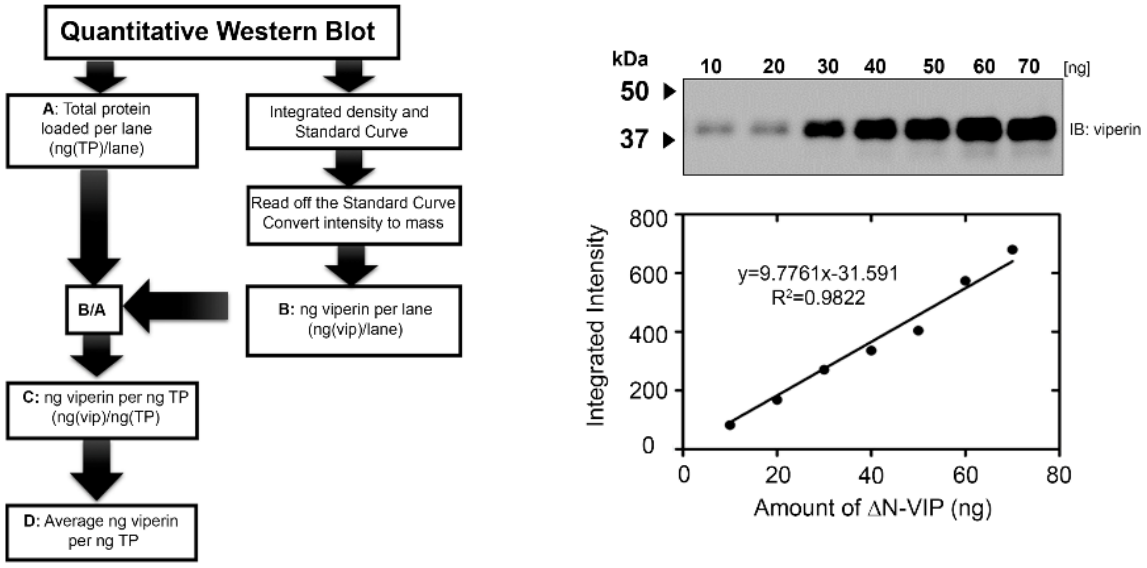

Appendix A2:

Figure A2 *(Left)* Flowchart illustrating the procedure used to determine the amount of viperin in HEK 293T lysates. *(Right)* Representative standard curve constructed from increasing concentrations of purified ΔN-viperin, visualize by immunoblotting and quantified. The standard curve was used to estimate the concentration of viperin in HEK cell lysates for assessing reductive SAM cleaving activity.

Appendix A3: Calculation of turnover number of viperin and viperin-ΔN50 in the presence of NS5A and VAP-33

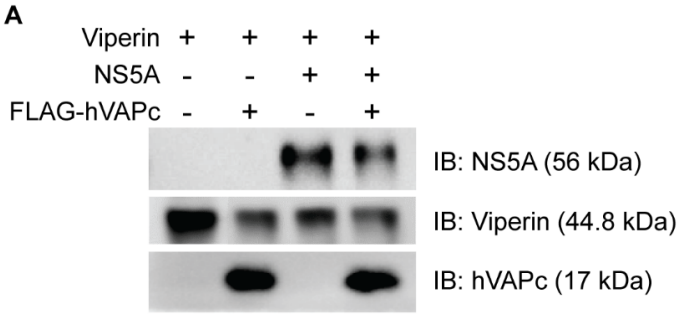

	5'dA (pmol)	Viperin (pmol)	Specific Activity (hr^{-1})
Viperin	3.58 ± 0.22	0.50 ± 0.05	7.60 ± 0.57
Viperin + hVAPc	1.92 ± 0.11	0.15 ± 0.02	13.07 ± 1.07
Viperin + NS5A	2.70 ± 0.20	0.32 ± 0.03	8.38 ± 0.70
Viperin + hVAPc + NS5A	0.72 ± 0.07	0.18 ± 0.01	3.95 ± 0.38

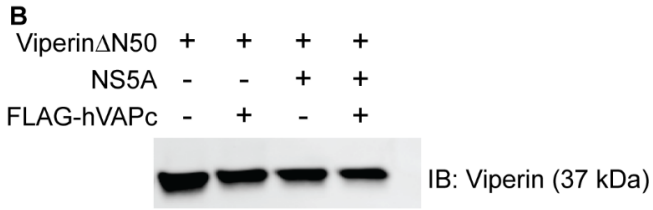

	5'dA (pmol)	Viperin (pmol)	Specific Activity (hr^{-1})
ViperinΔN50	1.00± 0.06	1.44± 0.08	0.69± 0.04
ViperinΔN50 + hVAPc	0.77 ± 0.05	1.1 ± 0.06	0.69 ± 0.05
ViperinΔN50 + NS5A	0.48 ± 0.08	0.98± 0.06	0.49 ± 0.08
ViperinΔN50 + hVAPc + NS5A	0.32± 0.04	0.66± 0.04	0.49 ± 0.06

Appendix A3: Co-expression of NS5A and VAP-33C inhibits reductive SAM cleavage activity of Viperin in HEK293T cell-lysates.

Figure A3 (A) Immunoblotting of vipeirn, NS5A and VAP-33C present in the samples. **(B)** Immunoblotting of viperinΔN50, in the presence of NS5A and VAP-33C in HEK293T cells.

Table A3 (A) The relative activity was of viperin was determined by the ratio of 5'-deoxyadenosine produced to amount of viperin present in the sample per hour. **(B)** Calculation of specific activity of viperinΔN50, determined by the ratio of 5'-deoxyadenosine produced to amount of viperin present in the sample per hour.

Appendix A4: Calculation of turnover number of viperin in the presence of TRAF6 and IRAK1

	5'dA (pmol)	Viperin (pmol)	Turnover (h^{-1})
Viperin	1.30 ± 0.01	1.38 ± 0.07	0.94 ± 0.04
Viperin +TRAF6	1.27 ± 0.01	1.10 ± 0.06	1.15 ± 0.06
Viperin + IRAK1	1.49 ± 0.02	0.70 ± 0.04	2.13 ± 0.13
Viperin +IRAK1+ TRAF6	1.72 ± 0.03	0.40 ± 0.02	4.30 ± 0.22
Viperin +CTP	3.10 ± 0.15	1.38 ± 0.07	2.25 ± 0.16
Viperin + IRAK1+CTP	5.09 ± 0.17	0.70 ± 0.04	7.27 ± 0.48
Viperin +IRAK1+ TRAF6+CTP	8.55 ± 0.48	0.40 ± 0.02	21.4 ± 1.6

Table A4: Calculation of specific activity of viperin in the presence of TRAF6 and IRAK1. The relative activity was of viperin was determined by the ratio of 5'-deoxyadenosine produced to amount of viperin present in the sample per hour.

Appendix A5: List of proteins as potential candidates for the interactome of viperin

PROTID	GENE	Descripton	Fold change_1	Fold Change_2	Fold Change_3	SAINT Score
Q8WXG1	RSAD2	Radical S-adenosyl methionine domain-containing protein 2 [OS=Homo sapiens]	388	431	455	
P48449	LSS	lanosterol synthase [OS=Homo sapiens]	53	27.5	29.5	1
Q14534	SQLE	squalene monooxygenase [OS=Homo sapiens]	18.5	18.5	52	1
Q6ZRQ5	MMS22L	Protein MMS22-like [OS=Homo sapiens]	22	24	28	1
Q6NUQ4	TMEM214	Transmembrane protein 214 [OS=Homo sapiens]	31	17.5	28	1
Q9UHG3	PCYOX1	prenylcysteine oxidase 1 [OS=Homo sapiens]	19	23	28	1
O95470	SGPL1	sphingosine-1-phosphate lyase 1 [OS=Homo sapiens]	19	24	22	1
P07099	EPHX1	epoxide hydrolase 1 [OS=Homo sapiens]	18	19	24	1
O94830	DDHD2	Phospholipase DDHD2 [OS=Homo sapiens]	14.5	33	19	1
Q9H497	TOR3A	Torsin-3A [OS=Homo sapiens]	17.5	17.5	21	1
Q9H6V9	LDAH	Isoform 2 of Lipid droplet-associated hydrolase [OS=Homo sapiens]	20	14	24	1
Q96AD5	PNPLA2	Patatin-like phospholipase domain-containing protein 2 [OS=Homo sapiens]	16	17	15	1
P23786	CPT2	Carnitine O-palmitoyltransferase 2, mitochondrial [OS=Homo sapiens]	16	12.33333333	20.5	1
Q15738	NSDHL	sterol-4-alpha-carboxylate 3-dehydrogenase, decarboxylating [OS=Homo sapiens]	17	16	13.4	1
Q9H3N1	TMX1	Thioredoxin-related transmembrane protein 1 [OS=Homo sapiens]	12	14	17	1
Q9HDC9	APMAP	Adipocyte plasma membrane-associated protein [OS=Homo sapiens]	21	10.5	13.5	1
Q96HA7	TONSL	Tonsoku-like protein [OS=Homo sapiens]	12.5	21	11.5	1
Q96BW9	TAMM41	CDP-diacylglycerol--glycerol-3-phosphate 3-phosphatidyltransferase, mitochondrial [OS=Homo sapiens]	10	21	10	1
O15270	SPTLC2	Serine palmitoyltransferase 2 [OS=Homo sapiens]	12	13	16	1
Q32NB8	PGS1	Isoform 3 of Phosphatidate cytidylyltransferase, mitochondrial [OS=Homo sapiens]	13	15	13	1

Q86UE4	MTDH	protein LYRIC [OS=Homo sapiens]	20	10.2	14.66666667	1
Q8WTS1	ABHD5	1-acylglycerol-3-phosphate O-acyltransferase ABHD5 [OS=Homo sapiens]	14	12	14	1
Q8NBM8	PCYOX1L	Prenylcysteine oxidase-like [OS=Homo sapiens]	9	24	12	1
O43156	TTI1	TELO2-interacting protein 1 homolog [OS=Homo sapiens]	19	8	15	1
Q13505	MTX1	Metaxin-1 [OS=Homo sapiens]	12	13	12	1
Q8N128	FAM177A1	Isoform 2 of Protein FAM177A1 [OS=Homo sapiens]	10	14	13	1
O15228	GNPAT	Dihydroxyacetone phosphate acyltransferase [OS=Homo sapiens]	20	8.2	13.66666667	1
Q8IZ81	ELMOD2	ELMO domain-containing protein 2 [OS=Homo sapiens]	12	11	12	1
Q8NBX0	SCCPDH	saccharopine dehydrogenase-like oxidoreductase [OS=Homo sapiens]	9	11	12	1
Q16850	CYP51A1	lanosterol 14-alpha demethylase [OS=Homo sapiens]	9	11	11	1
Q9UH92	MLX	MAX-like protein X [OS=Homo sapiens]	9	12	10	1
P33121	ACSL1	Long-chain-fatty-acid--CoA ligase 1 [OS=Homo sapiens]	8.25	10.66666667	12.33333333	1
Q9BSY9	DESI2	Desumoylating isopeptidase 2 [OS=Homo sapiens]	9	12	9	1
P56937	HSD17B7	3-keto-steroid reductase [OS=Homo sapiens]	8	12	10	1
P42345	MTOR	Serine/threonine-protein kinase mTOR [OS=Homo sapiens]	22	6.75	10	1
O15269	SPTLC1	serine palmitoyltransferase 1 [OS=Homo sapiens]	11	8	10	1
Q9HBH5	RDH14	Retinol dehydrogenase 14 [OS=Homo sapiens]	8	10	11	1
Q9BV23	ABHD6	Monoacylglycerol lipase ABHD6 [OS=Homo sapiens]	9	8	11	1
Q99487	PAFAH2	Platelet-activating factor acetylhydrolase 2, cytoplasmic [OS=Homo sapiens]	9	10	9	1
Q96KC8	DNAJC1	DnaJ homolog subfamily C member 1 [OS=Homo sapiens]	9	10	9	1
Q96E22	NUS1	Dehydrodolichyl diphosphate synthase complex subunit nus1 [OS=Homo sapiens]	8	10	9	1
Q8TC12	RDH11	Retinol dehydrogenase 11 [OS=Homo sapiens]	12	5.5	12	1
Q8NBQ5	HSD17B11	Estradiol 17-beta-dehydrogenase 11 [OS=Homo sapiens]	11	6	12	1
P50336	PPOX	protoporphyrinogen oxidase [OS=Homo sapiens]	9	11	7.5	1
P21964	COMT	Catechol O-methyltransferase [OS=Homo sapiens]	13	16	5	1
Q9UI26	IPO11	Isoform 2 of Importin-11 [OS=Homo sapiens]	10.5	7.25	7	1
P51648	ALDH3A2	Isoform 2 of Fatty aldehyde dehydrogenase [OS=Homo sapiens]	12	10	3.666666667	1
Q9NW68	BSDC1	BSD domain-containing protein 1 [OS=Homo sapiens]	6.5	7	7.5	1
P40855	PEX19	Peroxisomal biogenesis factor 19 [OS=Homo sapiens]	4.4	11	7.2	1
P47712	PLA2G4A	Cytosolic phospholipase A2 [OS=Homo sapiens]	5.6	6.4	8.2	1
O43681	ASNA1	ATPase ASNA1 [OS=Homo sapiens]	5.285714286	7.166666667	6	1
Q9BXW9	FANCD2	Isoform 1 of Fanconi anemia group D2 protein [OS=Homo sapiens]	9	7.833333333	3.909090909	1

O60313	OPA1	Isoform 2 of Dynamin-like 120 kDa protein, mitochondrial [OS=Homo sapiens]	6.2	5.666666667	6.090909091	1
Q13724	MOGS	Mannosyl-oligosaccharide glucosidase [OS=Homo sapiens]	6.333333333	4.2	8.333333333	1
O76071	CIAO1	Probable cytosolic iron-sulfur protein assembly protein Ciao1 [OS=Homo sapiens]	6.666666667	5.25	5.6	1
Q9Y4R8	TELO2	telomere length regulation protein TEL2 homolog [OS=Homo sapiens]	5.6	9.666666667	3	1
Q96T76	MMS19	Isoform 5 of MMS19 nucleotide excision repair protein homolog [OS=Homo sapiens]	5.25	4.066666667	4.857142857	1
P40939	HADHA	Trifunctional enzyme subunit alpha, mitochondrial [OS=Homo sapiens]	4.090909091	3.058823529	5.454545455	1
Q6NXR4	TTI2	TELO2-interacting protein 2 [OS=Homo sapiens]	6	9	12	0.99
Q86SQ9	DHDDS	Isoform 2 of Dehydrodolichyl diphosphate synthase complex subunit DHDDS [OS=Homo sapiens]	7	10	9	0.99
Q99653	CHP1	Calcineurin B homologous protein 1 [OS=Homo sapiens]	7	12	7	0.99
Q92575	UBXN4	UBX domain-containing protein 4 [OS=Homo sapiens]	8	10	7	0.99
P50897	PPT1	Palmitoyl-protein thioesterase 1 [OS=Homo sapiens]	13	5	8	0.99
Q13190	STX5	Syntaxin-5 [OS=Homo sapiens]	9	5	8	0.99
P00387	CYB5R3	Isoform 3 of NADH-cytochrome b5 reductase 3 [OS=Homo sapiens]	5	6	5.5	0.99
O95573	ACSL3	long-chain-fatty-acid--CoA ligase 3 [OS=Homo sapiens]	5.333333333	4	5.5	0.99
P55084	HADHB	Trifunctional enzyme subunit beta, mitochondrial [OS=Homo sapiens]	4.285714286	3.090909091	5.714285714	0.99
Q99807	COQ7	5-demethoxyubiquinone hydroxylase, mitochondrial [OS=Homo sapiens]	8	7	8	0.98
Q9H1E5	TMX4	Thioredoxin-related transmembrane protein 4 [OS=Homo sapiens]	6	9	8	0.98
Q9BRX8	FAM213A	Redox-regulatory protein FAM213A [OS=Homo sapiens]	7	10	6	0.98
Q6PIU2	NCEH1	Isoform 2 of Neutral cholesterol ester hydrolase 1 [OS=Homo sapiens]	6	9	7	0.98
Q9HAP2	MLXIP	MLX-interacting protein [OS=Homo sapiens]	7	6	4.5	0.98
P43378	PTPN9	Tyrosine-protein phosphatase non-receptor type 9 [OS=Homo sapiens]	4.5	5	9	0.98
O75155	CAND2	Cullin-associated NEDD8-dissociated protein 2 [OS=Homo sapiens]	4	6	5.333333333	0.98
Q86U38	NOP9	Nucleolar protein 9 [OS=Homo sapiens]	4	3.666666667	3.428571429	0.98
Q9H1A3	METTL9	Methyltransferase-like protein 9 [OS=Homo sapiens]	6	9	7	0.97
P37268	FDFT1	squalene synthase [OS=Homo sapiens]	11	3.5	8	0.97
Q9Y2Z9	COQ6	Ubiquinone biosynthesis monooxygenase COQ6, mitochondrial [OS=Homo sapiens]	6	6	9	0.96
Q6PI48	DARS2	Aspartate--tRNA ligase, mitochondrial [OS=Homo sapiens]	3.4	4.75	4	0.96
Q96AG4	LRRC59	Leucine-rich repeat-containing protein 59 [OS=Homo sapiens]	6.333333333	2.714285714	3.833333333	0.96
Q8WVC6	DCAKD	dephospho-CoA kinase domain-containing protein [OS=Homo sapiens]	8	8	6	0.95

Q3SXM5	HSDL1	Inactive hydroxysteroid dehydrogenase-like protein 1 [OS=Homo sapiens]	8	6	5	0.95
O14656	TOR1A	Torsin-1A [OS=Homo sapiens]	4.5	3.666666667	6	0.95
O75915	ARL6IP5	PRA1 family protein 3 [OS=Homo sapiens]	7	5	7	0.94
Q9Y673	ALG5	dolichyl-phosphate beta-glucosyltransferase [OS=Homo sapiens]	6	7	5	0.94
Q6UX53	METTL7B	Methyltransferase-like protein 7B [OS=Homo sapiens]	6	6	5	0.94
O75691	UTP20	Small subunit processome component 20 homolog [OS=Homo sapiens]	8	5.666666667	3.333333333	0.94
Q13637	RAB32	Ras-related protein Rab-32 [OS=Homo sapiens]	4	4	4	0.93
A6NDU8	C5ORF51	UPF0600 protein C5orf51 [OS=Homo sapiens]	6	7	1.857142857	0.93
Q99541	PLIN2	perilipin-2 [OS=Homo sapiens]	4.4	5.4	2.090909091	0.93
P02649	APOE	Apolipoprotein E [OS=Homo sapiens]	9	8	4	0.92
P53701	HCCS	Cytochrome c-type heme lyase [OS=Homo sapiens]	3	5	5	0.92
P01111	NRAS	GTPase NRas [OS=Homo sapiens]	3	5.5	7	0.92
A1L0T0	ILVBL	Acetolactate synthase-like protein [OS=Homo sapiens]	5	5	7	0.91
Q2TAA5	ALG11	GDP-Man:Man(3)GlcNAc(2)-PP-Dol alpha-1,2-mannosyltransferase [OS=Homo sapiens]	4	4	5	0.91
Q96CS3	FAF2	FAS-associated factor 2 [OS=Homo sapiens]	7	4	2.6	0.91
Q68D91	MBLAC2	Metallo-beta-lactamase domain-containing protein 2 [OS=Homo sapiens]	5	11	5	0.9
P04843	RPN1	Dolichyl-diphosphooligosaccharide--protein glycosyltransferase subunit 1 [OS=Homo sapiens]	8	3.333333333	4.5	0.9
P05023	ATP1A1	Sodium/potassium-transporting ATPase subunit alpha-1 [OS=Homo sapiens]	4	6	4	0.9

Table A5: List of most enriched proteins observed in the interactome of viperin

Appendix A6: Generation and screening of Tet-On stable cell-line, stably expressing viperin

Cell line Tet-On 3G HEK 293T cell line was purchased from CloneTech

Reagents pTRE3G-BI vector, linear puromycin marker,Tet-approved foetal bovine serum (FBS), Puromycin and Geneticin (G418) antibiotic were purchased from CloneTech. Doxycyclin Hyclate was purchased from Sigma. DMEM media, 0.05% Trypsin-EDTA and 1X Phosphate buffer saline were obtained from Gibco (Thermo Fisher Scientific).

Cloning of pTRE3G-3x FLAG viperin The viperin construct with N-terminal 3x FLAG tag was cloned between BamHI and NotI restriction sites in a pTRE3G-BI vector using Gibson Assembly method. The sequence of the construct was checked at the University of Michigan sequencing core.

Creating of Tet-On 3G cell line, stably expressing 3x-FLAG-viperin Tet-On 3G cells were plated on a 100 mm collagen-coated plate and grown in DMEM media, supplemented with 10% tet-approved FBS, 1% Penicilllin/Streptamycin antibiotics and 100 µg/ml Geneticin (G418). The cells were grown to 80% confluence (80% of the plate was covered by the cells) and passed in a well of a 6-well plate at 1: 4 dilution in DMEM. The cells were transfected with 2 µg of viperin construct, with 100 ng Puromycin selection marker, mixing with Fugene HD at 1:3 ratio. After 48 h post-transfection, the confluent cells were split into four 100-mm collagen coated plates. After

an additional 48 hr, the media was changed with fresh media, supplemented with 0.5 µg/ml Puromycin. The media was replaced every four days with Puromycin supplemented fresh media, until the colonies were formed. About 48 large, healthy colonies were isolated using glass cylinders and passed into the wells in a collagen coated 24-well plate. The colonies were cultured in DMEM media supplemented with 10% tet-approved FBS, 1% Penicilllin/Streptamycin antibiotics and 100 µg/ml Geneticin (G418) and 0.25 µg/ml Puromycin.

Screening of colonies that are expressing 3x-FLAG-viperin The cells in each well of the 24-well plate were allowed to grow to 80-90% confluence and split in to 3 wells of a 6-well collagen coated plates. The *stock plate* was propagated for future maintenance, depending on the result from the inducibility assay. The rest of the two wells were used for induction test. The experimental well was treated with 1000ng/ml Doxycycline Hyclate and the last well was treated as a negative control. 48 h post induction, the cells were harvested and immunoblotted to test the expression of viperin. Six colonies, out of 48, showed expression of viperin upon doxycycline induction, without expression at basal level.

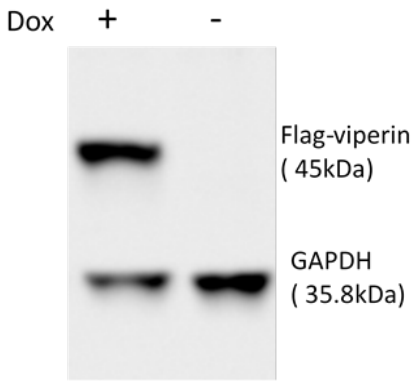

Figure A6: Screening of viperin expression in Tet-On 3G cell line, stably expressing under the control of pTRE3G promoter

Appendix A7: Cellular degradation pathway involved in the regulation of viperin expression

To investigate whether a degradation pathway is involved in regulating the cellular expression of viperin, we performed a time-dependent accumulation of viperin in HEK293T cells in the presence of proteasomal and lysosomal degradation inhibitors. Both transiently transfected viperin in HEK293T cells and stably expressed viperin in Tet-On 3G cells were assessed for monitoring the expression levels.

Upon blocking the proteasomal degradation pathway with reversible, cell permeable inhibitor MG132, a time-dependent degradation of viperin was observed *in vivo,* in comparison to the control cells treated with DMSO. On the contrary, treatment with lysosomal degradation inhibitors chloroquine and ammonium chloride resulted in an accumulation in the cellular expression level of viperin over 16 hours post-transfection (for transient transfection of viperin) or post-induction (for stably expressed viperin) ***[Figure A7]***, indicating that the expression level of viperin is regulated through lysosomal degradation pathway. However, the reason behind the reduction of cellular expression level of viperin upon treatment with proteasome-mediated degradation inhibitor MG132 is not well understood. As viperin was shown to interact with several ubiquitin ligases or ubiquitin-interacting proteins, it could be possible that inhibition of these proteins by MG132 may result in destabilization of viperin in turn.

Experimental Procedure

Cell HEK293T cells were obtained from ATCC. Tet-On 3G cells stably expressing viperin doxycycline induction were generated as mentioned in Appendix A6.

Materials MG132 in DMSO solution (M7449), ammonium chloride (213330) and chloroquine diphosphate salt (C6628) were purchased from Sigma.

Treatment of cells with protesome and lysosomal inhibitors HEK293T cells and Tet On 3G cells were grown to 60-70% confluency and transfected with 3X-FLAG tagged viperin gene in pcDNA3.1 or induced with 1000ng/ml doxycycline hyclate, respectively. After 24 hours of transfection or induction cells were treated with MG132 in DMSO (final concentration 50 μM) or ammonium chloride and Chloroquine solution in water together (final ceoncentration of each is 50 μM). Control cells were treated with DMSO. Cells were harvested at two hour time points till 16 hours post-transfection or post-induction and immunoblotted against anti-viperin antibody (rabbit polyclonal).

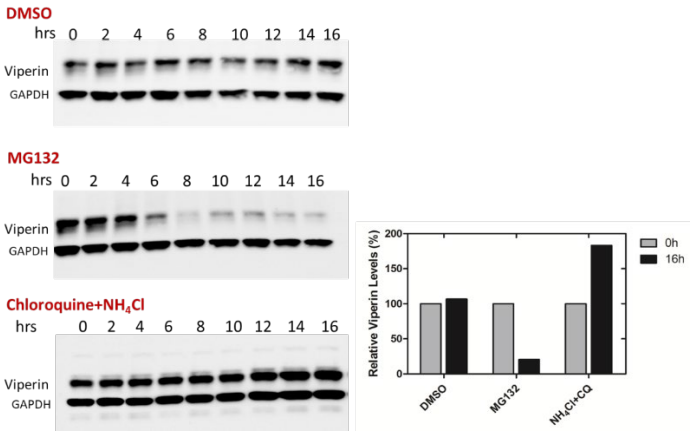

***Figure A7*: Cellular degradation pathway involved in the cellular expression level of viperin. HEK293T** cells expressing 3x-FLAG tagged viperin were treated with proteasomal degradation inhibitor MG132 (50 μM final concentration) or lysosomal degradation inhibitors Chloroquine (50 μM) and ammonium chloride (50 μM). Blocking of lysome-mediated degradation resulted in an accumulation of cellular level of viperin 16 hours post-transfection.

Appendix A8: Sinefungin and 5'deoxyadenosine reverses viperin mediated degradation of NS5A *in vivo*

To examine whether viperin requires its cofactor-bound (S-adenosyl-L-methionine) active state to degrade NS5A in vivo, we treated HEK293T cells, expressing NS5A, VAP-33C and viperin/viperinΔ3C with sinefungin, a competitive inhibitor of radical SAM-dependent enzymes. The cells were treated with sinefungin (final concentration 45 nM) at the same time of transfection to allow the maximum incorporation of sinefungin in viperin and followed for 12 hrs before expression test. It had been shown in previous studies that sinefungin binds to viperin and deactivates its radical SAM activity in producing 5'-deoxyadenosine from uncoupled reductive cleavage of SAM. Intriguingly, the sinefungin treated cells showed partial restoration of NS5A expression level, in presence of wild-type viperin and VAP-33C, in comparison to the un-treated cells ***[Figure A8(a)]***. Sinefungin did not show any effect on the expression level of viperin. However, intra-cellular expression of NS5A remained similar in sinefungin treated and untreated cells, when co expressed with viperinΔ3C and VAP-33C ***[Figure A8(a)]*****.** These results suggest that the SAM-bound active state of viperin might be required for its inhibitory activity against NS5A.

Similar results were observed when cells, expressing NS5A, viperin and VAP-33C, were treated with exogenous 5'-deoxyadenosine. Reductive SAM cleavage by product 5'-deoxyadenosine often acts as a product inhibitor for radical SAM enzymes. To

investigate whether 5’-deoxyadenosine can supress viperin’s ability to promote degradation of NS5A, we co-exoressed NS5A with viperin/viperinΔ3C and VAP-33C in HEK293T cells for 12 hours, followed by treatment with exogenous 5’-deoxyadenosine (final concentration 5μM) for 12 hours. Consistent with the results obtained from in vivo sinefungin treatment assay, NS5A expression level was partially restored in presence of wild type viperin and VAP-33C in 5’-deoxyadenosine treated cells ***[Figure A8(b)]*****,** whereas, the protein level of NS5A remained same in 5’-deoxyadenosine-treated and untreated cells in presence of viperinΔ3C ***[Figure A8(b)].*** The fact that 5’-deoxyadenosine only inhibits viperin’s activity by competing with SAM and not by altering its expression level, it implies that the SAM-bound active state of wild type viperin may play an important role in promoting degradation of NS5A *in vivo*.

Experimental Procedure

Cell HEK293T cells were obtained from ATCC.

Materials Sinefungin (567051-2MG-M) and 5'-deoxyadenosine (D1771) were purchased from Sigma Aldrich.

Treatment of cells with sinefungin and 5'-deoxyadenosine HEK293T cells and Tet On 3G cells were grown to 60-70% confluency and transfected with viperin/viperinΔ3C, NS5A and VAP-33C genes in pcDNA3.1. For sinefungin treatment, cells, sinefungin solution in water was added to 45 nM final concentrations at the same time of transfection and harvested 12 hours post transfection. For 5'-deoxyadenosine treatment, cells were treated with 5μM 5'-deoxyadenosine solution in water 12 hours post transfection and

harvested 12 hours post-treatment. Control cells were treated with water. The cells were lysed and immunoblotted for viperin, NS5A and VAP-33C.

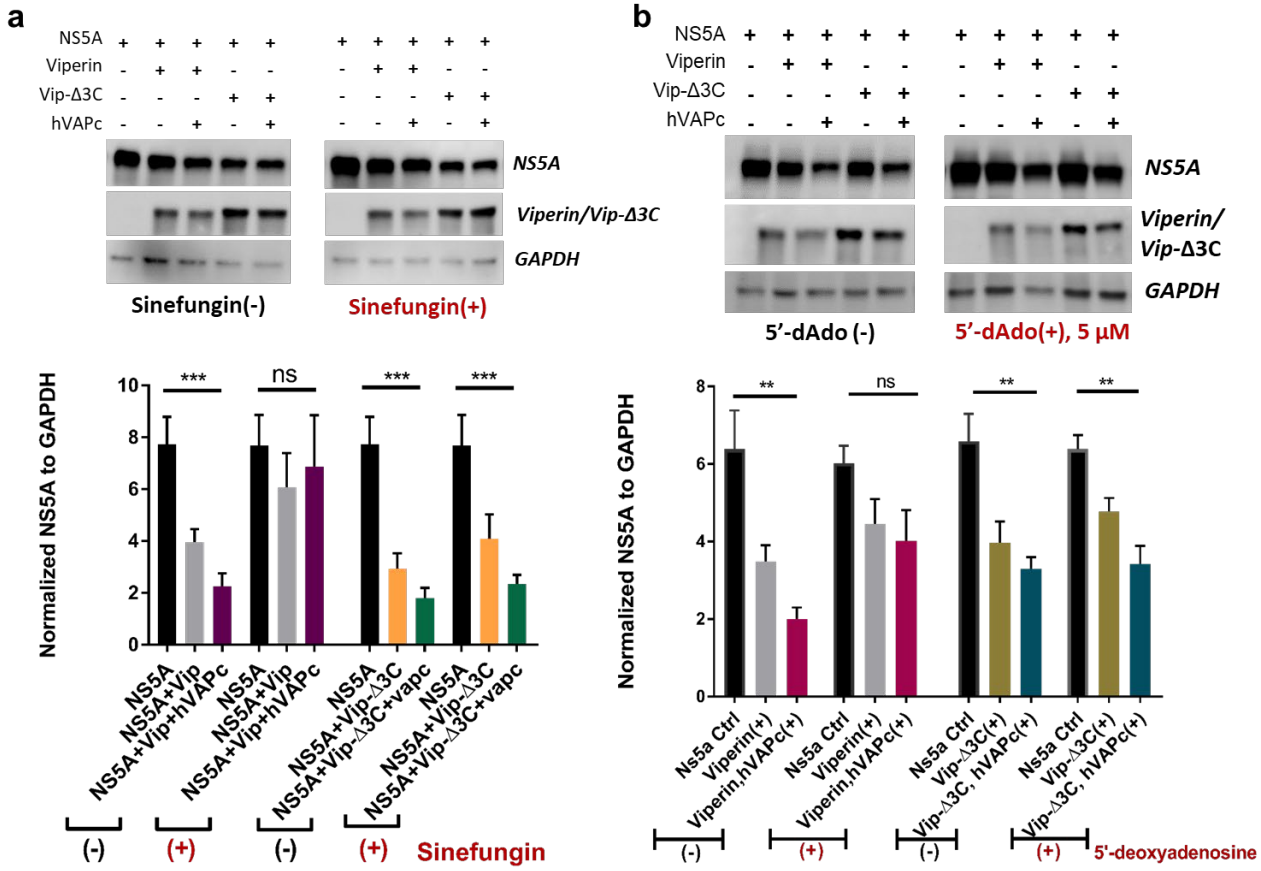

Figure A8. **SAM-bound active state of viperin is important for NS5A degradation in vivo** (a) HEK293T cells, transfected with genes of NS5A, FLAG-VAP-33C and viperin or viperin-Δ3C, were treated with *Sinefungin*, a competitive inhibitor of SAM at the same of transfection and immunoblotted 12 hours post-transfection/post-treatment. When treated with sinefungin, relative amount of NS5A, normalized to GAPDH were restored in presence of vipeirn and VAP-33C ($p>0.05$). However, the expression level of NS5A remain reduced in presence of mutant viperin (viperin-Δ3C) and VAP-33C, regardless the treatment with sinefungin. The comparisons between single-transfected and triple-transfected samples were executed by statistical analysis on the relative level of NS5A using student t-test (p_1***=0.0004; p_2***=0.0002; p_3***=0.0017; n=10). (b) Similar results were observed when cells, expressing above mentioned genes were treated with 5'-deoxyadenosine, a known product inhibitor of radical SAM enzymes. Relative amount of NS5A, normalized to GAPDH were partially restored in presence of vipeirn and VAP-33C ($p>0.05$) when treated with 5'-deoxyadenosine, but not in presence of the radical SAM domain mutant viperin. The comparisons between single-transfected and triple-transfected samples were executed by statistical analysis on the relative level of NS5A using student t-test (p_1***=0.0012; p_2***=0.0069; p_3***=0.0095; n=5).